Geology of the Milltown Alabama 7.5' Quadrangle and $^{40}Ar/^{39}Ar$ geochronology of muscovite from select rocks of the east-central Alabama Piedmont

By

John Paul Whitmore

A thesis submitted to the Graduate Faculty of

Auburn University

In partial fulfillment of the

Requirements for the Degree of

Masters of Science

Auburn, Alabama

December 15, 2018

Keywords: Milltown, Dadeville Complex, Jacksons Gap Group, Inner Piedmont, Hog Mountain, southernmost Appalachians

ABSTRACT

The Milltown 7.5' Quadrangle is located within east-central Alabama and contains features important to understanding the formation of the southern Appalachians. The Brevard fault zone passes through the Milltown Quadrangle and divides the Laurentian margin metasedimentary rocks of the eastern Blue Ridge from allochthonous metavolcanic units assigned to the Inner Piedmont terrane. In the study area, the eastern Blue Ridge is composed primarily of schists and phyllites separated from the Inner Piedmont by the Brevard fault zone, which is bounded by the Abanda and Katy Creek faults. Within the fault zone are lithologically distinct rocks of the Jacksons Gap Group which can be traced from the Upper Cretaceous onlap in Alabama all the way to Atlanta, Georgia. Within the study area and to the southwest the Jacksons Gap Group can be divided into several subunits that become less distinct to the northeast. The Inner Piedmont is composed of the Waresville Schist, a diverse group of metamorphosed volcanic and volcaniclastic rocks that has been intruded by the Rock Mills Granite Gneiss. Late-stage Alleghanian right-lateral shearing overprinted the Brevard zone mylonites and phyllites an extensive area of rocks in both the eastern Blue Ridge and Inner Piedmont and collectively the affected zone is referred to as the Brevard shear zone.

Geological mapping of the Milltown Quadrangle and $^{40}Ar/^{39}Ar$ cooling dates for muscovite have produced five key findings. (1) Within the Milltown Quadrangle, Brevard zone lithologies (i.e. Jacksons Gap Group) are not easily separable into individual map units as has been recognized for other areas to the southwest. Units have gradational

contacts and display only slight lithologic differences. The Jacksons Gap Group is subdivided into three units: a structurally lower section consisting predominantly of fine-grained garnetiferous, graphitic, quartz phyllites; a middle section of interlayered garnetiferous quartz schists and phyllites; and an upper section of sericitic quartz phyllites. Along-strike structural and/or stratigraphic variations have caused many units to pinch and swell or to be completely excised. (2) The Waresville Schist contains metamorphosed mafic and more felsic volcanics that are extensive enough to potentially be mapped as distinct lithologies. A previously unreported lithology, garnetite, was identified in the Waresville Schist that extends possibly 8 kilometers as a mapable unit, and likely extends farther to the east of the Milltown Quadrangle. The protolith is interpreted as a sedimentary deposit hosted within hydrothermal exhalatives. (3) Late D_2 deformation produced the large scale folding within the Dadeville Complex including the Penton synform that trends N70°E and plunges 28° with a half-wavelength of ~10 km and an amplitude of ~3 km. Notably, the Penton synform does not affect underlying units of the Jacksons Gap Group requiring its detachment from the lower plate along the Katy Creek fault. (4) $^{40}Ar/^{39}Ar$ Cooling ages for muscovite extracted from lithologies of the Inner Piedmont are ~319 Ma with a standard deviation of 0.47 Ma and those from the Jacksons Gap Group are ~315 Ma, consistent with dates reported for wholesale uplift and cooling of these terranes. And, (5) muscovite from en echelon quartz veins within the Hog Mountain tonalite are ~321 Ma, indicating that they were emplaced during early Alleghanian metamorphism at shallower depths than the Inner Piedmont, and not during later extension of the Southern Appalachians.

ACKNOWLEDGEMENTS

Funding was provided by the National Cooperative Geologic Mapping Program and the United States Geologic Survey (EDMAP) to Dr. Mark Steltenpohl, Auburn University. I am very appreciative of this research assistantship support. Additionally, I would like to thank Ben Smith for his invaluable assistance in the field and to Lainey Le Blanc for her support.

TABLE OF CONTENTS

LIST OF TABLES

List of Plates

LIST OF FIGURES

MINERAL ABBREVIATIONS

Am	amphibole
Ep	epidote
Grt	garnet
Hbl	hornblende
Or	orthoclase
Mag	magnetite
Oam	Orthoamphibole
Pl	plagioclase
Qtz	quartz
Zo	zoisite

INTRODUCTION

The primary study area is the Milltown Quadrangle, located in Randolph and Chambers counties in the east-central Alabama (Fig. 1), to the southwest of Roanoke. Geologically it straddles the Brevard fault zone, separating the eastern Blue Ridge and Inner Piedmont terranes of the southern Appalachians. Previous geological mapping of the area has been limited to large scale reconnaissance work (Bentley and Neathery, 1970). As such, the National Cooperative Geologic Mapping Program funded an EDMAP award to Dr. M. G. Steltenpohl for the creation of a 1:24,000 scale geologic map of the area. The purpose of this mapping is four-fold: 1) to map and characterize lithologies and clarify their distributions and boundaries within the Milltown Quadrangle; 2) to analyze structures and fabrics within and along the Brevard fault zone for studying the kinematics; 3) to produce a 1:24,000 scale geologic map of the Milltown Quadrangle; and 4) to synthesize the regional geological history.

In addition to the geologic mapping of the Milltown Quadrangle, a geochronological investigation was performed on rocks and quartz veins in the rocks of the Milltown Quadrangle and within the Hog Mountain tonalite, located in Tallapoosa County, Alabama approximately 13 miles to the northeast of Alexander City (Fig. 1). The purpose of this investigation was to determine whether there is a geologic, kinematic and temporal relationship between brittle faulting along the Brevard zone and the network of gold and other ore-bearing quartz veins within the Hog Mountain tonalite, and what the results might tell us about Appalachian evolution. Additional samples were

analyzed for lithologies from the Jacksons Gap Group and the Inner Piedmont in order to further constrain the overall cooling history of these terranes.

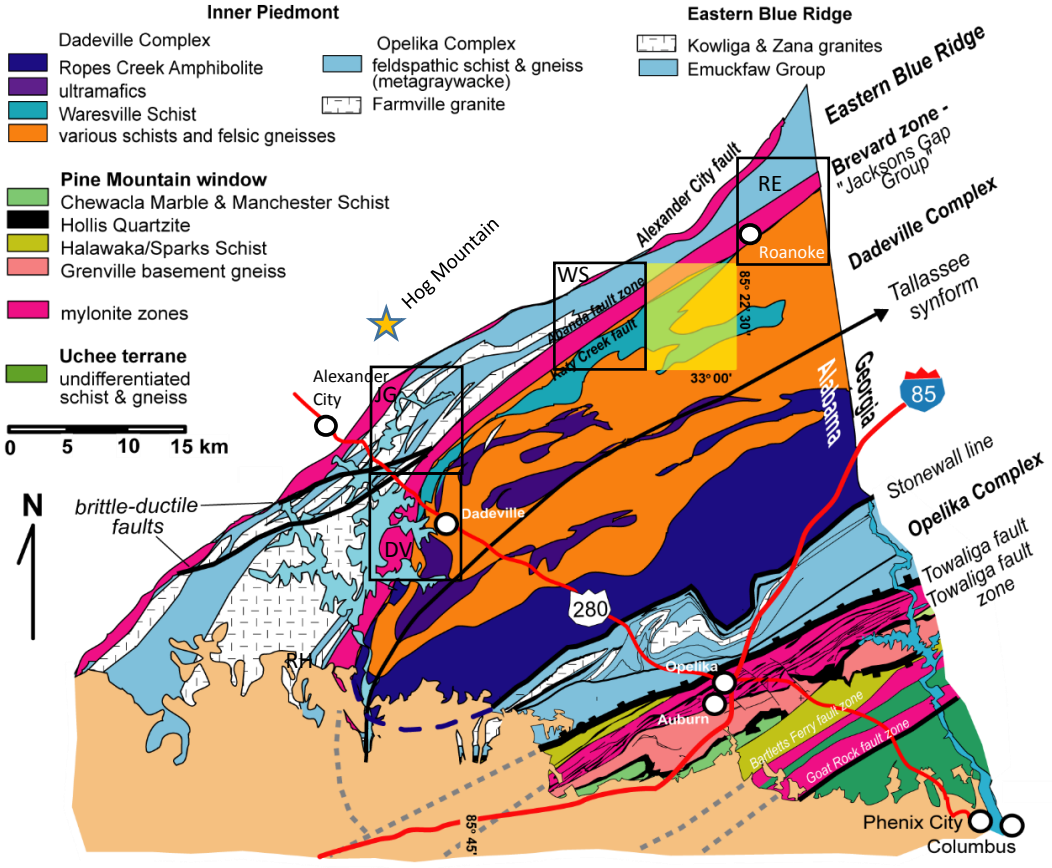

Figure 1 - Geologic map of a part of the Alabama Piedmont emphasizing the Inner Piedmont and eastern Blue Ridge terranes. The location of the Milltown quadrangle is highlighted yellow. The location of Hog Mountain is shown by the yellow star. Modified from Steltenpohl (2005). EDMAP Quadrangle abbreviations: DV = Dadeville; JG = Jacksons Gap; RE = Roanoke East; WS = Wadley South.

PREVIOUS INVESTIGATIONS

Previous work done within the area of the Milltown Quadrangle has largely been part of larger general surveys of the regional geology. Some of the earliest geologic investigations were performed by Adams (1926) who identified the basic regional lithologies and contacts. The most significant effort was the seminal Bentley and Neathery (1970) paper, which described the Brevard fault zone and Inner Piedmont and identified the extent of what is now known as the Emuckfaw Group, much of the Kowaliga Gneiss and Zana Granite, the Katy Creek and Abanda faults, and the Dadeville Complex. Bentley and Neathery (1970) were the first to suggest that much of the southern Appalachian Piedmont is an allochthonous terrane thrust upon the Laurentian margin along the Brevard fault zone. In the 1970's, COCORP (COnsortium for COntinental Reflection Profiling) investigated the southern Appalachians in Georgia, including the Brevard zone, using seismic-reflection profiles and developed a similar interpretation (Cook et al., 1979). Neathery and Reynolds (1975) further contributed to the current understanding of the eastern Blue Ridge by studying the Heard Group and renaming it the Emuckfaw Formation. It was further subdivided and renamed as the Emuckfaw Group by Raymond and others (1988).

While investigating the Brevard fault zone in Alabama both Bentley and Neathery (1970) and Wielchowsky (1983) described the rocks of the Jacksons Gap Group as being lithologically distinct from the Emuckfaw Group, which previously were interpreted as altered Wedowee Group (Adams, 1926). It is differentiated from the garnet schists of the Emuckfaw Group by the transition to graphitic phyllites and schists.

Wielchowsky (1983) verified that the geometry of the Brevard zone in Alabama is similar to that identified by COCORP in Georgia.

Finer scale 1:24,000 geologic mapping of 7.5' quadrangles and structural analyses and geochemical analyses have been conducted along the Brevard shear zone in Alabama as part of numerous Auburn University student theses under the direction of Dr. Mark Steltenpohl and others between 1988 and 2017. The goal is to gain a better understanding of the geologic significance of the Brevard fault zone in the southernmost exposures of the orogen and how it relates to the emplacement of the Dadeville Complex, and Opelika complex (Johnson, 1988; Keefer, 1992; Grimes, 1993; Reed, 1994; McCullars, 2001; Sterling, 2006; White, 2007; Hawkins, 2013; Poole, 2015; VanDervoort, 2016; Harstad, 2017). Of particular importance, Johnson (1988) and Reed (1994), mapping in the Jacksons Gap Group within the western Dadeville and eastern Jacksons Gap quadrangles (Fig. 2), delineated mappable units that were further defined by VanDervoort (2016) within the Wadley South Quadrangle. A compilation map of 1:24,000 quadrangles of the Brevard zone from Abanda, Alabama to Atlanta, Georgia was presented by Crawford and Kath (2017) and it includes the Milltown Quadrangle.

The Hog Mountain pluton is located in Tallapoosa County (Fig. 1) and has seen intermittent mining for gold since the nineteenth century (Aldrich, 1909; Park, 1935; Pardee and park, 1948; Stowell et al., 1996; Lambe, 1982; Guthrie and Lesher, 1989; Cook and Thomson, 1995; Ozsarac, 2016). Pardee and Park (1948) claimed that the veins attitude and extent along strike were not consistent with tension gashes as had earlier been hypothesized (Aldrich, 1909; Park, 1935). Stowell and others (1996) did extensive

work on the timing of mineralization, mechanisms of vein emplacement, and provided geochemical analyses of vein material and the surrounding rocks. They concluded that quartz veins within the Hog Mountain tonalite were emplaced at peak to near peak upper greenschist to lower amphibolite facies conditions at a pressure of 5.5 ± 1 kbar. As this report was written, Wellborn Mining Company LLC is actively performing a drilling program to assess its potential as a gold mine.

METHODS

Geologic mapping of the Milltown quadrangle was performed at a 1:24,000 scale along all primary and secondary roads, logging trails, public property, and private property where permission from the landowner could be acquired. Three hundred and forty-eight measurements were collected on structural, lithologic, and kinematic features over ~168 square kilometers. The U.S. Geological Survey U.S. Topo 7.5-minute map for Milltown, AL 20141001, was used as a base map for field work and for the production of the final Milltown geologic map generated using ArcMap® 10.4.1 (Fig. 2). A copy of the final geologic map is included as Plate 1.

Station locations were recorded using a Garmin eTrex® GPS in the Universal Transverse Mercator coordinate system. Twenty-one samples representing key lithologies and/or oriented samples for kinematic determination were selected to be made into thin sections. Billets were cut using equipment available at Auburn University before being sent to National Petrographic Service, Inc. A Nikon Labophot2-Pol polarizing microscope was used for the petrographic analyses. Images taken in the field

were captured with a Samsung Galaxy S7® cellphone. Photomicrographs were taken with a Canon Rebel® T5i attached to a Motic BA300pol binocular polarizing microscope.

Samples of vein material along with several major lithologies within the Milltown Quadrangle were collected for $^{40}Ar/^{39}Ar$ dating. Samples from Hog Mountain were taken from large quartz veins that were historically mined. These were mechanically disaggregated using a mortar and pestle before being sieved. Material was placed in a Petri dish with alcohol and muscovite was identified using a zoom binocular stereo microscope and removed with tweezers. The extracted muscovite samples were sent to the U.S. Geological Survey TRIGA Reactor in Denver, Colorado where they were irradiated for 16 hours. $^{40}Ar/^{39}Ar$ dating was performed in the Auburn Noble Isotope Mass Analysis Laboratory (ANIMAL). The determined dates represent cooling ages used to assess the possible emplacement ages of the quartz veins and the timing of regional metamorphism. A polished section containing material not sent for irradiation was made using the Auburn University thin section lab and analyzed in the JEOL JXA-8600 Superprobe in the Auburn University Electron Microprobe Analysis Lab. The Auburn X-ray diffractometer (XRD) laboratory was also utilized for the analysis of one sample.

LOCATION

The primary study area is the Milltown 7.5’ Quadrangle (33°07’30” and 33°00’N; 85°30’ and 85°22’30”W) located in Chambers and Randolph counties in east-central Alabama to the southwest of Roanoke (Fig. 1). The majority of the area of the quadrangle lies within the Inner Piedmont physiographic province, with only the

northwestern corner being within the eastern Blue Ridge. The topography is hilly and primarily dictated by dendritic drainage patterns with little topographic relief; elevation ranges from 190 to 275 meters and increases toward the northeast. The exception is a pair of linear ridges in the northwest corner that are the surface expression of the Brevard fault zone. The quadrangle is entirely within the Middle Tallapoosa watershed. High Pine, Caty and Chikasanoxee creeks are the primary waterways and are a part of the High Pine and Chikasanoxee subwatersheds respectively, which drain into the Tallapoosa River ~ 5 km to the west (CH2MHILL, 2004). Incorporated Roanoke extends into the northeastern corner of the quadrangle but the majority of the area is rural, made up of pasture and timberland. The exceptions are the small communities of Clackville, Doublehead, Milltown, Penton, Red Level, and Rock Fence.

A secondary field site is the Hog Mountain gold prospect, which is located in Tallapoosa County, Alabama approximately 13 miles to the northeast of Alexander City (Fig. 1). The gold prospect is hosted within the pre- to syn-metamorphic Hog Mountain tonalite which intruded the Wedowee Group (Guthrie and Lesher, 1989). Gold was discovered at the location in 1839 and produced ~17,300 ounces, with average ore grades of 0.1-0.2 ounces per ton (Pardee and park, 1948). More than a dozen large named veins occur within the tonalite (Fig. 3) and these were historically quarried in surface pits and mined underground. Numerous smaller veins occur along and oblique to strike.

Geologic Map of the Milltown Quadrangle, Alabama

John Whitmore

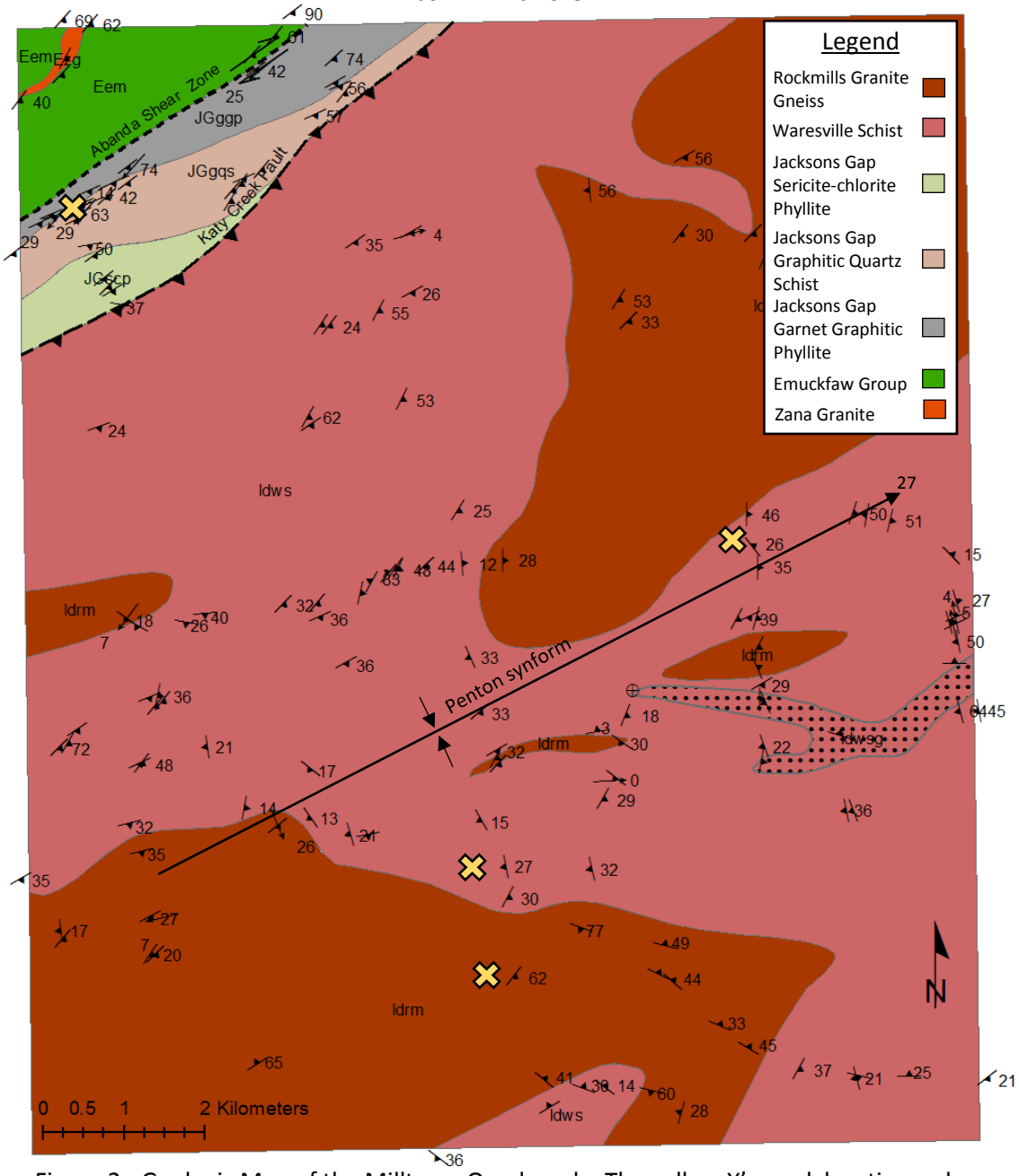

Figure 2 - Geologic Map of the Milltown Quadrangle. The yellow X's mark locations where samples were collected for $^{40}Ar/^{39}Ar$. From north to south they are samples: 72.1B, 28.2B, 8.3B, and 7.2B.

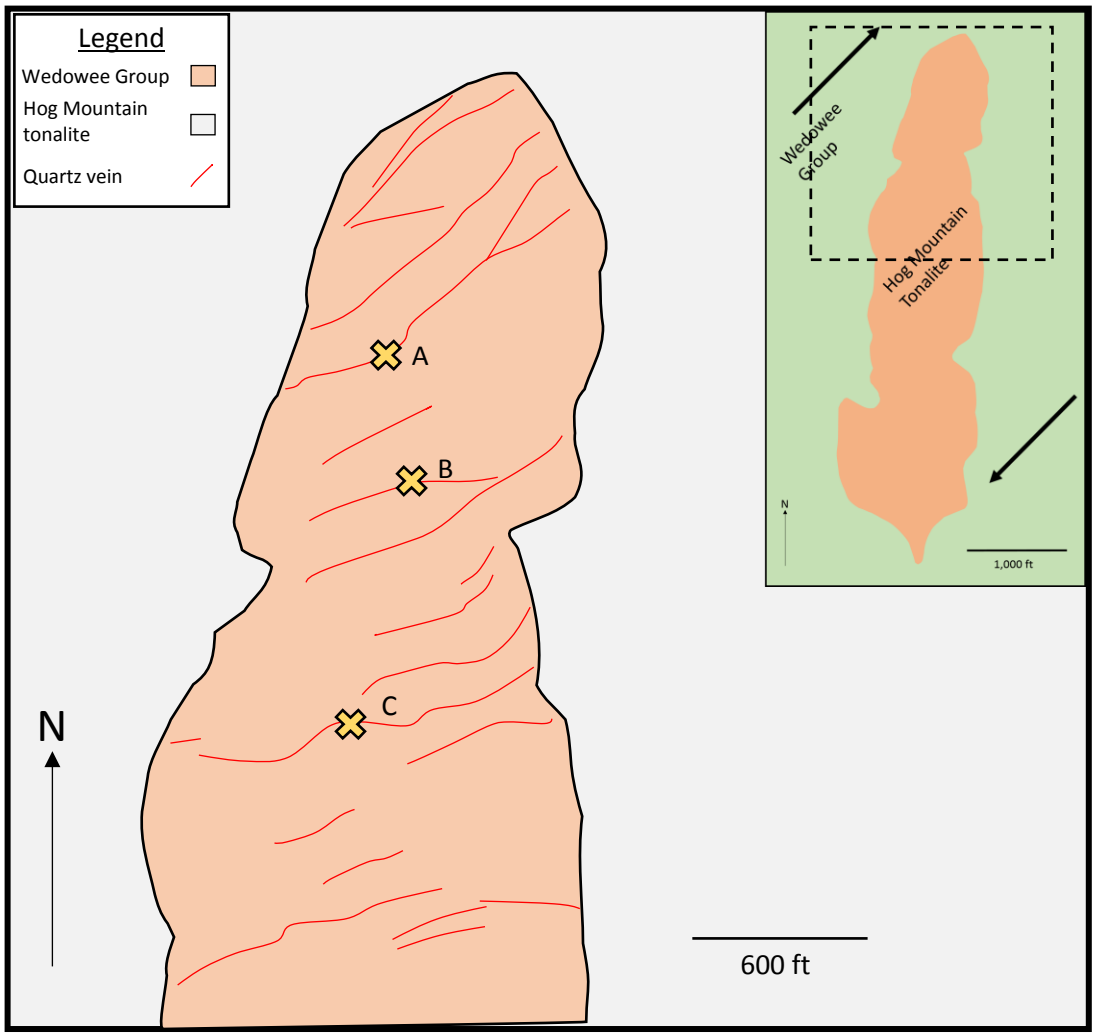

Figure 3 - Map of the northern portion of the Hog Mountain tonalite depicting significant ore bearing veins. Yellow X's mark locations where samples were collected: (A) Trippel vein (B) Barren vein (C) Tunnel vein. Based on map from Pardee and Park (1948). Inset map depicts the general horizontal maximum principle stress component (σ_1) based on the veins occurring as tension gashes. The overall dextral sense of shear reflects Alexander City and Brevard fault zone kinematics.

GEOLOGIC SETTING

Alabama contains the southernmost exposures of the crystalline Appalachians before plunging beneath the Coastal Plain onlap. Crystalline rocks of the Piedmont physiographic province are divided from northwest to southeast into the western Blue Ridge, eastern Blue Ridge, Inner Piedmont, Pine Mountain, and Uchee terranes (Bream et al., 2004; Steltenpohl et al., 2008; Steltenpohl et al., 2013). In Alabama, Paleozoic continental margin and foreland basin deposits of the Valley and Ridge have been overthrust by the metamorphosed Neoproterozoic-early Paleozoic Laurentian rift-to-drift-facies of the western Blue Ridge (Talladega slate belt) along the Talladega-Cartersville thrust fault (Williams and Hatcher, 1983; Gestaldo et al., 1993; McClellan et al., 2007; Tull et al., 2012). Estimated displacement along the fault is ~190 km (Cook et al., 1979; Tull et al., 2012). The eastern part of the Blue Ridge is separated from the western part by the Hollins Line fault and the former is differentiated by its higher degree of metamorphism and it being composed of deeper water slope/rise-facies (McClellan et al., 2007). The Hollins Line fault is a dextral transpressional fault that is duplexed along much of its extent; the roof fault contains up to several kilometers of mylonitized eastern Blue Ridge rocks (Mies, 1992; Steltenpohl et al., 2013). The eastern Blue Ridge contains the Ashland Supergroup, Wedowee Group, Emuckfaw Group, and numerous granitic plutons including the Elkahatchee Quartz Diorite, Kowaliga Gneiss, and Zana Granite (Bentley and Neathery, 1970; Steltenpohl, 2005; Merschat, 2009). The Brevard fault zone bounds the eastern Blue Ridge along its south eastern extent.

Two major fault systems cut the eastern Blue Ridge. The Goodwater-Enitachopco fault has experienced movement in at least two episodes. The first during the Alleghanian as an imbricated thrust, mostly within the eastern Blue Ridge and is generally sub-parallel with the Talledega-Cartersville fault, with a movement towards the northwest. The later period of movement is recorded by discrete crosscutting mylonitized shear zones that strike towards the northeast and have an oblique dextral and normal-slip component (Steltenpohl et al., 2013). The Alexander City fault locally separates the Wedowee Group from the Emuckfaw Group and is interpreted to have thrust the Emuckfaw onto the Wedowee, later having been reactivated as a dextral strike slip fault.

The Brevard zone in Alabama is a shear zone of varying dimensions but generally less than six kilometers wide separating the Inner Piedmont from the eastern Blue Ridge (Sterling et al., 2005). In Alabama it is bounded to the northwest by the Abanda fault and to the southeast by the Katy Creek fault (Bentley and Neathery, 1970; Neathery and Reynolds, 1975; Tull, 1978; Steltenpohl et al., 2013). The Jacksons Gap Group are the lithologies defining the Brevard fault zone in Alabama, and they could be part of the eastern Blue Ridge but no definitive terrane assignment is yet known. The Jacksons Gap Group is variably mylonitized and phyllonitized with low- strain volumes of rocks locally retaining primary sedimentary structures (Abrams, 2014).

The Inner Piedmont of Alabama traditionally has been interpreted as the Dadeville Complex and Opelika Complex (Bentley and Neathery, 1970; Raymond et al., 1988). The Dadeville Complex contains an allochthonous arc fragment and an associated

ocean floor sequence which is primarily composed of metavolcanics, metasedimentary, ultramafic, and granitoid units that were overthrust onto the eastern Blue Ridge (Steltenpohl and Kunk, 1993; VanDervoort et al., 2015; VanDervoort, 2016; Tull et al., 2018). The timing of the emplacement of the Dadeville Complex to its current place remains to be constrained. The timing of the arc magmatism, however, have been constrained to be ca. 467-457 Ma for the main magmatism following an earlier phase at ca. 479 Ma on the basis of zircon U-Pb dating of meta-igneous rocks of the arc-related intrusions (Ma et al., in preparation). Tull et al. (2018) also reported magmatic zircons of ca. 448–444 Ma that might reflect a late phase of arc magmatism. The arc fragment in the Dadeville Complex, therefore, is considered as a Taconic arc. The Franklin Gneiss in western Georgia (equivalent to the Rock Mills Granite Gneiss in Alabama) that was dated to be 460 Ma (Rb-Sr whole-rock isochron age; Seal and Kish, 1990) is consistent with the interpretation of a Taconic arc. Detrital zircons from the metasedimentary units of the Dadeville Complex suggest Laurentian and Taconian sources.

The Dadeville Complex lies in the core of the shallow northeast plunging Tallassee synform (Steltenpohl, 2005). After thrusting had ceased, the Dadeville arc terrane experienced dextral strike-slip movement along the Brevard and related shear zones resulting in its southwest translation (Hatcher. 1989; Merschat, 2009). The Stonewall line fault separates the Dadeville arc from the metasedimentary rocks of the Opelika Complex. Although traditionally included in the Inner Piedmont, Steltenpohl (2005) reports that the Opelika Complex shows lithologic and temporal affinities to the Jacksons Gap and Emuckfaw groups. The Opelika Complex is underlain to the southeast

by rocks of the Pine Mountain terrane (Fig. 1), a tectonic window into the Grenville basement complex and its attached Neoproterozoic to early Paleozoic cover (see Steltenpohl et al., 2010). The contact between them is marked by the Towaliga fault zone. Further southeast-ward, the Uchee terrane overlies the Pine Mountain terrane along some of the widest zones of mylonites in the Appalachians, the Goat Rock and Bartletts Ferry fault zones (Fig. 1; Steltenpohl, 1988; Steltenpohl et al., 1992). The Uchee terrane is a peri-Gondwanan or Gondwanan arc terrane (Steltenpohl et al., 2008)

LITHOLOGIC UNITS

Lithologies depicted in Figure 2 and plate 1 that were distinct and large enough to be mappable, below, include the map symbol parenthetically. Other lithologies that were minor components of mappable units are discussed under their subheadings.

Emuckfaw Group (Eem)

The tectonostratigraphically lowest unit in the study area, the Emuckfaw Group is a variably graphitic garnet-bearing muscovite-biotite-quartz-feldspar schist, commonly interbedded with quartzite and quartz phyllite in layers ranging from centimeters to meters. Within the study area it has been intruded by the Zana Granite, whereas outside of the study area it contains numerous plutons of Zana Granite and the Kowaliga Gneiss (Hawkins, 2013; VanDervoort, 2016). Rare amphibolite lenses are locally present within the Emuckfaw Group but were not observed in the current study area. Fresh exposures of schist are rare but are typically dark gray- to silver-colored weathering to a tan to orangish-red. Commonly, muscovite is peppered with sub-millimeter dark minerals,

possibly magnetite or chloritoid. Quartz veins and lenses are locally abundant, oriented along foliation and typically 1-10 mm thick. Where outcrops are not present, the Emuckfaw Group is identifiable by a surficial cover of garnet and muscovite grains. The Emuckfaw Group in the Milltown Quadrangle is typically highly sheared by dextral movements along the Brevard shear zone, producing a strong S-C fabric. Where garnets are present, they commonly form the center of a mica 'button'. Exposure of the Emuckfaw Group is limited by dense vegetation, intense weathering, and alluvium but small exposures can readily be found upon close inspection where land has been graded for dirt roads. The best exposures in the study area can be found along CR-830 and CR-3 (Plate 1)

Zana Granite (Ezg)

Within the Emuckfaw Group are numerous tabular, sill-like bodies of metagranite that range from meters to hundreds of meters in thickness and length along strike. Based on mineralogy, these have historically been divided into the Kowaliga Gneiss and Zana Granite (Bentley and Neathery, 1970). Their mineralogical and geochemical similarity led previous workers to suggest that they were derived from the same intrusive suite (Bentley and Neathery, 1970; Stoddard, 1983; Hawkins, 2013). The majority of Zana Granite is concentrated along strike to the southwest of the Milltown Quadrangle, although recent work has correlated smaller pods of metagranite both to the northeast and southwest of the study area with the Zana Granite (VanDervoort 2016; Harstad, 2017).

The Zana Granite is a highly sheared, foliated, and lineated medium- to coarse-grained biotite-muscovite-alkali feldspar gneiss. Within the Milltown Quadrangle it crops out as distinctive dark fins that rise above the surface up to a couple of meters; they are up to 200 meters thick. Bands of white feldspar, several centimeters thick mixed with sparse biotite, muscovite, and quartz appear and taper out along foliation over ~20-200 cm. Sporadic feldspar porphyroclasts up to 1 cm long, and quartz ribbons ~1 cm thick are common. The mineralogy consists of muscovite, biotite, quartz, plagioclase, potassium feldspar, and minor amounts of epidote, hornblende, and sericite.

Foliation is mainly defined by muscovite, which is concentrated in distinct 3-5 mm bands, or present as either individual books 1-2 mm thick or as mica fish up to 4 mm in length. Rarely, where mica is more abundant, there is what appears to be a c-prime fabric is present. Biotite is present throughout as sub-millimeter thick drapes between quartz and feldspar crystals, and is commonly present with sericite and very fine quartz grains. Quartz grains are inequigranular with larger grains up 1 mm but typically they are 0.5 mm in length. Domains of interlobate quartz bulges smaller than 0.2 mm surround larger grains indicating grain boundary bulging and recrystallization of the larger grains.

Quartz grains exhibit undulose extinction exclusively. Larger grains are stretched along the primary foliation and are commonly bounded by bands of much smaller recrystallized strain-free grains forming a seriate interlobate texture. Plagioclase is identified by relict albite twinning and isolated sub-millimeter crystals with intact albite

twins. Potassic feldspars include both microcline and orthoclase. Epidote is present throughout but primarily associated with the same bands that contain muscovite, and they range from 0.3 to 1 mm in diameter with isolated larger crystals. Brown hornblende is also present in small quantities.

Jacksons Gap Group

Generally, the Jacksons Gap Group is differentiated from the garnet schists of the Emuckfaw Group by the former having a greater abundance of graphitic phyllites and schists. Bentley and Neathery (1970) report that the Brevard fault zone in Alabama is primarily composed of muscovite and sericite schists, phyllites and quartzites of the Jacksons Gap Group, with a central core of mylonite (Figs. 2, 4 and 5). Recent work indicates, however, that mylonites and cataclasites are interspersed throughout the fault zone and its component units (VanDervoort, 2016; Barkley and Hawkins, 2016). Upper greenschist facies metamorphism and locally low-degrees of strain allows the Jacksons Gap Group to preserve primary sedimentary structures such as quartz pebble conglomerates and relic cross-bedded quartzites, clearly reflecting a shallow marine setting (Sterling, 2006; Abrahams, 2014; Poole 2015). No primary sedimentary structures were observed, however, in the current study of rocks in the Milltown Quadrangle.

It is generally accepted that the Jacksons Gap Group lies within the confines of the two bounding faults of the Brevard fault zone, the Abanda and Katy Creek faults. How the Jacksons Gap Group is distinguished from the Emuckfaw Group in areas where

the Abanda fault is not observed, however, varies depending on the observations of different investigators. Hawkins (2013) and Poole (2015) distinguish the Jacksons Gap Group by its anomalously low metamorphic grade as compared to the Emuckfaw Group. Harstad (2017), on the other hand, defined the base of the Jacksons Gap Group where pods of amphibolite cease to be present moving upward within the Emuckfaw Group. Along CR-856 the contact between the Emuckfaw and Jacksons Gap groups is marked by a thin zone of ultramylonites of the Abanda fault (see Plate 1).

VanDervoort (2016) reported that the Jacksons Gap Group within the Wadley South Quadrangle was composed of three units: garnetiferous graphitic phyllite (JGggp); garnetiferous quartz schist (JGgqs); and sericite-chlorite phyllite (JGscp). The same units carry through into the area of the Milltown quadrangle and are described individually.

Garnetiferous Graphitic Phyllite (JGggp)

The unit is a fine- to medium-grained graphitic muscovite, quartz, and garnet phyllite. Locally it is sericitized and contains garnets that range in diameter from < 1 to 6 mm. In outcrops the unit generally has a silverish gray appearance that may be stained reddish yellow. Sheets of fine-grained white mica are commonly found peppered with submillimeter chloritoid grains. The unit is strongly sheared, locally exhibiting a well-developed S-C fabric; mylonites and ultramylonites locally form within more quartzofeldspathic layers. Locally, steeply plunging, dextral kink folds have 1 - 3 meter amplitudes. Discrete zones of multiple quartz veins from 10 - 18 cm thick are also common.

The JGggp is bounded to the northwest by the Abanda fault where it contains zones of discrete mylonization (Fig. 6). A sample (Figs. 4 & 5) of ultramylonite was collected near the Abanda fault from a quartz-rich layer of the JGggp (33.119864°, 85.4683124°W). The ultramylonite has a fine crystalline matrix that is divided into bands of quartz and opaque layers. Mica fish are rare but are present throughout the sample as sub-millimeter fish. Rare delta porphyroclasts of feldspar and numerous sheath and asymmetric flow folds indicate a dextral shear sense. In the middle of CR-53 (33.09989°N, 85.50064°W) after it had been freshly graded an isolated example of a gneissic biotite-muscovite-feldspar-quartz mylonite was observed. This mylonite is 10 cm thick, contains whiteish to tan porphyroclasts up to 7 mm and boudins of quartz and feldspar up to 4 cm long.

Figure 4 - Ultramylonitized quartzite in the garnetiferous graphitic phyllite of the Jacksons Gap Group, associated with the Abanda fault. Sample next to notebook is from where thin section 68.3B was made (see Figure 5).

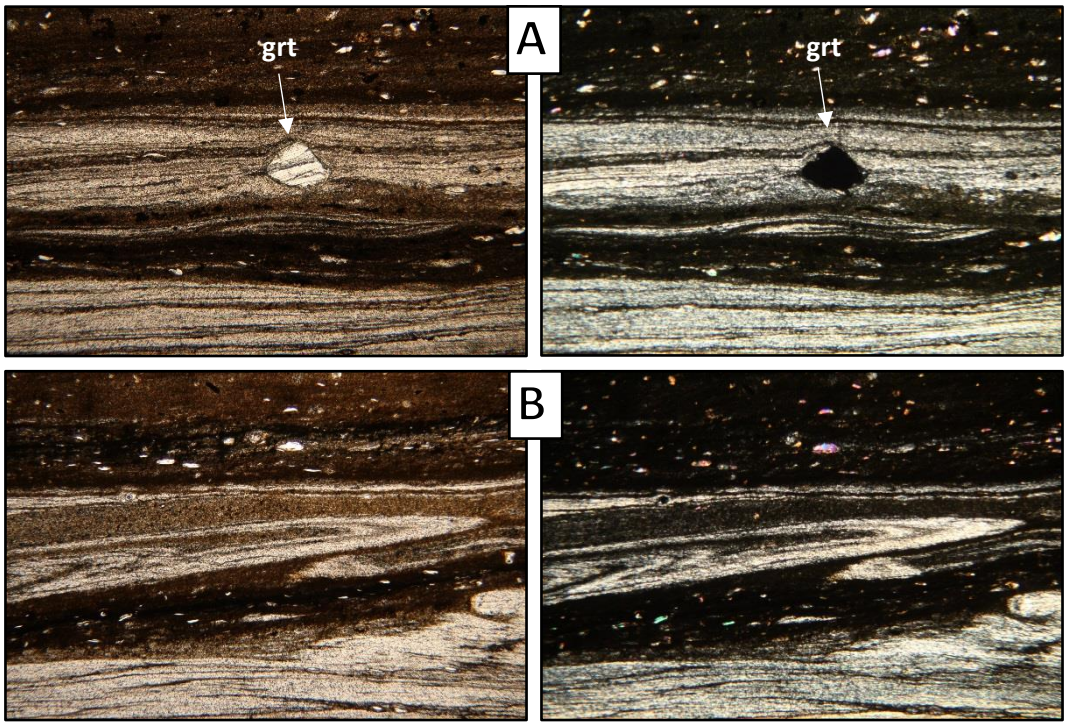

Figure 5 – Photomicrographs in plane- (left) and cross- polarized (right) light of a JGG ultramylonite. Field of view is 4 mm. (A) Compositional banding between more quartz-rich bands and darker band. Below the garnet porphyroclasts is a curtain fold (Passchier and Trouw, 2005). (B) Sheath fold which has rolled over itself.

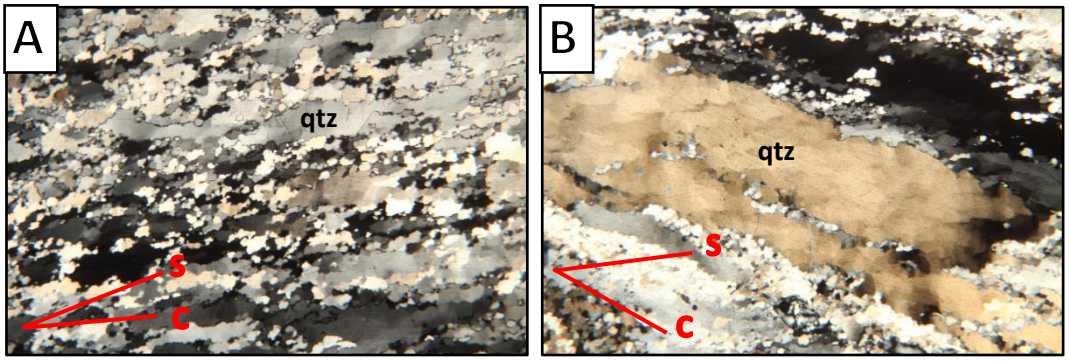

Figure 6 – Photomicrographs in cross-polarized light of a mylonitized quartzite from the JGG. Field of view is 4 mm. Grain preferred orientations indicate a dextral shear.

Garnetiferous Quartz Schist (JGgqs)

Southeast of and overlying the garnetiferous graphitic phyllite is a medium- to coarse-grained muscovite, garnet, quartz schist that contains occasional quartz veinlets and graphitic layers. Garnets range from < 1 to 4 mm in diameter. Locally the schist has a strong S-C fabric where there is abundant muscovite (Fig. 7). In fresh exposures of the JGgqs it appears gray to tannish brown, but is typically iron stained to a more reddish hue. It weathers to a tannish orange soil with plentiful muscovite and garnet. Phyllonites are present in volumes of rock where areas of higher discrete shear have affected the unit. Lenses of muscovite schist are commonly contained within more phyllitic sections and form symmetrical or dextral lenses (Fig. 6). Post- and pre- or syn-metamorphic quartz veins are present, with the post-metamorphic veins being distinguished by a lack of a metamorphic fabric and dextral folding. The JGgqs appears to be in fault contact with the Waresville Schist near the intersection of Louina Street and CR-861 where amphibolite was observed on the south side of Louina Street. The Katy Creek fault was interpreted to lie between outcroppings of the JGgqs and Waresville Schist in areas with no exposure.

Between the JGgqs and JGscp in one location (33.10045°, 85.49090°) is a distinct dark grey to black unit ~8 m thick that contains numerous orthoclase porphyroclasts up to 2 cm in size with carlsbad twinning (Fig. 8). In hand sample it is a homogenously gray with foliation defined by quartz ribbons and stretched white feldspar porphyroclasts. A strong S-C fabric is defined by asymmetric biotite drapes surrounding sigma-type

Figure 7 - A pod of muscovite schist with a strong S-C fabric inside a phyllite. From the garnetiferous quartz schist on CR-143 just south of CR-53 (33.10422°, 85.49171°W).

porphyroclasts. In thin section the primary foliation is defined by muscovite, biotite, and a crystal-preferred orientation. The large orthoclase grains that are conspicuous in hand sample can be seen in thin section to have grown around and included other minerals in two distinct orientations. It is possible that the inclusion trails are evidence of an earlier relic fabric, but different clasts contain trails in different orientations and so they are interpreted as being preferentially aligned along the feldspars crystal lattice. The mantles of some feldspar clasts are interlobate and suggest core-mantle rotational crystallization. Allanite is observed throughout the sample, some as large as 2 mm and zoned (Fig. 8B). Large euhedral crystals of allanite contrast with the finer grained ones which are a product of regional metamorphism. Additionally, the later partial alteration to epidote indicates that they likely formed prior to metamorphism. The protolith which contained them was likely a granite or a rhyolite. Quartz is strongly undulose and fills the spaces between plagioclase and micas. Rare garnet and staurolite are present. The feldspathic two-mica schist crops out as fins almost a meter high in relief within the bed of Caty Creek ~50 meters to the east of CR-143.

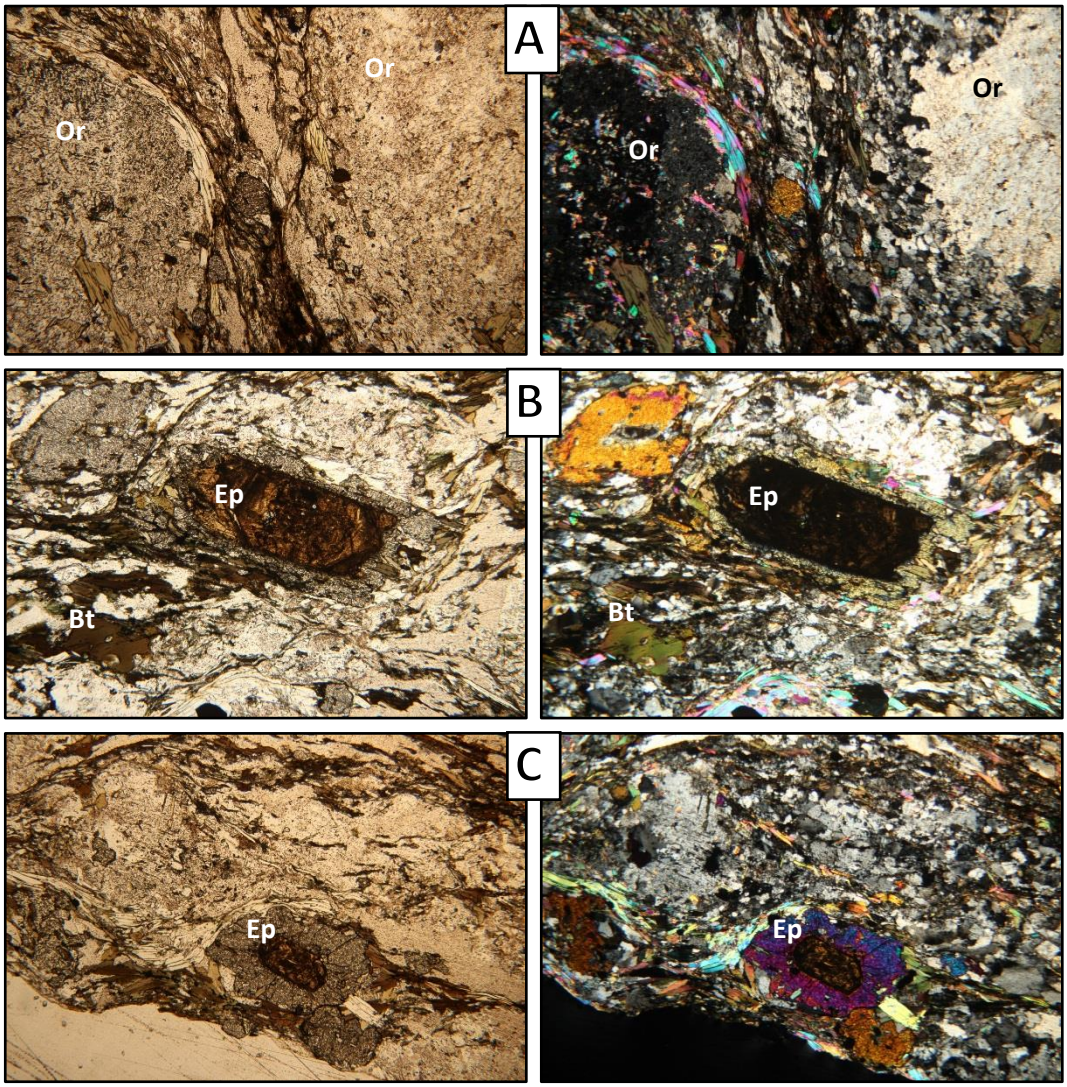

Figure 8 - Photomicrographs of feldspathic two-mica schist of the Jacksons Gap Group, sample 5.2B in both plane (left) and crossed (right) polarized light. Field of view is 4 mm. (A) Two orthoclase porphyroblasts with faint Carlsbad twinning in the left crystal. (B) Large zoned allanite crystal with epidote alteration rim. (C) Unzoned allanite with a corona of epidote.

Sericite-Chlorite Phyllite (JGscp)

The tectonostratigraphically highest member of the Jacksons Gap Group, a fine- to medium-grained sericite, quartz, chlorite phyllite, is only found in the western half of the Milltown Quadrangle. The unit is locally graphitic and garnetiferous, and on dirt roads where the ground has been scraped it appears as an almost completely white saprolite. Dextral curtain folds are common with amplitudes up to 30 cm, and are defined by layers that contain mostly sericite. The sericite-chlorite phyllite appears to either pinch out or become truncated by the Katy Creek fault, as all outcrops of the Jacksons Gap Group northeast of CR-143 are garnetiferous schists or amphibolites of the Dadeville Complex.

Dadeville Complex

The Dadeville Complex is separated from the Jacksons Gap Group by the Katy Creek fault. The Dadeville Complex is an allochthonous terrane composed of mainly metavolcanic and metaplutonic rocks, with subordinate metasiliciclastics (VanDervoort, 2016; Harstad, 2017). The primary lithologies are the Waresville Schist and the Rock Mills Granite Gneiss, the latter of which intruded the Waresville prior to the peak of metamorphism. Multiple episodes of overprinting deformation have led to a complex interfingering of the two units.

Waresville Schist (ldws)

The Waresville Schist is a compositionally banded to massive amphibolite, interlayered with fine- to medium-grained tonalitic schist. It is highly sheared with

foliation defined by hornblende, commonly with a distinctive submillimeter thick continuous cleavage. In areas where the Waresville Schist is deeply weathered the only evidence of its presence is dark red soil and relic black hornblende that collects in surface depressions and ditches. Large portions have been mostly or entirely weathered to a very light-weight, orange- to brick-red, clay-rich rock that is colloquially called a brickbat (Fig. 15) (M.G. Steltenpohl, personal communication). Areas that have been altered to brickbat are also associated with fractures filled with an amorphous black mineral that has been identified by X-ray powder diffraction as lithiophorite, an aluminum, lithium, manganese oxide. Centimeter-scale thick tonalitic schists are commonly interlayered with amphibolite and are readily apparent as white-to-tan colored bands. Sporadically the tonalitic schists may cover large areas where they appear as sericitic quartz schist and feldspathic muscovite schist. Basaltic lavas are likely the protolith of hornblende-rich amphibolite, and volcanoclastic rocks or tonalitic ash deposits or lavas the protolith to the tonalitic schist.

The most common lithology within the Waresville Schist is a massive amphibolite (Fig. 10A) which is black to dark green with millimeter-sized white flecks of plagioclase, giving it a salt-and-pepper appearance. Foliation is defined by a preferred orientation of hornblende crystals and commonly a subtle submillimeter layering of amphibole and plagioclase that, where weathered, breaks off in thin millimeter to submillimeter thick sheets. These massive amphibolites are interpreted as metamorphosed basaltic lava flows. Less commonly there is compositional banding up to a centimeter thick with dark bands rich in amphiboles and lighter bands dominated by plagioclase and epidote. An

example of this can be found west of the intersection of county roads 155 and 158 (33.064799°, 85.44175040°W). These latter units are interpreted as more mafic volcanics interlayered with felsic ashes.

Small scale outcrops of metagabbro appear within the more massive amphibolite (Fig. 9). Typically less weathered than the surrounding rock, it is composed of dark green amphibole surrounded by fine white plagioclase feldspar. In thin section the amphiboles are poikiloblastic hornblende grains which are agglomerated into asymmetric delta and sigmoidal structures (Fig. 14B). These are interpreted as evidence of recrystallization after shearing or of pseudomorphic replacement of pyroxene, because the interlocking blades of hornblende and the random orientation of inclusions appear to have grown in place. Between the hornblende porphyroblasts is primarily plagioclase with some quartz and minor amounts of epidote, rutile and actinolite.

Over a strike length of ~ 4 km in the east-central portion of the quadrangle, the Waresville Schist contains a distinctive brownish red rock that contains > 80% of interlocked submillimeter-sized red garnets in a quartz matrix (Figs. 11 and 17). Its extent was large enough that it was broken out as the Waresville Schist Garnetite (ldwsg; Fig. 9). In outcrop, the garnetite has the appearance of a rusty red quartzite, with the garnets not readily distinguished unless a sample is cut. In contrast, an outcrop along CR-232 (33.045627°, 85.392892°W) contained a lens several meters in length of very coarse quartzite (> 2 mm grains) with bands of garnet greater than 10 mm thick. In thin section the majority of garnet porphyroblasts contain spiraled inclusion trails of

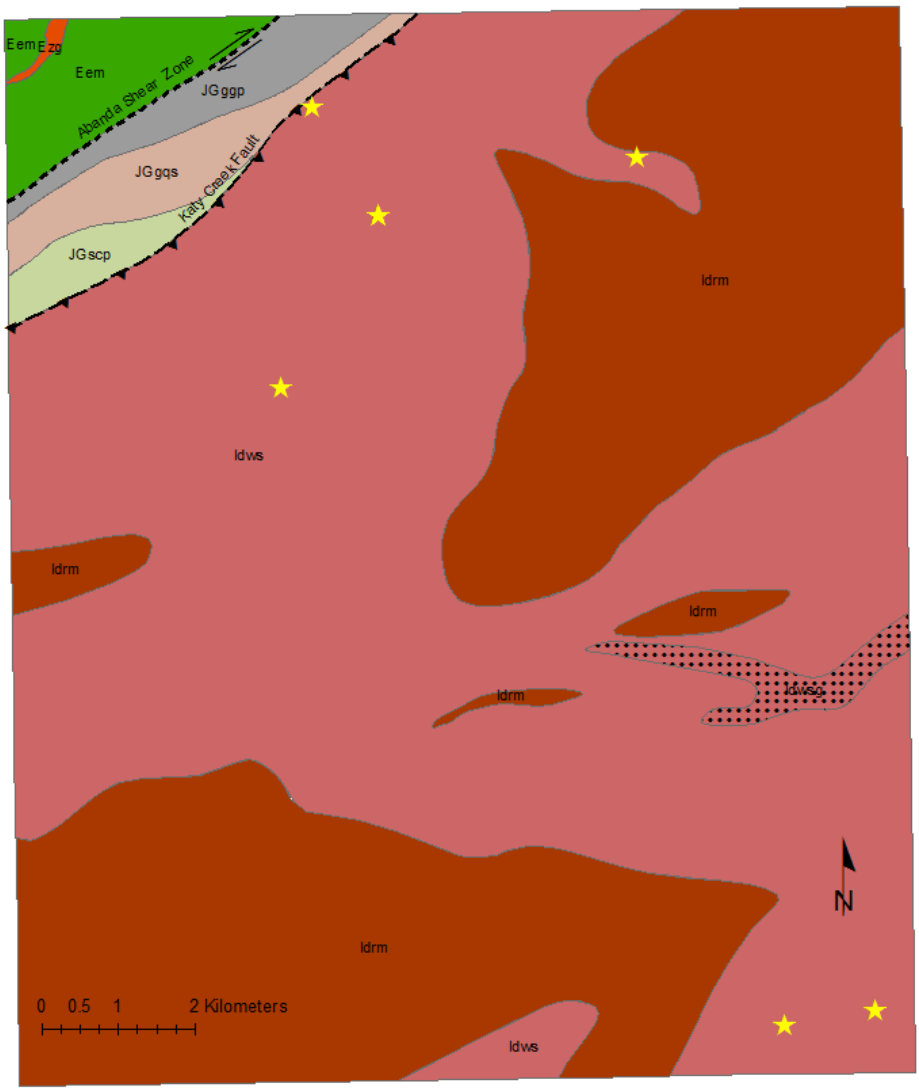

Figure 9 – Geologic map of the Milltown Quadrangle showing locations of the stations where metagabbro was identified.

quartz and opaque minerals. Garnet growth occurred during the formation of the D_2 fabric, which rotated garnets in relation to the fabric as growth continued, forming the spiral pattern of inclusions. Garnetite shows compositional banding, with ~1 mm garnet porphyroblasts in bands up to 5 mm thick and separated by bands of predominantly quartz. The garnet bands commonly contain rutile. Weathering has caused a significant amount of replacement of rutile, likely by goethite, to varying degrees, with many smaller crystals having been entirely replaced. Quartz crystals are mostly uniform in size (~ 1 mm), and through grain boundary area reduction have straight grain boundaries that come together in triple points. In bands containing garnets, quartz crystals are variable in size, commonly down to 0.1 mm. Some samples have a minor <<1% modal abundance of hornblende which is partially altered to an unidentified mineral.

Adjacent to where garnetite was found, a single outcrop, 1 meter across, of folded magnetite quartzite was observed (33.042274°, 85.402890°W) (Fig. 12). Fresh samples appear as a very clean white quartzite, black magnetite, and rare muscovite. In thin section, quartz is inequigranular interlobate with mild undulose extinction, large polycrystalline grains range from 1 to 5 mm, and smaller grains are on average 0.5 mm. Quartz crystals have a grain shape preferred orientation indicating a dextral shear sense. Grains of magnetite are on average 0.5 mm and disseminated throughout the sample but occur predominantly in bands 5 to 15 mm thick. These bands of concentrated magnetite contain crystals up to 2 mm across and have a strong attraction to a magnet. Most magnetite crystals are euhedral with minor weathered rims, however some have been entirely weathered away.

The garnetite and banded magnetite quartzite are contained within the amphibolites of the Waresville Schist, locally interlayered on the scale of centimeters. Brown (1982) reports similar lithologies within the Ropes Creek amphibolite and interpreted them as the result of a volcanogenic exhalative-sedimentary processes involving metalliferous brines.

A grayish amphibole quartzite interbedded with sericite schist was found along CR-237 in the western part of the study area (33.080243°, 85.48969714°W). In thin section (Fig. 16) it was found to be a fine grained a muscovite-amphibole quartzite, with an almost uniform crystal size of 0.5 mm. Foliation is defined by a grain preferred orientation of amphibole. Quartz is dynamically recrystallized with an oblique dextral foliation defining the s-plane. There is distinct compositional banding, typically 1.5 mm thick, of amphibole, fine grained quartz, and muscovite alternating with quartz ribbons. The quartz ribbons are composed of ~ 0.3 mm interlobate equigranular grains, indicating a bulging recrystallization. In some areas where muscovite is more abundant a c-prime fabric is variably developed (Fig. 16A). The majority of amphiboles are hornblende with less than 5% of actinolite observed.

On CR-258 (33.04393°, 85.4033212°W) is an outcrop of highly weathered amphibolite that is largely composed of translucent bladed crystals up to 5 mm long, and located between more competent layers of the common salt-and-pepper amphibolite. In thin section it is composed of hornblende, an unidentified green amphibole, plagioclase, and anthophyllite-gedrite, all preferentially aligned to form the primary foliation (Fig. 13). Hornblende is euhedral with a strong 60°/120° cleavage, and

are on average 1.5 mm long. A second unidentified amphibole presents prisms up to 2.5 mm long with a strong 60°/120° cleavage but no pleochroism and a significantly lower birefringence than the hornblende. Throughout the sample are large prismatic blades of an orthoamphibole, of the anthophyllite-gedrite series, up to 14 mm long (Fig. 13B). Plagioclase crystals are typically less than 1 mm between the large amphibole grains and is difficult to distinguish from quartz unless twinning is present.

The heavily weathered byproduct of amphibolite, brickbat (Fig. 15), is more common in outcrop than fresh amphibolite. It does not appear to be the byproduct of a different lithology as it is distributed evenly throughout all areas in which amphibolite is found. The brickbat is orange- to brick-red and feels unusually light weight in hand sample. In thin section (Fig. 15) it is primarily composed of various reddish weathering products with the outlines of relic bladed crystals not uncommon. Relic crystal habit and size are similar to that observed in other amphibolites of the Waresville Schist, and was likely identical to it before being altered by fluids.

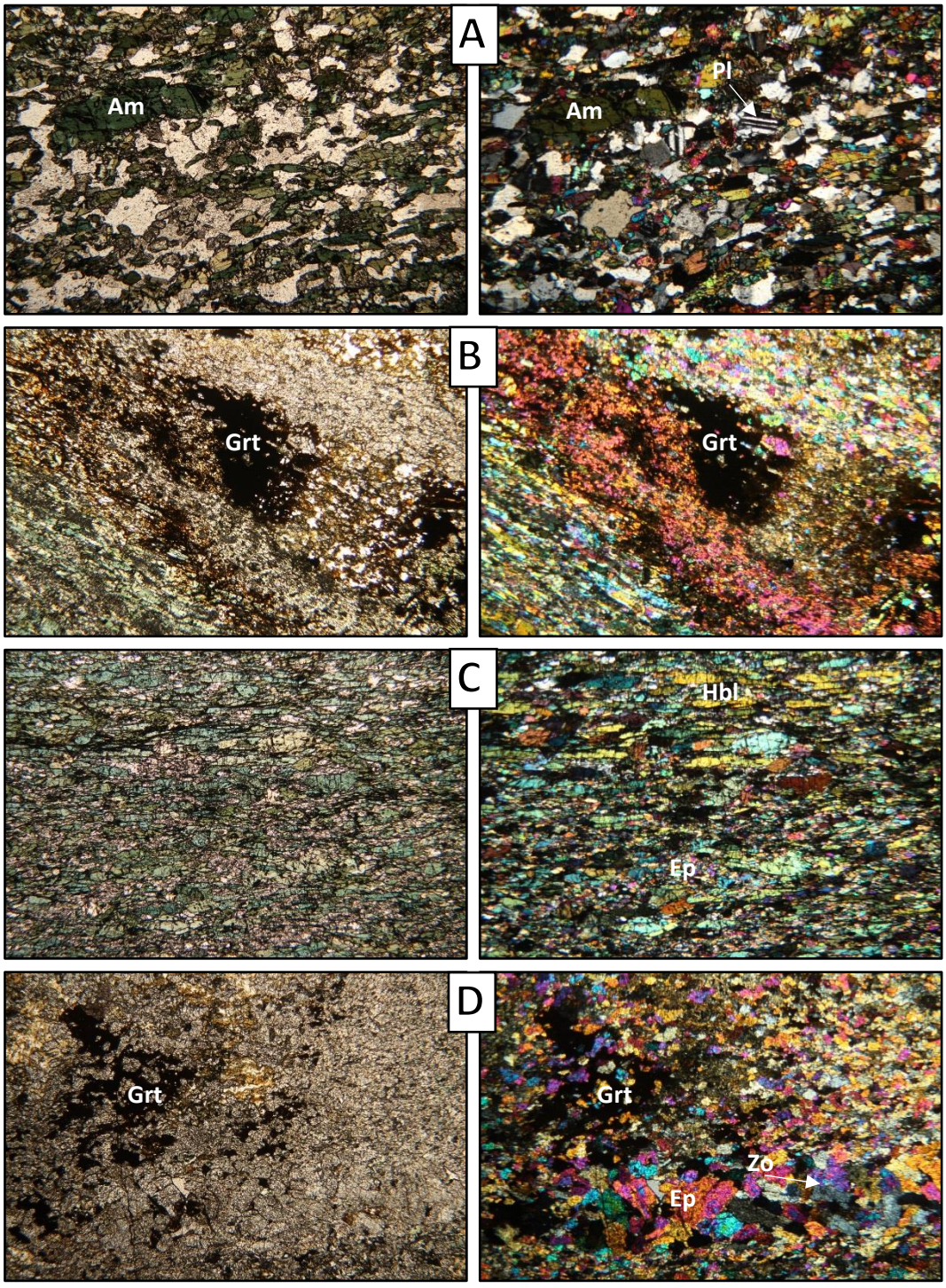

Figure 10 – Photomicrographs in plane (left) and crossed polarized (right) light of massive and compositionally banded amphibolite. Field of view is 4 mm. (A) Typical massive amphibolite with salt and pepper texture. (B) Opaque and epidote between amphibole and epidote bands. (C) Hornblende and epidote from a compositionally banded amphibolite. (D) Sample 10.3B: Skeletal opaque from a lighter band of amphibolite surrounded by epidote and zoisite.

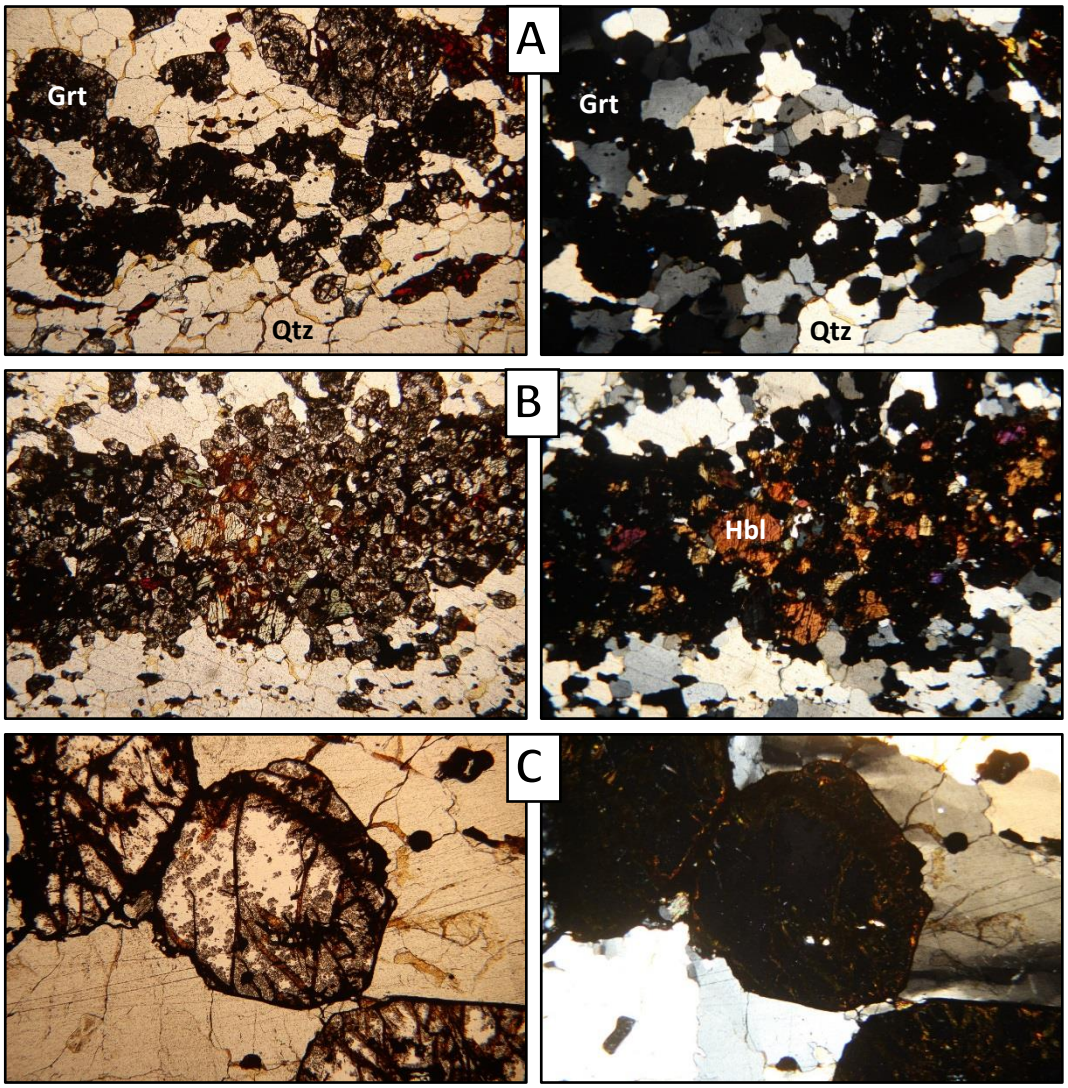

Figure 11 – Photomicrographs in plane (left) and cross-polarized (right) light of garnetite. Field of view is 4 mm. (A) typical garnetite with submillimeter garnets surrounded by quartz. (B) Rare hornblende clustered with submillimeter garnets. (C) Rare 2 mm garnets with undulose quartz.

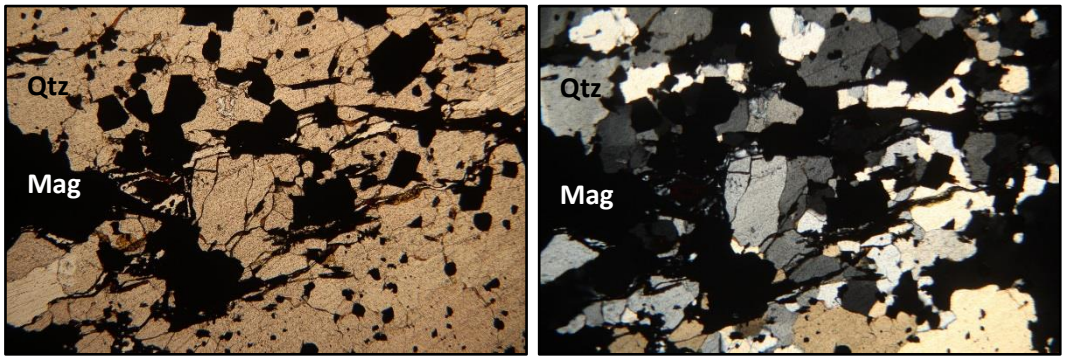

Figure 12 – Photomicrograph in plane (left) and cross-polarized (right) light of a banded magnetite quartzite. Field of view is 4 mm.

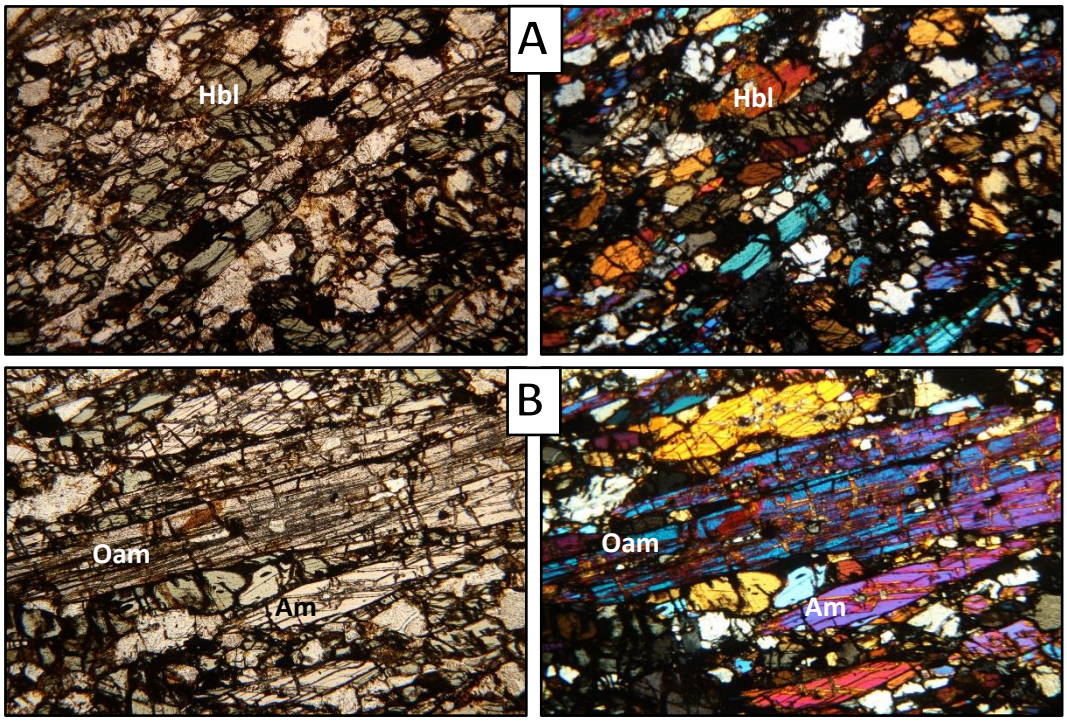

Figure 13 – Photomicrographs in plane (left) and cross-polarized (right) light of a hornblende-epidote schist. Field of view is 4 mm. (A) Pleochroic green hornblende and clear epidote crystals with a grain preferred orientation. (B) Example of a large bladed anthophyllite-gedrite crystals and the non-pleochroic amphibole.

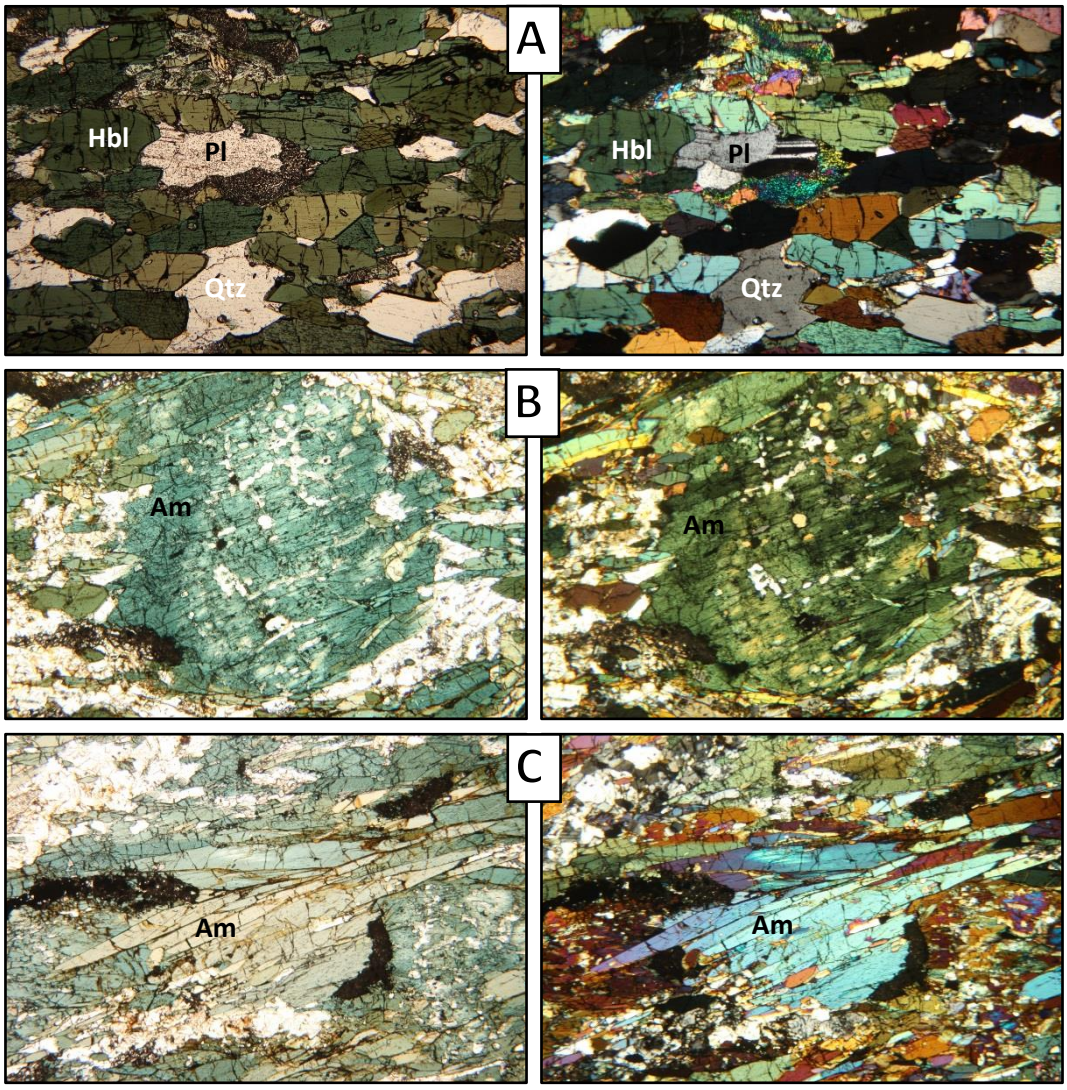

Figure 14 – Photomicrographs of metagabbro in plane (left) and cross-polarized (right) light. Field of view is 4 mm. (A) Typical section of coarse grained metagabbro. Plagioclase shows simplectic alteration to epidote and quartz. (B) Amphibole pseudomorphically replacing primary pyroxene. (C) Amphibole crystals with a grain preferred orientation.

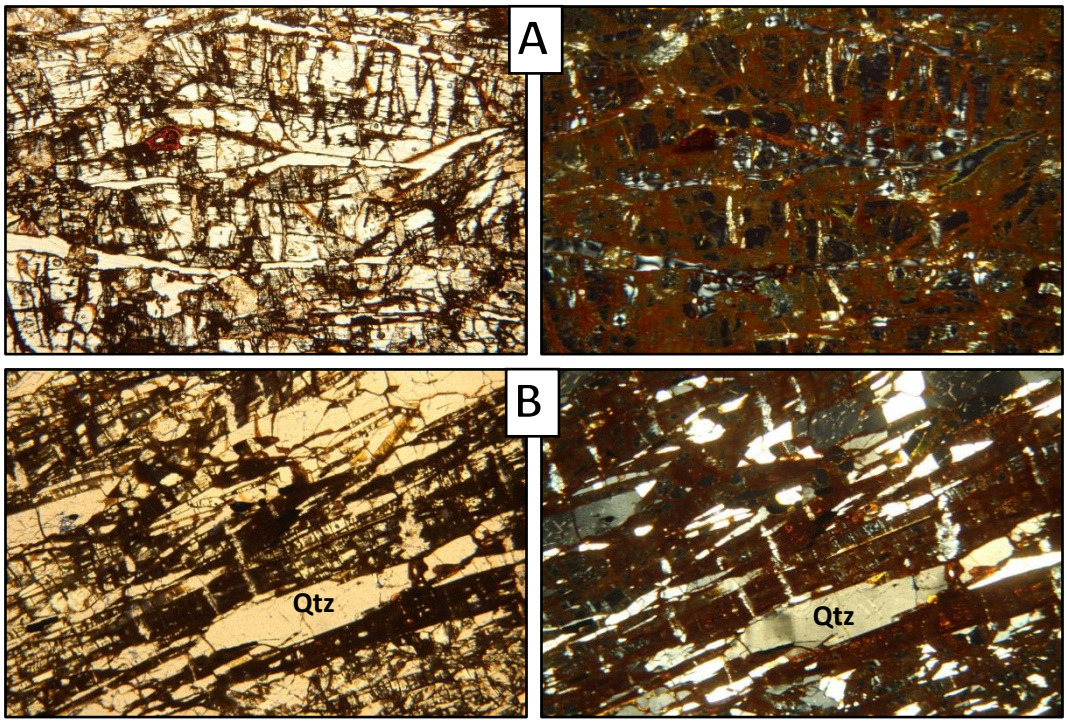

Figure 15 – Photomicrographs in plane (left) and cross-polarized (right) light of brickbat. Two samples from different locations show almost identical reddish alteration products and quartz pseudomorphs developed after amphibole. Field of view is 4 mm.

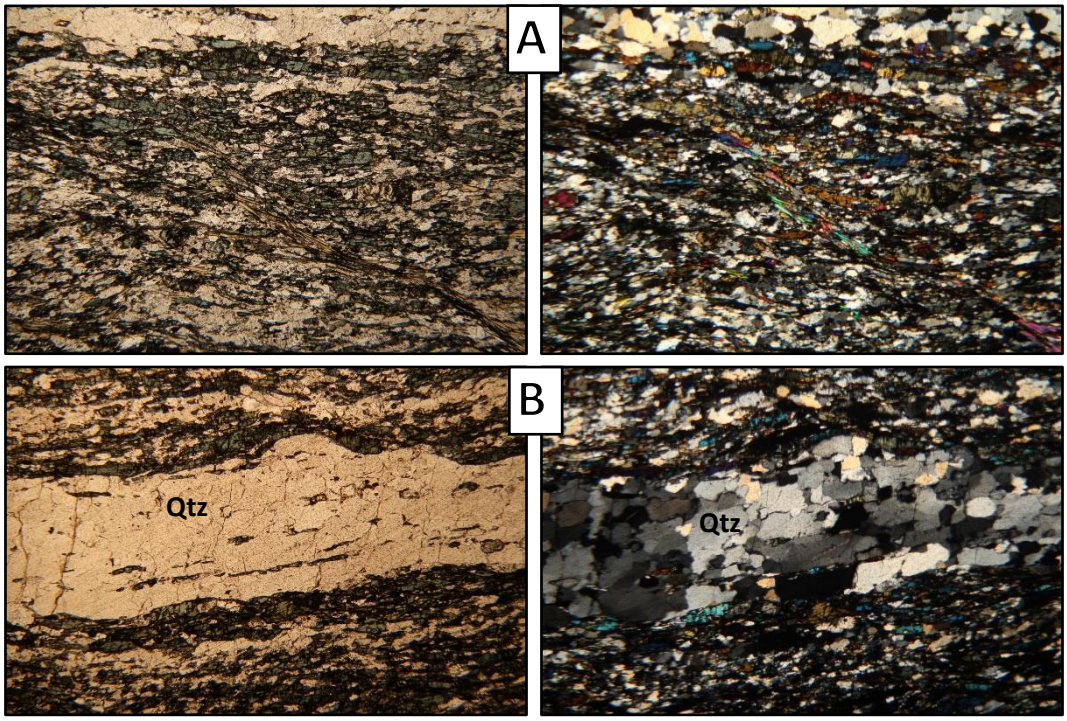

Figure 16 – Photomicrographs of amphibole quartzite (60.1B) in plane (left) and cross-polarized (right) light. Field of view is 4 mm. (A) Fine grained amphibole and quartz with muscovite defining a c-prime fabric. (B) Ribbon of quartz which has been dynamically recrystallized and indicates a dextral shear sense.

Figure 17 - Cut and polished slab sample (65.3B) of garnetite from the Waresville Schist. It typically appears as a nearly uniform massive reddish brown rock, as in the top left part of this sample.

Rock Mills Granite Gneiss (ldrm)

The Rock Mills Granite Gneiss is a medium- to coarse-grained biotite, muscovite, alkali-feldspar gneiss that locally contains garnet, tourmaline, and rare fluorite. Millimeter to submillimeter crystals of a dark ferrous mineral are commonly found throughout and concentrated along foliation planes. Foliation is weakly defined by streaky elongated biotite and quartz ribbons (Fig. 18). The unit weathers to a reddish tan saprolite with hard-cored spheroidal boulders remaining. Remnant mica in the saprolite commonly preserves the foliation, allowing for measurement of strike and dip. A large area of Rock Mills is exposed as pavement just south of the town of Milltown, to the east of AL-77 (33.026233°, 85.483296°W). This area has been quarried in the past on a small scale and is readily visible in aerial imagery. Locally, pods of muscovite schist are found as xenoliths within outcrops of Rock Mills saprolite, particularly along the contact with the Waresville Schist.

In thin section the Rock Mills Granite Gneiss is found to contain ~ 85% feldspar, predominantly orthoclase and microcline with a smaller proportion of plagioclase. There are usually lobate grain boundaries between the potassic feldspars and surrounding quartz, whereas boundaries between orthoclase and microcline are often indistinct. Deformation twinning makes it difficult to distinguish the potassic feldspars. Tapered albite twins and plastic bends of twin planes indicate that the latest deformation occurred at low-medium temperatures of 400-500°C (Passchier and Trouw, 2005). Orthoclase contains albite exsolution and perthitic texture. Using the Michel-Levy

method, plagioclase was measured to have an average anorthite content of ~17 making it predominantly oligoclase, and commonly has antiperthetic texture.

Following feldspar, quartz is the next most common mineral, making up ~13% of the rock based on a visual estimate. It forms polycrystalline aggregates 4 mm and larger in diameter, which are in turn composed of individual submillimeter inequigranular seriate-interlobate grains. Quartz commonly has undulose extinction, bulging grain boundaries indicating migration recrystallization, and linear arrangements of inclusions. Biotite makes up ~ 1 % of the sample and is almost entirely submillimeter, occurring preferentially along individual foliation planes. A significant percentage of biotite has been altered to white mica and chlorite. Disseminated throughout the rock are crystals of magnetite from 0.5 to 1 mm in diameter; isolated entrained magnetite crystals are up to 5 mm in diameter. There is evidence of fluid alteration where feldspars have been altered to sericite along fractures, and one sample contained isolated submillimeter euhedral apatite crystals along and within fracture zones.

Figure 18 - Rock Mills Granite Gneiss exposed as a pavement along AL-77. Abandoned quarry is visible on the right hand side of the photo. Inset photo of a foliation plane of the Rock Mills Granite Gneiss showing mineral elongation and streaky quartz and biotite lineations. Pencil is 14 cm in length.

Table 1. Summary of deformational events in the Milltown quadrangle

Deformational Phases	Structural Elements	Description
D_1	M_1	Regional prograde dynamothermal metamorphism of the eastern Blue Ridge, Jacksons Gap Group, and Dadeville Complex
	S_1	Regional foliation (schistosity and gneissosity) early movement along the Brevard fault zone
		Syn- to late-peak metamorphic Katy Creek fault movement
	L_1	Elongation lineation within mylontized units
D_2	M_2	Retrogressive reactivation of the Katy Creek fault
		Early movement along the Abanda and Alexander City faults
	F_2	Isoclinal, intrafolial folding of $S_{0/1}$
		Late-F_2 folding of the Tallassee and Penton synforms
	S_2	Local transposition of S_1 into S_2 in the Jacksons Gap Group, Composite S-C mylonitic fabric indicating oblique dextral-normal movement
D_3	M_3	Upper greenschist-facies reactivation of the Abanda fault
	F_3	Asymmetric folds associated with movement along the Abanda fault
	S_3	Composite S-C mylonitic fabric indicating oblique dextral-normal movement along the Abanda fault

METAMORPHISM

The Milltown Quadrangle contains rocks that make up the core of the crystalline Appalachians in Alabama, which have experienced several periods of metamorphism and deformation (Table 1). The oldest identifiable metamorphic event, M_1, is a regional event that affected the entire eastern Blue Ridge, Jacksons Gap Group, and the Dadeville Complex (Fig. 19). This amphibolite facies event produced the S_1 primary regional foliation. The second metamorphic event, M_2, is a retrogressive reactivation of the Katy Creek fault and the early stages of movement along the Abanda and Alexander City faults. S-C mylonization of the Jacksons Gap Group units, isoclinal folding in eastern Blue Ridge units, and the generation of the Tallassee and Penton synforms was also associated with the M_2 event. The final metamorphic episode, M_3, resulted in upper greenschist-facies reactivation of the Abanda fault with associated asymmetric folding and a dextral-normal composite S-C fabric development.

Eastern Blue Ridge

The Emuckfaw Group within the Milltown Quadrangle is mostly limited to rocks of pelitic compositions, containing predominantly muscovite + quartz + garnet (Fig. 19). Workers in adjacent quadrangles (VanDervoort, 2015; Harstad, 2016) report the presence of amphibolite in the Emuckfaw Group, but no amphibolites were found within the Emuckfaw Group in the current investigation. Metamorphosed granites typically do not supply assemblages that are diagnostic of metamorphic conditions. Nonetheless, the S_1 foliation of the Zana Granite Gneiss parallels that observed in the

amphibolite-facies country rock surrounding it, indicating that the unit experienced the same M_1 event. Additionally, the Zana Granite contains tapered albite twins, undulose extinction in quartz, and dynamic recrystallization of quartz and feldspar indicating that following S_1 strains it experienced lower amphibolite-facies conditions (Passchier and Trouw, 2005). Fractures crosscutting retrograded minerals allowed fluid to alter feldspar to sericite, likely representing D_3 deformation.

Jacksons Gap Group

The Jacksons Gap Group within the Milltown Quadrangle contains mainly metapelites, primarily as muscovite and sericite schists and phyllites with variably quartzose, graphitic, and garnetiferous members. Prograde mineral assemblages include muscovite + garnet + orthoclase + epidote + quartz, suggestive of upper greenschist-facies to lower amphibolite-facies peak M_1 metamorphic conditions (Fig. 19). These were in turn retrograded to lower-to-middle greenschist-facies mineral assemblages containing chlorite + chloritoid + sericite. M_1 minerals, including biotite are replaced by chlorite, and muscovite replaced with sericite. M_2 chloritoid occurs as euhedral and undeformed porphyroblasts. The Jacksons Gap Group within the Milltown and Wadley South quadrangles have no identifiable sedimentary structures and contain evidence of significant hydrothermal alteration to sericite.

Dadeville Complex

Metasedimentary rocks of the Dadeville Complex in the Milltown Quadrangle are limited to metamorphosed volcanoclastic rocks, which have a prograde mineral

assemblage of hornblende + actinolite + muscovite + quartz. Within the study area these are exclusively found within the Waresville Schist as either discrete layers or boudins.

Mafic rocks are common within the Dadeville Complex as foliated amphibolites of the Waresville Schist derived from basalt and gabbro. They typically have a prograde mineral assemblage of hornblende ± muscovite ± epidote ± garnet, which is indicative of lower to middle amphibolite-facies conditions (Fig. 19). Metagabbro appears in meter scale outcrops (Fig. 9) with a prograde mineral assembly of hornblende + actinolite + zoisite + plagioclase ± biotite. Retrograde mineral assemblages are typically white mica alteration of plagioclase, hornblende to chlorite, and garnet to ilmenite.

Garnetite (Fig. 11) and banded magnetite quartzite (Fig. 12) are primarily composed of quartz and interpreted as being derived from exhalatives deposited by hydrothermal fluids onto the bed of a body of water. Garnetite has a prograde mineral assemblage of garnet + quartz + rutile ± hornblende + opaques, which is compatible with amphibolite facies conditions. Garnets contain helicitic inclusion trails and are weathered to goethite. Hornblende is altered to actinolite likely during D_3 greenschist facies retrogression.

The Rock Mills Granite Gneiss contains primarily alkali feldspar and quartz with generally minor amounts of plagioclase and biotite. As such it does not preserve a diagnostic prograde mineral assemblage. However, a fine mantle of feldspar is preserved around larger feldspar grains, which indicates a temperature of 450°-600° C

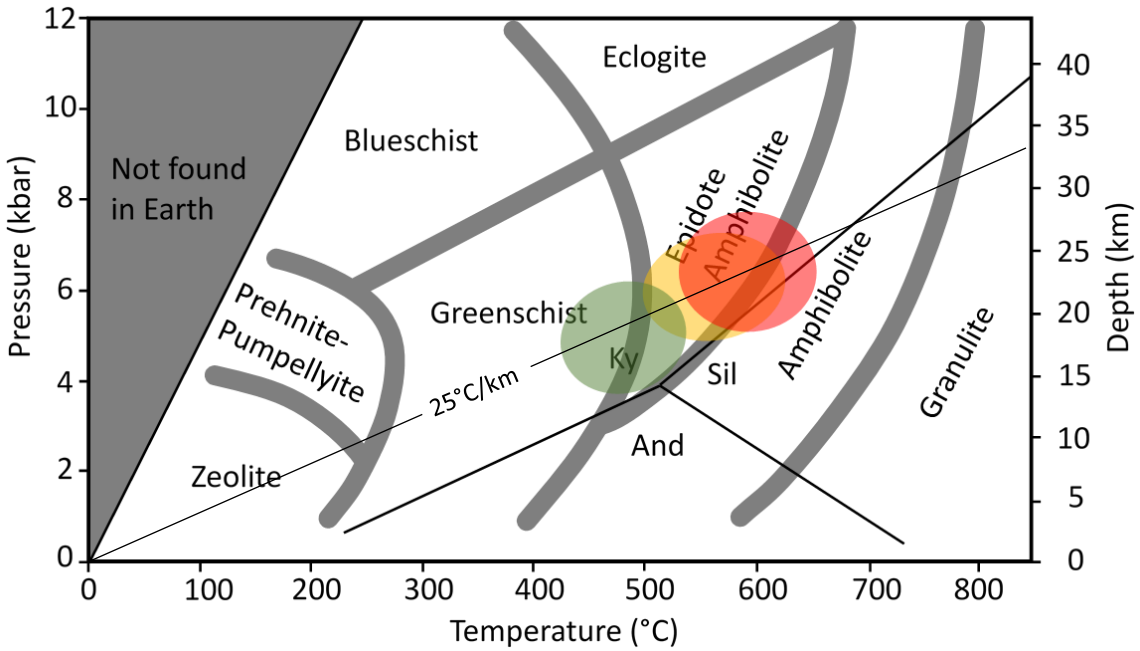

Figure 19 - Peak metamorphic conditions for the eastern Blue Ridge (yellow), Jacksons Gap Group (green), and Dadeville Complex (red). Figure adapted from Nesse (2012) and Spear (1993).

(Passchier and Trouw, 2005). It also contains retrograde greenschist-facies alteration of feldspar to muscovite and epidote minerals as well as biotite to chlorite.

The Dadeville Complex contains prograde assemblages which are indicative of lower to middle amphibolite-facies metamorphic conditions before being retrograded to greenschist-facies. This mirrors the findings of Johnson (1988), Steltenpohl et al. (1990), Reed (1994), Sterling (2006), Abrahams (2014), Singleton and Steltenpohl (2014), Poole (2015), VanDervoort (2016), and Harstad (2017).

STRUCTURE

The Milltown Quadrangle contains the rocks of three fault separated terranes, each of which has experienced a complex deformational history. Structural analysis was performed by gathering measurements of primary metamorphic foliation, S-C fabrics, mineral and elongation lineations, and fold hinge measurements. Together, there is evidence for at least three periods of deformation, D_1 through D_3 (Table 1). The dominant regional foliation, S_1, is associated with peak metamorphic conditions (lower- to middle-amphibolite facies) and is defined by lattice- and dimensional-preferred orientation of phyllosilicate and inequant minerals. S_1 is interpreted as having formed due to Acadian-Neoacadian thrusting and metamorphism (Hatcher, 1987; Steltenpohl et al., 2013). Given late and post-metamorphic faults separate the Jacksons Gap Group from the eastern Blue Ridge and the Dadeville Complex, structural analysis requires the study area to be divided into three subareas, (I) the eastern Blue Ridge, (II) the Jacksons Gap Group/Brevard fault zone, and (III) the Dadeville Complex. Below, each subarea is

described and then followed by a discussion of differences and similarities between them.

Subarea I: Eastern Blue Ridge

The eastern Blue Ridge makes up only a small fraction of the study area in the northwestern corner. The primary S_1 foliation is defined by muscovite sheets and a grain preferred orientation of quartz and opaque minerals. Garnets commonly are surrounded by drapes of muscovite forming sigma clasts which define a secondary fabric. From figure 20A it can be seen that poles to S_1 have a mean strike and dip ofN42°E, 66°S. There is a weak pi-girdle at N39°W, 74°S indicating a post-S_1 fold with an axis of N51°E, 14°. Figure 20B indicates that shear zone movements were mostly right-slip with a minor normal-slip component.

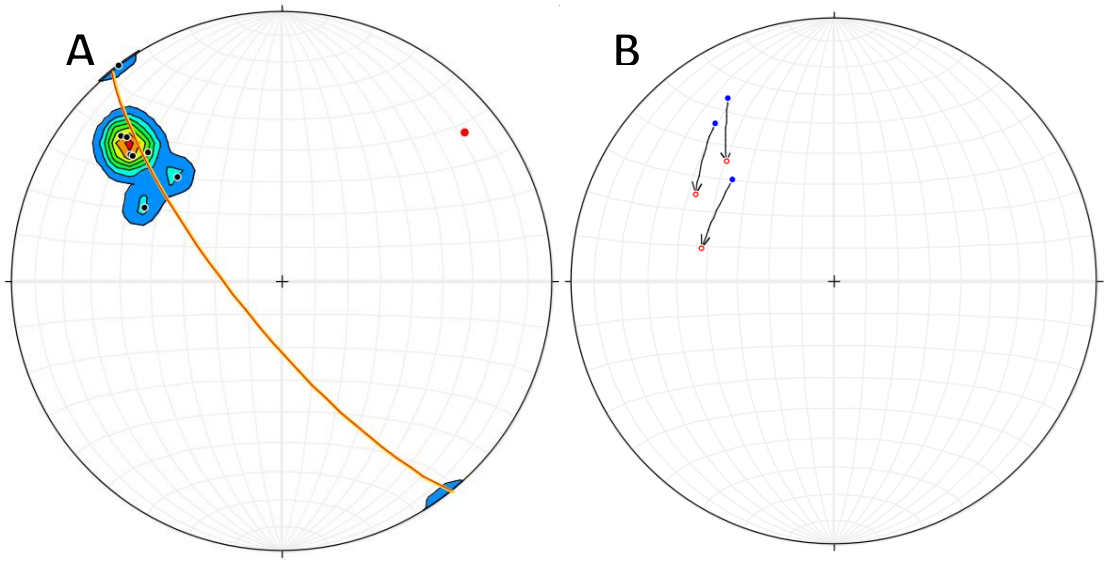

Figure 20 – Subarea I: Lower hemisphere equal-area stereoplots of S_1 foliation from the eastern Blue Ridge. (A) Poles-to-plane of foliation n = 8 with 1% contour intervals. The red line is the cylindrical best fit of the poles-to-plane data which gives an S_2 fold-axis of N51°E, 14°. (B) Poles to C-planes are unornamented end of arrows (blue dots) and poles to S-planes are the tip of the arrows (red circles). N = 3.

Subarea II: Brevard fault zone /Jacksons Gap Group

The Jacksons Gap Group are the lithologies that lie between the Abanda and Katy Creek faults. The primary S_1 foliation of the Jacksons Gap Group is defined by alignment of muscovite and sericite, and by compositional layering. Isoclinal folds are common and their axial surfaces parallel S_1. A strong point maximum of S_1 poles is shown in figure 21A indicating the average strike and dip is N53°E, 57°S. The associated mineral lineation and mineral stretching lineations (L_1) plunge shallowly (~25°) to the southwest, and are defined by a grain shape preferred orientation of inequant grains.

An ultramylonite zone exposed CR-856 (33.119864°, 85.4683124°W) formed through extreme plastic shearing of the Waresville Schist and is interpreted to be associated with movement along the Abanda fault. The exposed thickness of the ultramylonite zone is at least 25 centimeters (Fig. 4) and it contains finely-recrystallized quartz and numerous sheath folds of the ultramylonitic foliation with amplitudes of 1-6 centimeters (Fig. 5). The attitude of the ultramylonite zone is N55°E, 72°N. The dip direction of the ultramylonite foliation likely does not reflect that of the original fault plane, however, as rocks both above and below it dip to the south, and outcrop-scale sheath folds are commonplace. To the south along CR-143 (33.0937561°, 85.4868129°W), rocks the Katy Creek fault were identified in a road cut where Jacksons Gap Group units crop out and are separated from crenulated amphibolite of the Waresville Schist by several tens of meters. No direct observations or measurements on fault rocks of the Katy Creek fault were collected. Figure 21B illustrates S-C plane data

measured from phyllonites of the Jacksons Gap Group and they indicate mainly right-slip with local oblique reverse-slip movements.

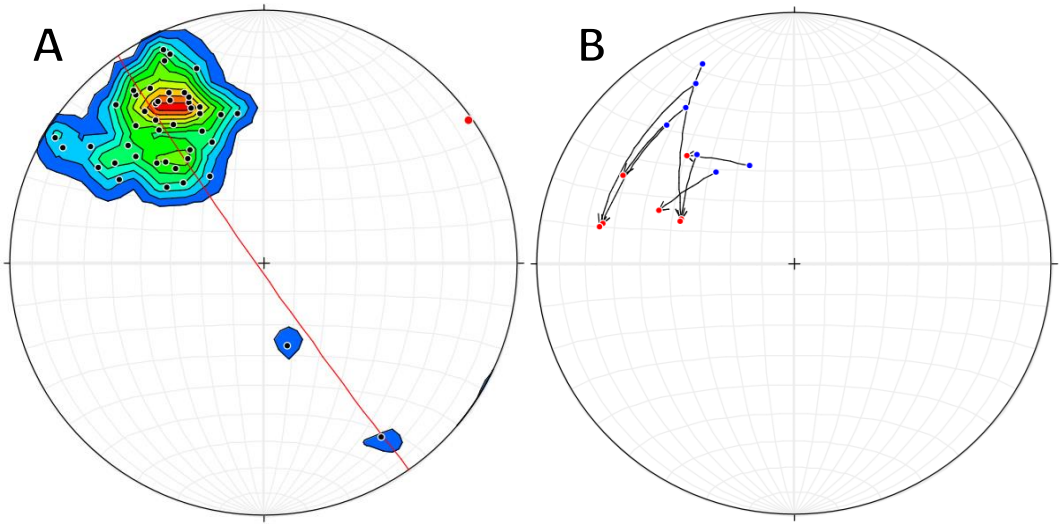

Figure 21 – Subarea II: Lower hemisphere equal-area stereoplots of S_1 foliation within the Jacksons Gap Group. (A) Poles-to-plane of foliation n = 45 with 1% contour, and mineral stretching lineations (green diamonds) n = 5. The red line is the cylindrical best fit of the weak pi girdle (N35°W, 88°S). The red circle is the fold-axis (N55°E, 2°). (B) Poles to C-planes are unornamented end of arrows (blue dots) and poles to S-planes are the tip of the arrows (red circles) n = 6.

Subarea III: Dadeville Complex

The Dadeville Complex as this terrane occupies ~85% of the area of the Milltown Quadrangle and the majority of measurements for subarea III were made in the Waresville Schist and the Rock Mills Gneiss. A total of 173 strike-and-dip measurements were made on S_1 and Figure 22A shows an amoeboidal point maximum indicating a mean strike and dip of N42°E, 24°SE.

A weak S-C fabric can be found locally within the Dadeville Complex which is associated with D_2 shearing (Fig. 22B). Retrograde mineral assemblages adorn the S-C

fabric indicate lower-amphibolite to upper-greenschist facies conditions. The shear sense indicates mostly right-slip and a slight oblique, reverse-slip component of movement along the Katy Creek fault.

Late stage, post-S_1, F_2 folding produced the open, regional scale (~40 km half-wavelength), shallow north-east plunging Tallassee synform that affects the entire Dadeville Complex. A smaller scale, but still large (~10 km half-wavelength), F_2 fold, the Penton synform, is identified in the Milltown Quadrangle and extending toward the northeast out of the area of the quadrangle (Plate 1 and Figure 2). The Penton synform trends N66°E and plunges 27° (Fig. 22C). The study area is on the northwestern limb of the Tallassee synform (Fig. 1). The Penton synform has a similar open style, and is also post-D_1, but trends somewhat oblique to the Tallassee synform, which has a trend and plunge of N40°E, 12° (Abrahams, 2014). The contact between the Dadeville Complex and the Brevard zone partly defines the western limb of the Penton synform, while the eastern limb is located ~10 km to the southeast (Fig. 2).

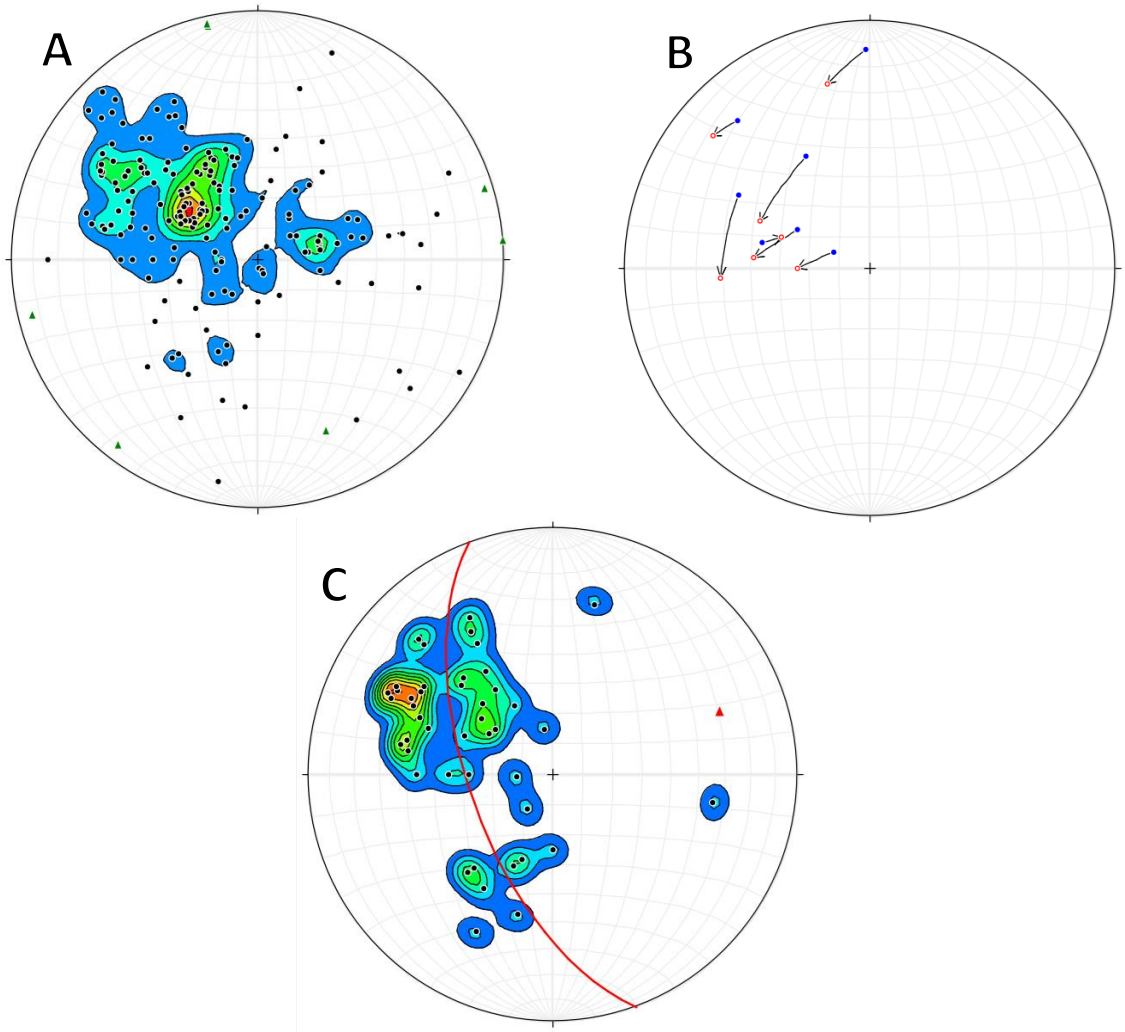

Figure 22 – Subarea III: Lower hemisphere equal-area stereoplots of S_1 foliation within the Dadeville Complex. (A) Poles-to-plane of foliation with 1% contouring. N = 173. (B) Poles-to C-planes are unornamented end of arrows (blue dots) and poles to S-planes are the tip of the arrows (red circles) n = 7. (C) Poles-to-plane of measurements in sub areas around the limbs of the Penton synform with 1% contouring. N = 44. The red great circle is the Pi circle and the red triangle the beta axis. The fold axis is 066°, 27°.

Discussion of Structural Analysis

Structural observations from rocks of the Milltown Quadrangle show evidence for at least three deformational events, D_1 through D_3 (Table 1). The effects of an M_1 metamorphic peak and the associated D_1 structures and fabrics are clearly manifest in each of the three terrane subareas: (I) the eastern Blue Ridge records lower- to middle-amphibolite facies; (II) the Jacksons Gap Group is upper-greenschist to lower-amphibolite facies; and (III) the Dadeville Complex is middle to upper amphibolite facies (Fig. 19). The post-M_1 peak, D_2 Abanda fault has juxtaposed the Jacksons Gap Group upon the eastern Blue Ridge, and the syn- to late-M_1 Katy Creek fault emplaced the Dadeville Complex upon the Jacksons Gap Group. The absolute timing of the M_1 metamorphic peak in rocks from all three terranes is not precisely constrained but reported $^{40}Ar/^{39}Ar$ mineral cooling dates, and those reported herein, below, indicate that each likely had cooled from a Devonian-to-Mississippian peak (Steltenpohl and Kunk, 1993; Steltenpohl, 2005; Steltenpohl et al., 2013). Stereoplots of poles to S_1 for each subarea (Figs. 20, 21, and 22) have overlapping point maxima that reflect their positions on the west-limb of the F_2 Tallassee synform and also indicate that the three terranes had been amalgamated either during or just prior-to D_2. The S_1 plot for the Dadeville Complex (Fig. 22), however, is skewed by (n=44) measurements from rocks affected by the F_2 Penton synform. Weak partial girdles in figures 20 and 21 are compatible with folding about the Tallassee synform axis. Figure 22, on the other hand, implies that the Dadeville Complex behaved in a disharmonic fashion relative to the underlying Jacksons Gap Group and eastern Blue Ridge terranes. This is interpreted to

reflect decoupling along the oblique dextral-reverse slip Katy Creek fault to accommodate detached Penton-synform folding within the Dadeville hanging-wall block. A similar scale post-S_1 antiform occurs in precisely the same structural position as the Penton synform (i.e., in the Dadeville Complex adjacent to the Katy Creek fault) is reported by Abrahams (2014) 5 kilometers south of Dadeville, and other truncations of basal upper-plate Dadeville Complex lithologies and structures are clearly indicated on geologic maps of the Brevard zone in Alabama (e.g.: Wielchowsky, 1983; Osborne et al., 1988; Poole, 2015; VanDervoort, 2016; Harstad, 2017). The third deformational event, D_3, represents a prominent retrograde oblique dextral-normal/±reverse movement shearing event along the Abanda fault. D_3 shear zones in the study area are interpreted to correspond to the array of Alleghanian dextral strike-slip shear zones that extend throughout the hinterland to as far east as the Goat Rock fault zone (Fig. 1) and as far west as the Goodwater-Enitachopco fault (Steltenpohl et al., 2013).

$^{40}Ar/^{39}Ar$ ISOTOPIC DATING OF MUSCOVITE

The main objective for the $^{40}Ar/^{39}Ar$ isotopic study was to constrain and compare the ages of quartz veins associated with the Hog Mountain gold prospect to those found in the Jacksons Gap Group and Inner Piedmont terranes. A secondary objective was to date muscovite from select lithologies of the Jacksons Gap Group and the Inner Piedmont from the area of the Milltown Quadrangle to compare them with dates reported elsewhere for the same units in order to further constrain the timing of regional uplift and cooling. For objective one, it was hypothesized that many of the quartz veins in the eastern Blue Ridge were emplaced after the peak of metamorphism

at relatively shallow-depths in a brittle shear zone, as they were only weakly deformed seem characteristic of shallow depths, and thus muscovite ages from them should provide new constraints to the latest-stages (i.e., late Pennsylvanian-Permian, or perhaps Mesozoic) of development of the southernmost Appalachians. The temperature of fluids that had emplaced quartz veins within the Hog Mountain tonalite has been calculated to exceed that of the closure temperature for argon-isotopic equilibrium in muscovite, which is dependent on uplift rate and grain size but generally ~350°C (Dodson, 1973; Harrison and McDougall, 1981; Stowell et al., 1996; McDonald 2008). If the veins did indeed occur due to brittle shearing after peak metamorphism then age dates on the muscovite contained within the veins could constrain the time of this important event.

Much of the area mined on Hog Mountain in the late 19th and early 20th centuries has since been overgrown and the quartz veins now generally are no longer

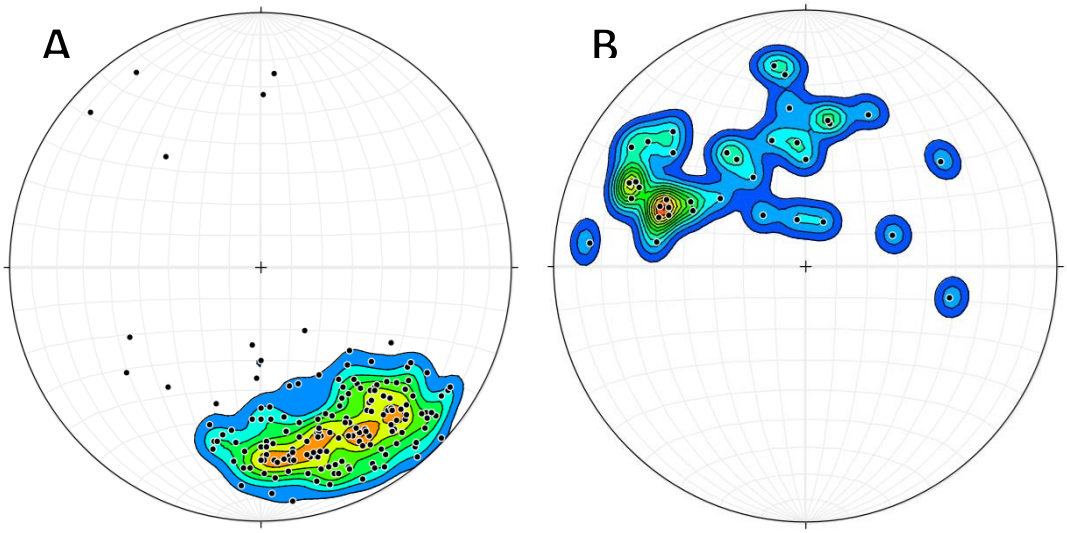

Figure 23 - Lower hemisphere equal-area stereoplots of poles-to-plane of quartz veins investigated in the current study area with 1% contour. (A) Attitude of quartz veins mapped by Pardee and Park (1948) in the Hog Mountain tonalite. N = 168. (B) Attitude of quartz veins mapped within the Milltown Quadrangle. n = 25.

exposed on the surface. Structural data was obtained from a mine map created by Pardee and Park (1948) which included vein locations, attitudes, and names. The tonalite is crosscut by a series of right-stepping en echelon, bifurcating quartz veins. (1996) performed extensive geochemical and thermobarometric work at Hog Mountain. They concluded that the veins were emplaced after peak metamorphic conditions based on the alteration envelope mineral assemblage and a K-Ar muscovite cooling age of 294 ± 16 Ma. Their attitude is dissimilar to quartz veins found within the Milltown Quadrangle (Fig. 23), with veins in the Hog Mountain tonalite striking from N45°E to E-W and dipping 63°NW and those in the Milltown Quadrangle striking N70°E to due-north and dipping to the southeast and east. The en echelon, right-stepping arrangement of veins at Hog Mountain is very clear (Fig. 3) and it is inescapable that they formed in a late-stage right-slip brittle shear zone. The author, therefore, collected samples of quartz vein material from the Hog Mountain gold prospect where they are easily accessed and the large quartz veins contain muscovite (Ozsarac, 2016). Unfortunately, quartz veins sampled from the area of the Milltown Quadrangle were found to be barren of muscovite such that no direct comparison could be made as to the relative timing of vein emplacement between the two study areas.

Seven samples were collected for $^{40}Ar/^{39}Ar$ dating (Table 2), three from the Hog Mountain prospect and four from the area of the Milltown Quadrangle. The three samples from Hog Mountain were from quartz vein material from named gold producing veins including the Tunnel, Trippel, and Barren veins (Fig. 3). Muscovites separated from sample 50.1B were initially only clumps of sericite, additional picking

produced larger euhedral books of muscovite crystals. These were each separately dated as samples 50.1B.b and 50.1B.a, respectively. Muscovite-bearing country-rock samples collected from terranes underlying the Milltown Quadrangle (Fig. 2) for investigating the cooling and uplift history, i.e., the second objective of the study, were selected as follows: one from the Rock Mills Granite Gneiss; one from the Jacksons Gap Group; and two from the Waresville Schist. These were each separately dated and correlate with samples 7.2B, 72.1B, 8.3B and 28.2B, respectively.

^{40}Ar/^{39}Ar analyses and interpretation

Of the three naturally occurring isotopes of ^{40}K is the only one that is radioactive, naturally decaying into ^{40}Ca and ^{40}Ar. The majority of ^{40}K decays to ^{40}Ca but 10.72% becomes ^{40}Ar, with a half-life of 1.248 x 10^{9} years (Brookhaven National Laboratory, 2005). All radiometric dating requires that the daughter particles produced by radioactive decay stay in the sample with the parent elements. A sample that contains only parent elements will give an age of zero. As time passes, and depending on an elements half-life, daughter products are generated and if conditions are right they will accumulate, allowing for an age to be calculated. The point where daughter products begin to accumulate in a sample is called the closure temperature. If a mineral is heated above its closure temperature atoms and molecules trapped within the crystal lattice can migrate or escape. In such a case what is actually being dated is the time a mineral cooled below the conditions of argon retention. For muscovite the closing temperature can range from ~300°C to greater than 500°C depending on the cooling rate and crystalize (Dodson, 1973; Hames and Bowring, 1994).

The $^{40}Ar/^{39}Ar$ method is where ^{39}Ar is created by irradiating a sample with neutrons. Given the known decay constant of ^{40}K and a constant for ^{39}Ar production from ^{39}K (the J-factor) an age can be found using the equation:

$$t = \frac{1}{\lambda} \ln(J \times \frac{40_{Ar*}}{39_{Ar}} + 1)$$

(McDougall & Harrison, 1999). This method can be performed on individual or multiple muscovite crystals.

The $^{40}Ar/^{39}Ar$ dating was performed using the Auburn Noble Gas Isotopic Mass Analysis Laboratory (ANIMAL) under the supervision of Dr. Willis Hames. A disk mill was avoided because it could crush larger muscovite crystals. Instead, each sample was manually pulverized with a 5 pound hammer in a bucket until the majority was the size of coarse sand. Two size fractions were collected using 14 mesh, 18 mesh, and 25 mesh sieves, the larger fragments and fines also being retained. A portion of each sample was then placed in a petri dish containing alcohol and viewed under a binocular microscope, while muscovite crystals were handpicked for each sample. Approximately 10-30 muscovite crystals for each sample were encapsulated into an aluminum disk (Fig. 24) and irradiated for 16 hours at the USGS TRIGA reactor in Denver, Colorado. Single Crystal analyses were performed on all samples 97 days after irradiation using ANIMAL. The raw data can be found in appendix A and table 2 contains information about each sample.

Results

The three samples from the Inner Piedmont units (7.2B; 8.3B; 28.2B) give consistent plateau cooling ages of ~319 Ma and a standard deviation of 0.47 Ma (Fig. 25). This precision encompasses samples from different formations and from both individual muscovite crystals and clusters of sericite.

The one sample from the Jacksons Gap Group gave a cooling age of ~315 Ma. The samples from quartz veins in the Hog Mountain tonalite (Fig. 26) produced ages of ~321 Ma, while sample 49.2B was discordant, with no age plateau reached during step heating. The majority of samples have a 'spike' of earlier ages in the initial heating steps before reaching a plateau. This is interpreted to indicate that the plateau age is an average, produced as crystals homogenized during heating, either of multiple crystals within sericite clusters or of domains within the muscovite. Sericitic clusters contain individual crystals that are smaller than larger sheets of muscovite. Smaller crystals have a lower closure temperature than larger crystals which experience identical conditions (Dodson, 1973). The initial spikes with a maximum age of 360 Ma could represent a Neoacadian signal which is masked either by a younger event, or the average age for each sample could be reduced by a larger number of small crystals.

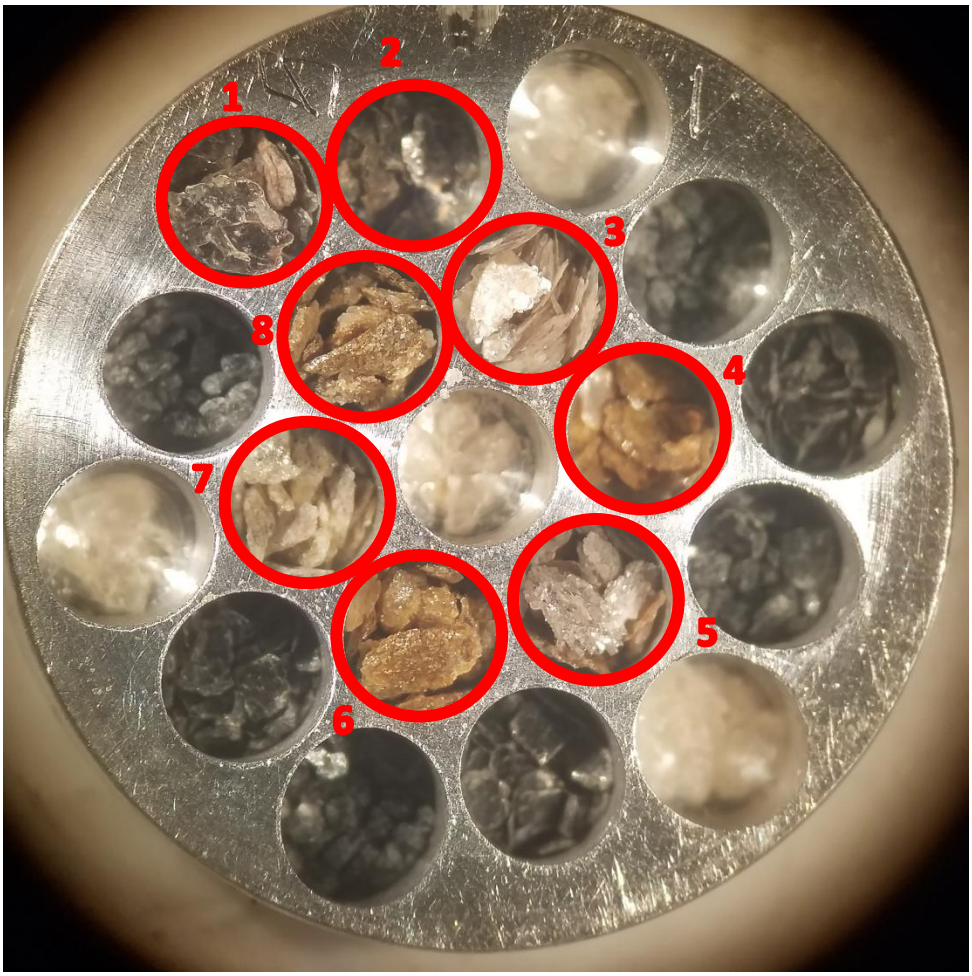

Figure 24 – Sample puck sent for irradiation with cells containing material dated for this study circled in red. (1) 7.2B (2) 8.3B (3) 28.2B (4) 49.2B (5) 50.1B.a (6) 49.3B (7) 72.1B (8) 50.1B.b.

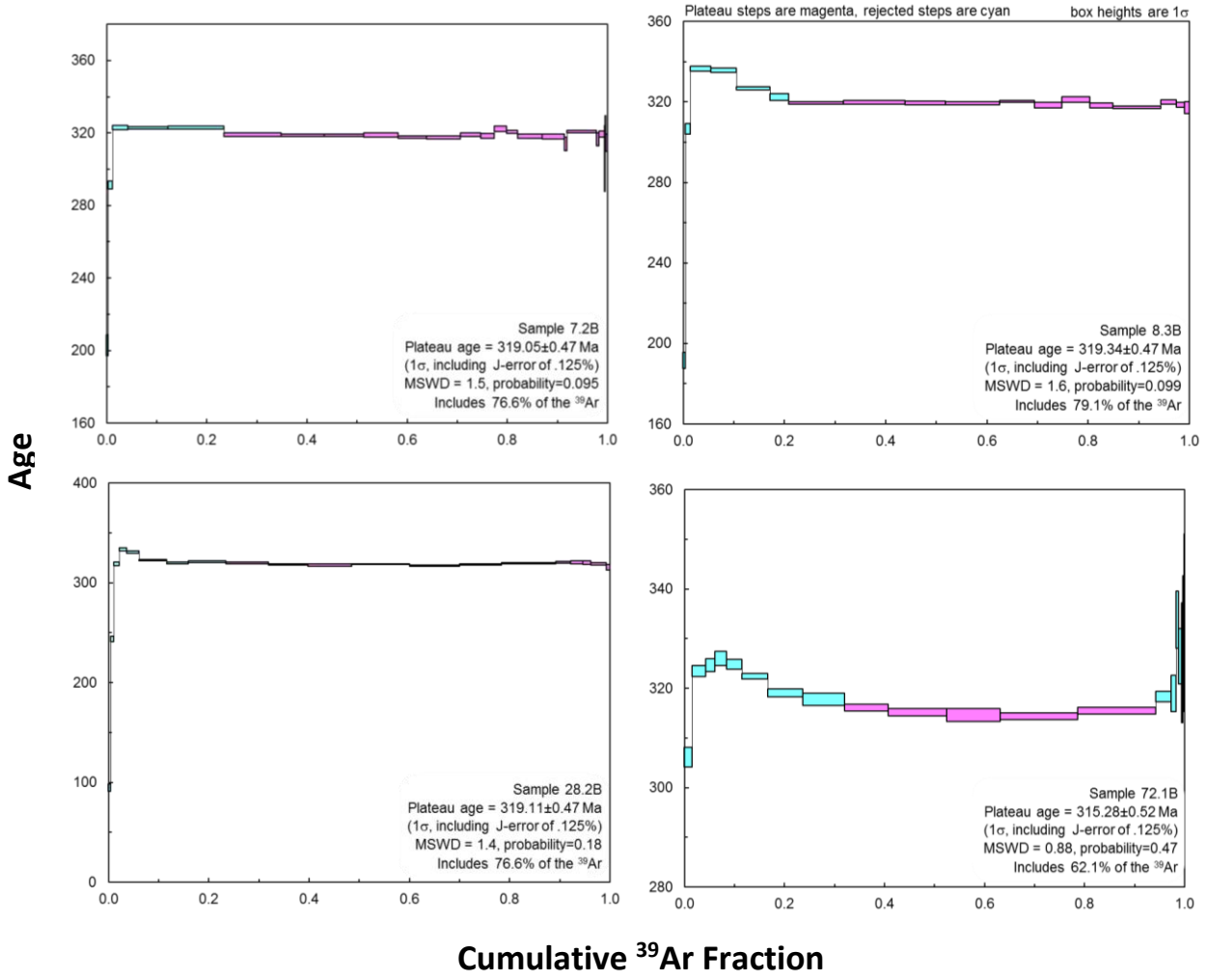

Figure 25 - Laser single crystal $^{40}Ar/^{39}Ar$ incremental heating spectra and plateau ages for muscovite crystals. Samples 7.2B, 8.3B, and 28.2B are located within the Inner Piedmont, while sample 72.1B is taken from the Brevard fault zone.

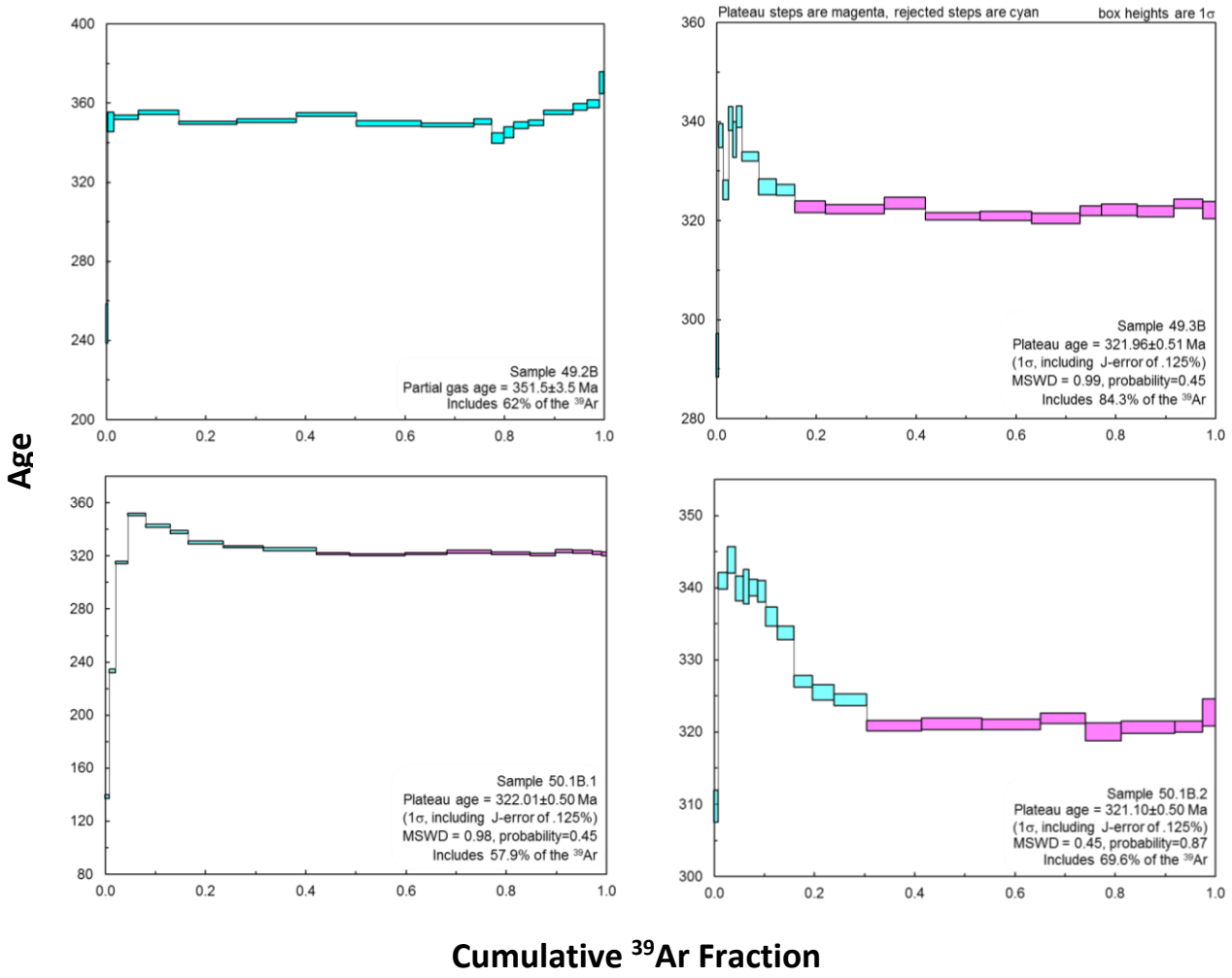

Figure 26 - Laser single crystal $^{40}Ar/^{39}Ar$ incremental heating spectra and plateau ages of muscovite crystals. All samples muscovite were extracted from quartz veins within the Hog Mountain tonalite in the eastern Blue Ridge. Sample 49.2B is discordant.

Table 2. Samples collected and results of $^{40}Ar/^{39}Ar$ dating with ANIMAL

Sample	Lithologic unit	isotopic date	Lattitude	Longitude	Comments
7.2B	Rockmills	319.05 ± 0.47 Ma	33.0187	-85.4359	Coarse muscovite gneiss, very quartz rich.
8.3B	Waresville	319.34 ± 0.47 Ma	33.0310	-85.4375	Weathered amphibolite with a large percentage of muscovite.
28.2B	Waresville	319.11 ± 0.47 Ma	33.0697	-85.4042	Yellowish muscovite + sericite schist.
72.1B	Jacksons Gap Group	315.28 ± 0.52 Ma	33.0138	-85.4954	Garnet + muscovite + sericite phyllite. Highly sheared with numerous z-folds.
49.2B	Quartz Vein / Hog Mountain Tonalite	Discordent 350 - 370	33.0733	-85.8503	Tunnel vein
50.1B.a	Quartz Vein / Hog Mountain Tonalite	322.01 ± 0.50 Ma	33.0700	-85.8519	Trippel vein
50.1B.b	Quartz Vein / Hog Mountain Tonalite	321.10 ± 0.50 Ma	33.0700	-85.8519	Trippel vein
49.3B	Quartz Vein / Hog Mountain Tonalite	321.96 ± 0.51 Ma	33.0719	-85.8502	Barren vein

Electron Microprobe Analysis

The muscovite samples dated included individual crystals aggregates of submillimeter sericitic crystals. It was desirous to know what percentage of the samples was actually muscovite, which contains potassium, and how much was paragonite which substitutes sodium. Electron microprobe analysis was, therefore, performed on samples that had been picked but not irradiated. This was done by encasing the samples in epoxy and polishing the exposed surface with abrasives of increasing grit before polishing with diamond paste and 0.3 micron alumina. The samples were then mapped using background electron imaging to find ideal spots for spot analyses using the AU EMPA lab (Figs. 27 and 28). A minimum of three spot analyses were performed on each sample.

The results (Table 3 and Appendix B) indicate that all samples were primarily muscovite with only minor percentages of paragonite. Dated samples which were composed of clusters of sericite are therefore reliable.

Table 3. Ratio of K and Na in samples used for $^{40}Ar/^{39}Ar$ dating

Sample	Ideal Formula	Age
28.2B	$(K_{0.95},Na_{0.05})_2Al_4[Si_6Al_2O_{20}](OH,F)_4$	319.11 +/- 0.47
72.1B	$(K_{0.90},Na_{0.10})_2Al_4[Si_6Al_2O_{20}](OH,F)_4$	315.28 +/- 0.52
49.3B	$(K_{0.91},Na_{0.09})_2Al_4[Si_6Al_2O_{20}](OH,F)_4$	321.96 +/- 0.51
49.2B	$(K_{0.90},Na_{0.10})_2Al_4[Si_6Al_2O_{20}](OH,F)_4$	Discordant
50.1B	$(K_{0.94},Na_{0.06})_2Al_4[Si_6Al_2O_{20}](OH,F)_4$	322.01 +/- 0.50
8.3B	$(K_{0.97},Na_{0.03})_2Al_4[Si_6Al_2O_{20}](OH,F)_4$	319.34 +/- 0.47
7.2B	$(K_{0.79},Na_{0.21})_2Al_4[Si_6Al_2O_{20}](OH,F)_4$	319.05 +/- 0.47

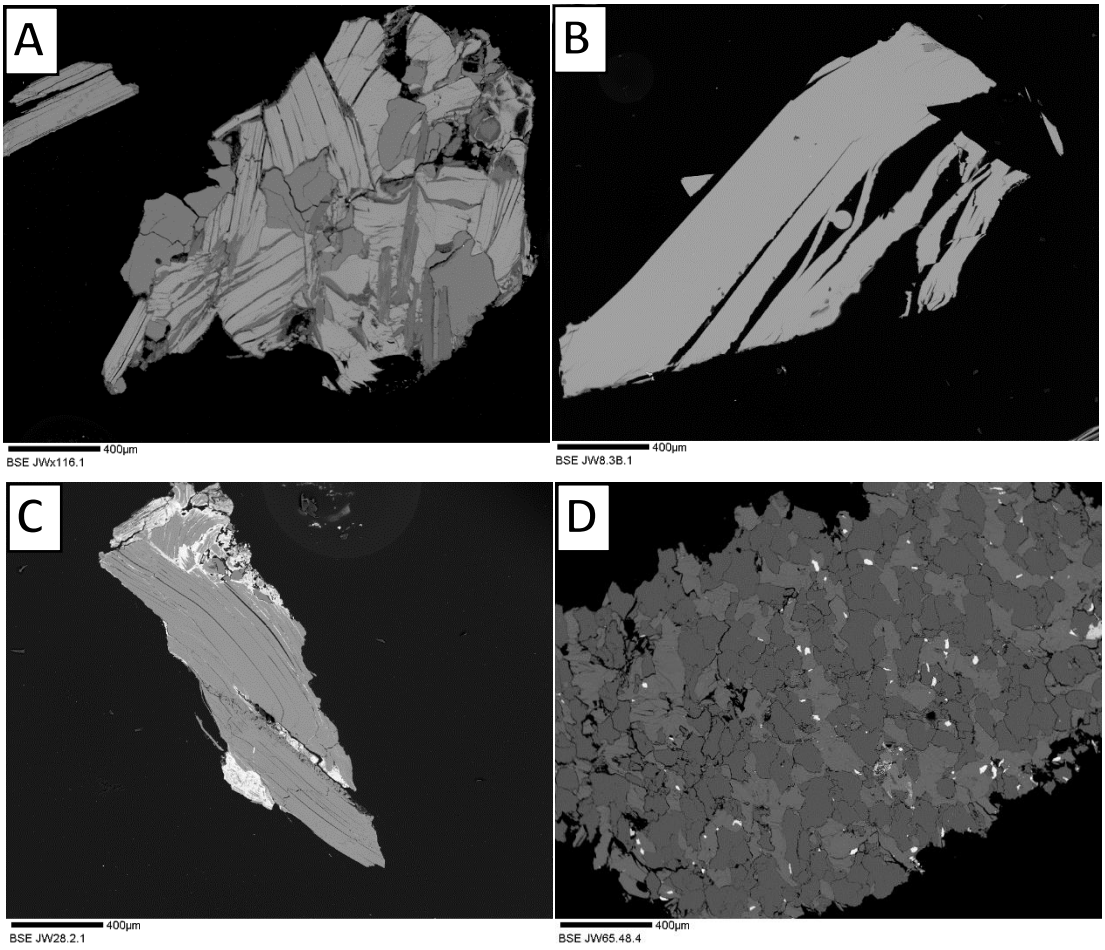

Figure 27 – Electron Backscatter images of four of the samples dated for the cooling/uplift study. Lighter colors indicate a greater density of high atomic number elements. (A) Sample 7.2B taken from within the Rock Mills Granite Gneiss and composed of primarily quartz and muscovite. (B) Sample 8.3B taken from a muscovite schist within the Waresville Schist. (C) Sample 28.2B taken from the Rock Mills Granite Gneiss. (D) Sample 72.1B taken from a phyllite within the Jacksons Gap Group.

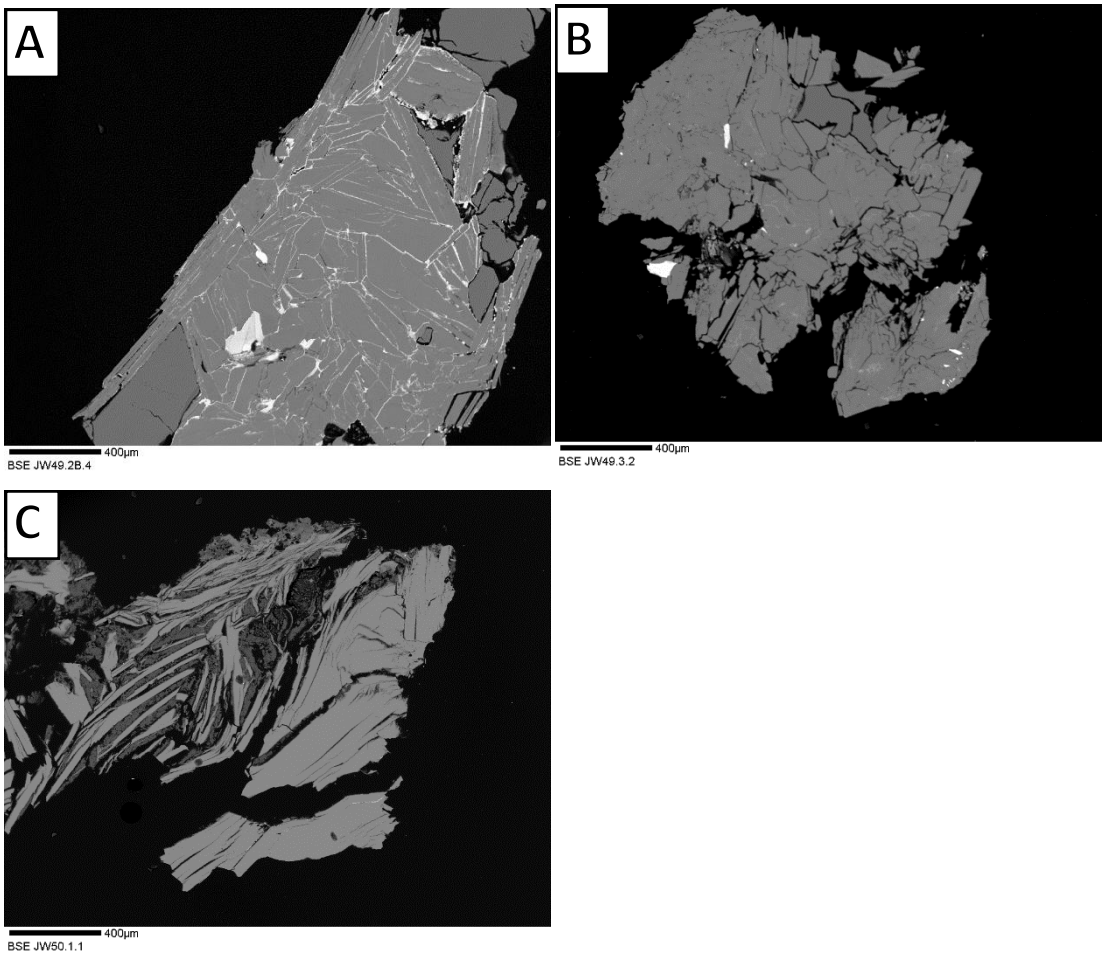

Figure 28 – Electron backscatter images of the three samples that were dated from the Hog Mountain prospect. (A) Sample 49.2B taken from the Tunnel Vein within the Hog Mountain pluton. (B) Sample 49.3B taken from the Barren Vein within the Hog Mountain pluton. (C) Sample 50.1B taken from the Trippel Vein within the Hog Mountain pluton.

CONCLUSIONS

- The Jacksons Gap Group has historically been recognized to contain diverse lithologies that vary across and along strike. Within the Milltown Quadrangle three main upper greenschist-facies to lower amphibolite-facies lithologies were observed to be at least partially continuous along strike to the southwest. The structurally lowest is a fine-grained garnetiferous, graphitic, quartz phyllite that is separated from the eastern Blue Ridge Emuckfaw Group by a discrete zone of ultramylonitized rock. The middle lithology is composed of interlayered garnetiferous quartz schists and phyllites with isolated quartz-feldspathic schists and mylonites. The tectonostratigraphically highest lithology is a sericitic quartz phyllite that pinches out toward the eastern part of the quadrangle.
- The Waresville Schist presents a much more highly diverse range of lithologies than earlier reported. Metamorphosed lower to middle amphibolite-facies mafic and more felsic volcanics are distinguishable and extensive enough to potentially be mapped as distinct lithologies. A previously unreported lithology, garnetite, was identified in the Waresville Schist that extends possibly 8 kilometers as a mapable unit, and likely extends further to the east of the Milltown Quadrangle. The protolith is interpreted to have resulted from sediment and hydrothermal exhalatives.

- The late D_2 large scale (~10 km half-wavelength) Penton synform was discovered. Trending N70°E and plunging 28° it has a medium amplitude of ~3 km. The Penton synform only affects rocks of the Dadeville Complex, where it is defined by the folded metamorphic foliation and coplanar compositional layering. The adjacent Jacksons Gap Group appears unaffected, following the characteristic N55°E trend of the Brevard fault zone. This disharmony is explained by detachment of the upper plate from the lower plate along the Katy Creek fault
- Muscovite cooling ages as measured by $^{40}Ar/^{39}Ar$ of lithologies within the Inner Piedmont give consistent plateau ages of ~319 Ma, which reflects the end of early Alleghanian metamorphism and possible unroofing. A cooling age of ~315 Ma for the Jacksons Gap Group indicates that right lateral movement occurred after early Alleghanian metamorphism while Gondwana was still colliding with Laurentia. All the ages are compatible with reported cooling dates throughout the eastern Blue Ridge and Jacksons Gap Group of Alabama (Steltenpohl, 2005; White, 2007; Steltenpohl et al., 2013; Abraham, 2014; Poole, 2015).
- Cooling ages for muscovite extracted from quartz veins within the Hog Mountain tonalite give an age across different veins of ~321 Ma, indicating that they were emplaced during early Alleghanian brittle shearing at shallower depths than the Inner Piedmont, and not during

later extension of the Southern Appalachians, which occurred between 278 and 230 Ma (Steltenpohl et al., 1992, 2013).

REFERENCES

Aldrich, T.H., Jr., 1909, The treatment of the gold ores of Hog Mountain, Alabama: American Institute of Mining and Metallurgical Engineers Transactions, v. 39, p. 578.

Abrahams, J.B., 2014, Geology of the Dadeville Quadrangle and the Tallassee Synform in characterizing the Dog River Window: unpublished M.S. thesis, Auburn University, Auburn, Alabama, 142 p.

Adams, G.I., 1926, The crystalline rocks, in Adams, G.I., Butts, D., Stephenson, L.W., and Cooke, C.W., eds., Geology of Alabama: Alabama Geological Survey Special Reports 14, p. 40-223.

Barkley, M.N., and Hawkins, J.F., 2016, Ductile fabric anomalies concerning the alleged Alexander City Fault in the eastern Blue Ridge of central Alabama: Geological Society of America Abstracts with Programs, v. 48, no. 7, doi: 10.1130/abs/2016AM-285891.

Bentley, R.D., and Neathery, T.L, 1970, Geology of the Brevard fault zone and related rocks of the Inner Piedmont of Alabama: Alabama Geological Society Field Trip Guidebook, no. 8, 119 p.

Bream, B.R., Hatcher, R.D., Jr., Miller, C.E., Fullager, P.D., 2004, Detrital zircon ages and Nd isotopic data from the southern Appalachian crystalline core, Georgia, South Carolina, North Carolina, and Tennessee: New provenance constraints for part of the Laurentian margin: Geological Society of America Memoirs, no. 197, p. 459-475.

Brookhaven National Laboratory, developed by the National Nuclear Data Center, 2005, NuDat 2.0: http://www.nndc.bnl.gov/nudat2 (accessed May 2018)

Brown, D. E., 1982, A study of the petrology and structure of a portion of the Boyds Creek mafic-ultramafic complex, Chambers country, Alabama: Unpublished M.S. thesis, Auburn University, Auburn, Alabama, 154 p.

CH2MHILL, prepared for the Alabama Clean Water Partnership, 2004, Tallapoosa River Basin Management Plan: http://www.adem.alabama.gov/programs/water/nps/files/TallapoosaBMP.pdf (accessed July 2017)

Cook, F.A., Albuagh, D.S., Brown, L.D., Kaufman, S., Oliver, J.E., and Hatcher, R.D., Jr., 1979, Thin-skinned tectonics in the crystalline southern Appalachians; COCORP seismic-reflection profiling of the Blue Ridge and Piedmont: Geology, v. 7, p. 563-567.

Cook, R.B., and Thomson, I., 1995, Characteristics of Brevard zone gold mineralization in the Sessions Vicinity, Tallapoosa County, Alabama, in Guthrie, G.M., ed., The

timing and tectonic mechanisms of the Alleghanian orogeny, Alabama Piedmont: Alabama Geological Society, 32nd Annual Field Trip Guidebook, p. 43-51.

Crawford, T.J., and Kath, R.L., 2015 Geologic map of the Brevard zone from central Georgia to eastern Alabama: Geological Society of America Abstracts with Programs, v. 47, no. 2, p.31.

Dodson, M.H., 1973, Closure temperature in cooling geochronological and petrological systems: Contributions to Mineralogy and Petrology, v. 40, p. 259-274.

Gestaldo, R.A., Guthrie, G.M., Steltenpohl, M.G., 1993, Mississippian fossils from southern Appalachian metamorphic rocks and their implications for late Paleozoic tectonic evolution: Science, v. 262, p. 732-734.

Grimes, J.E., 1993, Geology of the Piedmont rocks between the Dadeville Complex and the Pine Mountain Window in parts of Lee, Macon, and Tallapoosa Counties, Alabama: unpublished M.S. Thesis, Auburn University, Auburn, Alabama, 129 p.

Guthrie, G.M., and Lesher, C.M., 1989, Geologic setting of lode gold deposits in the Northern Piedmont and Brevard zone, Alabama: Geological Survey of Alabama Bulletin 136, p. 11-32.

Hames, W.E., and Bowring, S.A., 1994, An empirical evaluation of the argon diffusion geometry in muscovite: Earth and Planetary Science Letters, v. 124(1-4), p. 161-169.

Harrison, T. M., and McDougall, I., 1981, Excess Ar in metamorphic rocks from Broken Hill, New South Wales: Implications for $^{40}Ar/^{39}Ar$ age spectra and the thermal history of the region: Earth and Planetary Science Letters, v. 55, p. 123-149.

Harstad, R.P., 2017, Geology of the 1:24,000 Roanoke East Quadrangle and investigations of the Long Island Creek Gneiss within the southernmost Appalachians, Alabama and Georgia: unpublished M.S. thesis, Auburn University, Auburn, Alabama, 81 p.

Hatcher, R.D., Jr., 1989, Tectonic synthesis of the U.S. Appalachians, Chapter 14, in Hatcher R.D., Jr., Thomas, W.A., and Viele, G.W., eds., The Appalachian-Ouachita Orogen in the United States: Geology of North America, Geological Society of America, v. F-2, p. 511-535.

Hawkins, J.F., 2013, Geology, petrology, and geochronology of rocks in the Our Town, Alabama Quadrangle: unpublished M.S. thesis, Auburn University, Auburn, Alabama,118 p.

Johnson, M.J., 1988, Geology of the gold occurrences near Jacksons Gap, Tallapoosa County, Alabama: unpublished M.S. thesis, Auburn University, Auburn, Alabama, 156 p.

Keefer, W.D., 1992, Geology of the Tallassee synform hinge zone and its relationship to the Brevard fault zone, Tallapoosa and Elmore Counties, Alabama: unpublished M.S. thesis, Auburn University, Auburn, Alabama, 195 p.

Lambe, R.L., 1982, Hog Mountain Gold Project Alabama: Phase 2 Exploration program, unpublished report, 13 p.

McClellan, E.A., Steltenpohl, M.G., Thomas, C., Miller, C.F., 2007, Isotopic Age Constraints and Metamorphic History of the Talladega Belt: New Evidence for Timing of Arc Magmatism and Terrane Emplacement along the Southern Laurentian Margin, The Journal of Geology, v. 115, no. 5, p. 541-561.

McCullars, J.M., 2001, Geology and trace-element geochemistry of the Brevard zone near Martin Lake, Tallapoosa County, Alabama: unpublished M.S. thesis, Auburn University, Auburn, Alabama, 74 p.

McDonald, W.M., 2008, $^{40}Ar/^{39}Ar$ ages of muscovite from the Western Blue Ridge and Talladega Belt, Georgia, and North Carolina: unpublished M.S. thesis, Auburn University, Auburn, Alabama, P. 114.

McDougall, I., and Harrison, M.T., 1999, Geochronology and thermochronology by $^{40}Ar/^{39}Ar$ method: New York, Oxford University Press, 269 p.

Merschat, A.J., 2009, Assembling the Blue Ridge and Inner Piedmont: Insights into the Nature and Timing of Terrane Accretion in the Southern Appalachian orogen from Geologic Mapping, Stratigraphy, Kinematic Analysis, Petrology, Geochemistry, and Modern Geochronology [Ph.D. thesis]: Knoxville, University of Tennessee, 455 p.

Mies, J.W., 1992, Structural analysis of the Hollins Line Fault, southern Cleburne County, Alabama: Geological Survey of Alabama, Bulletin 148, 55 p.

Neathery, T.L., and Reynolds, J.W., 1975, Geology of the Lineville East, Ofelia, Wadley North and Mellow Valley Quadrangles, Alabama: Geological Survey of Alabama Bulletin, v. 109, 120 p.

Nesse, W.D., 2012, Introduction to mineralogy: New York, Oxford University Press, 480 p.

Ozsarac, S., 2016, Igneous-rock hosted orogenic gold deposit at Hog Mountain, Tallapoosa County, Alabama: unpublished M.S. thesis, Auburn University, Auburn, Alabama, 88 p.

Pardee, J.T. and Park, C.F., Jr., 1948, Gold Deposits of the southern Piedmont, U.S., Geological Survey Professional Paper 213,156 p.

Park, C.F., 1935, Hog Mountain gold district, Alabama: American Institute of mining and Metallurgical Engineers Transactions, Mining Geology, v. 115, p. 209-228.

Passchier, C.W., and Trouw, R.A., 2005, Microtectonics: Springer-Verlag, Berlin, Germany, 289 p.

Poole, J.D., 2015, Geology of the Jacksons Gap, Alabama, Quadrangle and structural implications for the Brevard fault zone: Unpublished M.S. thesis, Auburn University, Auburn, Alabama, 174 p.

Raymond, D.E., Osborne, W.E., Copeland, C.W., and Neathery, T.L., 1988, Alabama Stratigraphy: Geological Survey Circular 140, 97 p.

Reed, A.S., 1994, Geology of the western portion of the Dadeville 7.5' Quadrangle, Tallapoosa County, Alabama: unpublished M.S. thesis: Auburn University, Auburn, Alabama, 108 p.

Seal, T.L., and Kish, S.A., 1990, The geology of the Dadeville Complex of the western Georgia and eastern Alabama Inner Piedmont; initial petrographic, geochemical, and geochronological results, in Steltenpohl, M.G., and others, eds., Geology of the southern Inner Piedmont, Alabama and southwest Georgia, Southeastern Section of the Geological Society of America Field Trip Guidebook, v. 39, p. 65-77.

Singleton, R.F., and Steltenpohl, M.G., 2014, Geology of the 1:24,000 Buttston, Alabama, 7.5-Minute Quadrangle, Tallapoosa County, Alabama: Alabama Geological Survey Open-File Report, 30 p.

Spear, F.S., 1993, Metamorphic Phase Equilibria and Pressure-Temperature-Time Paths: Washington, DC: Mineralogical Society of America. Vol. 1.

Steltenpohl, M.G., 1988, Kinematics of the Towaliga, Bartletts Ferry, and Goat Rock fault zones: The late Paleozoic dextral shear system in the southernmost Appalachians: Geology, v. 16, p. 852-855.

Steltenpohl, M.G., Neilson, M.J., Bittner, E.I., Colberg, M.R., and Cook, R.B., 1990, Geology of the Alabama Inner Piedmont terrane: Geological Survey of Alabama Bulletin 139, 80 p.

Steltenpohl, M.G., and Kunk, M.J., 1993, $^{40}Ar/^{39}Ar$ thermochronology and Alleghanian development of the southernmost Appalachian Piedmont, Alabama and southwest Georgia: Geological Society of America Bulletin, v. 105, p. 819-833.

Steltenpohl, M.G., Goldberg, S.A., Hanley, T.B., Kunk, M.K., 1992, Alleghanian development of the Goat Rock fault zone, southernmost Appalachians: Temporal compatibility with the master decollement: Geology, v. 20. p. 845-848.

Steltenpohl, M.G., editor, 2005, New perspectives on southernmost Appalachian terranes, Alabama and Georgia: Alabama Geological Society 42nd Annual Field Trip Guidebook, 212 p.

Steltenpohl, M.G., Heatherington, A., Mueller, P., and Miller, B.V., 2005, Tectonic implications of new isotopic dates on crystalline rocks from Alabama and Georgia, in Steltenpohl, M.G. ed., Southernmost Appalachian terranes, Alabama and Georgia: Southeastern Section of the Geological Society of America Field Trip Guidebook, p. 51-67.

Steltenpohl, M.G., Mueller, P.M., Heatherington, A.L., Hanley, T.B., Wooden, J.L., 2008, Gondwanan/peri-Gondwanan origin for the Uchee terrane, Alabama and Georgia: Carolina zone or Suwannee terrane(?) and its suture with Grenvillian basement of the Pine Mountain window: Geosphere, v. 4, no. 1, p.131-141.

Steltenpohl, M.G., Hatcher, R.D., Jr., Mueller, P.A., Heatherington, A.L., and Wooden, J.L., 2010, Geologic history of the Pine Mountain window, Alabama and Georgia: Insights from a new geologic map and U-Pb isotopic dates, in Tollo, R.P., Bartholomew, M.J., Hibbard, J.P., and Karabinos, P.M., eds., From Rodinia to Pangea: The Lithotectonic Record of the Appalachian Region: Geological Society of America Memoir 206, p. 837–857.

Steltenpohl, M.G., Schwartz, J.J., and Miller, B.V., 2013, Late to post-Appalachian strain partitioning and extension in the Blue Ridge of Alabama and Georgia: Geosphere, v. 9; no. 3, p. 647-666.

Sterling, J.W., Steltenpohl, M.G., Cook, R.B., 2005, Petrology and geochemistry of igneous rocks in the southernmost Brevard zone of Alabama and their implications for southern Appalachian tectonic evolution: Alabama Geological Society, p. 96-124.

Sterling, J.W., 2006, Geology of the southernmost exposures of the Brevard zone in the Red Hill Quadrangle, Alabama: unpublished M.S. thesis, Auburn University, Auburn, Alabama, 118 p.

Stoddard, P.V., 1983, A petrographic and geochemical analysis of the Zana Granite and Kowaliga Augen Gneiss: Northern Piedmont, Alabama: unpublished M.S. thesis, Memphis State University, Memphis, Tennessee, 74 p.

Stowell, H.H., Lesher, C.M., Green, N.L., Sha, p., Guthrie, G.M., Sinha, A.K., 1996, Metamorphism and Gold Mineralization in the Blue Ridge, Southernmost Appalachians: Economic Geology, v. 91, p. 1115-1144.

Tull, J.F., 1978, Structural development of the Alabama Piedmont northwest of the Brevard zone: American Journal of Science, v. 278, no. 4, p. 442-460.

Tull, J.F., Baggazi, H., Groszos, M.S., 2012, Evolution of the Murphy synclinorium, southern Appalachian Blue Ridge, USA: Journal of Structural Geology, v. 44, p. 151-166

Tull, J.F., Mueller, P.M., Farris, D.W., and Davis, B.L., 2018, Taconic suprasubduction zone magmatism in southern Laurentia: Evidence from the Dadeville Complex:

Geological Society of America Bulletin, v. 130 (7-8), p. 1339-1354, https://doi.org/10.1130/B31885.1.

VanDervoort, D.S., Steltenpohl, M.G., and Schwartz, J.J., 2015, U-Pb ages from the Dadeville Complex, southernmost Appalachians, eastern Alabama: an accreted Taconic arc: Geological Society of America Abstracts with Programs, v. 47, no. 7, p. 159.

VanDervoort, D.S., 2016, Geology of the Wadley South Quadrangle and geochronology of the Dadeville Complex, southernmost Appalachians of east Alabama: unpublished M.S. thesis, Auburn University, Auburn, Alabama, 127 p.

White, T.W., 2007, Geology of the 1:24,000 Tallassee, Alabama, Quadrangle, and its implications for southern Appalachian tectonics: unpublished M.S. thesis, Auburn University, Auburn, Alabama, 74 p.

Wielchowsky, C.C., 1983, The geology of the Brevard zone and adjacent terranes in Alabama: unpublished Ph.D. dissertation, Rice University, Houston, Texas, 237 p.

Williams, H., Hatcher, R.D., Jr., 1983, Appalachian suspect terranes: Geological Society of America Memoirs, no. 158, p. 33-53.

APPENDIX A

$^{40}Ar/^{39}Ar$ ISOTOPIC DATA

Sensitivity (Moles/volt):	6.32E-15	±6.32E-17
Measured 40/36 of Air:	289	±1.5
Mass Discrimination (% per amu):	-0.55%	±0.10%
(36/37)Ca:	0.0003046	±0.0000084
(39/37)Ca:	0.000738	±0.0000370
(40/39)K:	0	±4E-04
(38/39)Cl:	0.01	±0.01
% of Sample in Split	0.58	
GA1550 Biotite Monitor Age Assignment :	9.88E+07	
FC Sanidine Monitor Age Assignment:	2.80E+07	
Date (midpoint) of Irradiation:	12/17/2017	
Date of Analysis:	3/24/2018	

Data are in volts and errors are the standard deviation unless indicated otherwise. P=laser power setting, t=time (s)

Plateau ages include error in estimating the J-value.

Single Crystal Total-Fusion Analyses

7.2B (33° 01' 7.62" N, 85° 26' 9.36" W), Inner Piedmont, Milltown Quadrangle, Alabama

Monitor	P	t	40V	39V	38V	37V	36V	Mol 40Ar	%Rad	R	Age	%sd
au33.5k.mus.1a.txt	0.6	30	0.30074 ± 0.000823	0.0091 ± 0.000092	0.00016 ± 0.000045	-0.00017 ± 0.000132	0.00009 ± 0.000025	1.90E-15	90.84 %	30.0132	203.09 ± 5.98	2.94 %
au33.5k.mus.1b.txt	0.7	30	1.88138 ± 0.00123	0.03124 ± 0.000102	0.00081 ± 0.000051	-0.00034 ± 0.000138	0.0017 ± 0.000029	1.19E-14	73.32 %	44.1569	291.41 ± 2.25	0.77 %
au33.5k.mus.1c.txt	0.8	30	5.08141 ± 0.005263	0.10159 ± 0.000311	0.00141 ± 0.000037	0.00005 ± 0.000159	0.00022 ± 0.000029	3.21E-14	98.72 %	49.3803	322.96 ± 1.2	0.37 %
au33.5k.mus.1d.txt	0.9	30	13.27037 ± 0.00519	0.26874 ± 0.000326	0.0036 ± 0.000085	-0.00018 ± 0.000209	0.00002 ± 0.000067	8.39E-14	99.95 %	49.354	322.8 ± 0.63	0.2 %
au33.5k.mus.1e.txt	1	30	18.35873 ± 0.009218	0.37088 ± 0.000703	0.00508 ± 0.000088	0.00096 ± 0.000273	0.00011 ± 0.000036	1.16E-13	99.83 %	49.4152	323.17 ± 0.66	0.2 %
au33.5k.mus.1f.txt	1	30	18.53321 ± 0.00834	0.38021 ± 0.00104	0.00492 ± 0.000065	0.00151 ± 0.000088	-0.0001 ± 0.000048	1.17E-13	100.15 %	48.7451	319.15 ± 0.92	0.29 %
au33.5k.mus.1g.txt	1	30	13.84953 ± 0.008411	0.28438 ± 0.000624	0.00367 ± 0.000059	-0.00013 ± 0.000359	0.00003 ± 0.000038	8.76E-14	99.94 %	48.671	318.71 ± 0.77	0.24 %
au33.5k.mus.1h.txt	1.1	30	12.86785 ± 0.008392	0.264 ± 0.000527	0.00346 ± 0.000059	0.00141 ± 0.000141	0.00003 ± 0.00004	8.13E-14	99.93 %	48.7081	318.93 ± 0.73	0.23 %
au33.5k.mus.1i.txt	1.1	30	11.35869 ± 0.007487	0.23321 ± 0.000692	0.00309 ± 0.000097	0.00133 ± 0.000202	-0.00002 ± 0.000033	7.18E-14	100.04 %	48.7056	318.91 ± 1.01	0.32 %
au33.5k.mus.1j.txt	1.2	30	9.09792 ± 0.009313	0.18742 ± 0.000306	0.00242 ± 0.000051	0.0001 ± 0.000168	0.00002 ± 0.000022	5.75E-14	99.92 %	48.5032	317.7 ± 0.65	0.21%
au33.5k.mus.1k.txt	1.2	30	11.00623 ± 0.007383	0.22653 ± 0.000643	0.00288 ± 0.000083	0.00118 ± 0.000198	0.00007 ± 0.000034	6.96E-14	99.81%	48.4917	317.63 ± 0.97	0.31%
au33.5k.mus.1l.txt	1.3	30	6.53893 ± 0.00697	0.13418 ± 0.000355	0.00157 ± 0.000072	0.00026 ± 0.000197	0 ± 0.000024	4.13E-14	99.98 %	48.7222	319.01 ± 0.97	0.3 %
au33.5k.mus.1m.txt	1.4	30	4.30423 ± 0.002765	0.08852 ± 0.000302	0.00118 ± 0.000046	0 ± 0.000169	-0.00006 ± 0.000037	2.72E-14	100.44 %	48.6228	318.42 ± 1.37	0.43 %
au33.5k.mus.1n.txt	1.5	30	4.08528 ± 0.003634	0.08288 ± 0.000272	0.00108 ± 0.000044	0.00019 ± 0.000123	-0.00003 ± 0.000044	2.58E-14	100.22 %	49.2928	322.43 ± 1.5	0.47 %
au33.5k.mus.1o.txt	1.6	30	3.64539 ± 0.002031	0.0742 ± 0.000142	0.00092 ± 0.000072	0.00006 ± 0.000161	0.00003 ± 0.000025	2.30E-14	99.75 %	49.0034	320.7 ± 0.91	0.28 %
au33.5k.mus.1p.txt	1.8	30	7.91231 ± 0.005519	0.16278 ± 0.000603	0.00208 ± 0.000052	0.00015 ± 0.000164	-0.00001 ± 0.000021	5.00E-14	100.03 %	48.608	318.33 ± 1.23	0.39 %
au33.5k.mus.1q.txt	2	30	7.11484 ± 0.008083	0.14623 ± 0.000586	0.00182 ± 0.000048	-0.00002 ± 0.000035	0.00003 ± 0.000025	4.50E-14	99.89 %	48.6011	318.29 ± 1.37	0.43 %
au33.5k.mus.1r.txt	2.2	30	0.82379 ± 0.000758	0.0172 ± 0.000116	0.00016 ± 0.000049	0.00005 ± 0.000218	-0.00001 ± 0.000026	5.21E-15	100.3 %	47.9038	314.1 ± 3.65	1.16 %
au33.5k.mus.1s.txt	2.5	30	9.62981 ± 0.002999	0.19648 ± 0.000353	0.00251 ± 0.000043	0.00009 ± 0.000271	-0.00005 ± 0.00003	6.09E-14	100.15 %	49.0109	320.75 ± 0.65	0.2 %
au33.5k.mus.1t.txt	2.6	30	0.73225 ± 0.000768	0.01515 ± 0.000083	0.00013 ± 0.000047	-0.00013 ± 0.000099	-0.00001 ± 0.000024	4.63E-15	100.48 %	48.3381	316.71 ± 3.56	1.12 %
au33.5k.mus.1u.txt	2.8	30	1.81625 ± 0.001733	0.03701 ± 0.000103	0.00044 ± 0.000041	0.00008 ± 0.000198	0.00004 ± 0.000024	1.15E-14	99.42 %	48.7883	319.41 ± 1.58	0.5 %
au33.5k.mus.1v.txt	3	30	0.16353 ± 0.000847	0.00335 ± 0.000103	0.00002 ± 0.00004	-0.00079 ± 0.000283	0.00002 ± 0.000027	1.03E-15	95.52 %	46.5746	306.08 ± 18.37	6 %
au33.5k.mus.1w.txt	3.2	30	0.37495 ± 0.000739	0.00765 ± 0.000159	0.00006 ± 0.000042	-0.00025 ± 0.000144	0 ± 0.000023	2.37E-15	100.14 %	49.0392	320.91 ± 8.79	2.74 %
au33.5k.mus.1x.txt	3.3	30	0.59264 ± 0.000934	0.01234 ± 0.000117	0.00015 ± 0.000047	0.00019 ± 0.00012	-0.00002 ± 0.000024	3.75E-15	101.06 %	48.0305	314.86 ± 4.8	1.52 %

Single Crystal Total-Fusion Analyses

8.3B (33° 01' 51.95" N, 85° 26' 15.29" W), Inner Piedmont, Milltown Quadrangle, Alabama

Monitor	P	t	40V	39V	38V	37V	36V	Mol 40Ar	%Rad	R	Age	%sd
au33.5l.mus.2a.txt	0.6	30	0.35924 ± 0.000688	0.01168 ± 0.000114	0.0002 ± 0.000054	-0.00012 ± 0.000267	0.0001 ± 0.00002	2.03E-05	91.89 %	28.2649	191.86 ± 4.06	2.12 %
au33.5l.mus.2b.txt	0.7	30	1.16107 ± 0.001242	0.02339 ± 0.000108	0.00029 ± 0.000043	-0.00019 ± 0.000132	0.00023 ± 0.000024	2.40E-05	94.08 %	46.6958	306.81 ± 2.52	0.82 %
au33.5l.mus.2c.txt	0.8	30	5.4783 ± 0.003183	0.10366 ± 0.000327	0.00134 ± 0.000055	0.00025 ± 0.000182	0.00041 ± 0.000024	2.41E-05	97.8 %	51.6838	336.7 ± 1.19	0.35 %
au33.5l.mus.2d.txt	0.8	30	6.46781 ± 0.006364	0.12463 ± 0.000295	0.00151 ± 0.000059	0.00004 ± 0.000131	0.00015 ± 0.000039	3.86E-05	99.33 %	51.5468	335.89 ± 1.05	0.31%
au33.5l.mus.2e.txt	0.9	30	8.20371 ± 0.006901	0.16314 ± 0.000246	0.0021 ± 0.000051	0.00045 ± 0.00022	0.00016 ± 0.000029	2.85E-05	99.44 %	50.0062	326.7 ± 0.66	0.2 %
au33.5l.mus.2f.txt	0.9	30	4.68505 ± 0.003302	0.09474 ± 0.000424	0.00114 ± 0.000036	-0.00003 ± 0.000202	0.00005 ± 0.000025	2.46E-05	99.69 %	49.2975	322.46 ± 1.55	0.48 %
au33.5l.mus.2g.txt	1	30	12.99373 ± 0.007005	0.26583 ± 0.000467	0.00338 ± 0.000074	0.00118 ± 0.00023	0.00009 ± 0.00003	2.97E-05	99.8 %	48.7842	319.39 ± 0.63	0.2 %
au33.5l.mus.2h.txt	1	30	14.88118 ± 0.005293	0.3046 ± 0.000928	0.00404 ± 0.000056	0.00185 ± 0.000103	-0.00004 ± 0.000048	4.82E-05	100.07 %	48.8569	319.82 ± 1.03	0.32 %
au33.5l.mus.2i.txt	1	30	9.86286 ± 0.01234	0.20173 ± 0.000472	0.00255 ± 0.000045	0.00022 ± 0.000169	0.00005 ± 0.000022	2.18E-05	99.84 %	48.8118	319.55 ± 0.87	0.27 %
au33.5l.mus.2j.txt	1.1	30	12.92352 ± 0.007443	0.26471 ± 0.000486	0.00346 ± 0.000057	0.00132 ± 0.000205	0.00005 ± 0.000037	3.73E-05	99.89 %	48.7696	319.3 ± 0.67	0.21%
au33.5l.mus.2k.txt	1.1	30	8.42769 ± 0.005469	0.17195 ± 0.000196	0.00223 ± 0.000057	0.00013 ± 0.000107	0.00003 ± 0.000023	2.31E-05	99.88 %	48.9531	320.4 ± 0.5	0.15 %
au33.5l.mus.2l.txt	1.2	30	6.48977 ± 0.00617	0.13315 ± 0.000543	0.0017 ± 0.000059	0.00004 ± 0.000256	0.00005 ± 0.000036	3.58E-05	99.78 %	48.6365	318.5 ± 1.43	0.45 %
au33.5l.mus.2m.txt	1.2	30	6.89805 ± 0.008059	0.1405 ± 0.000583	0.00178 ± 0.000047	0.00021 ± 0.000154	-0.00005 ± 0.000037	3.73E-05	100.21%	49.0952	321.25 ± 1.48	0.46 %
au33.5l.mus.2n.txt	1.3	30	5.49218 ± 0.00442	0.1129 ± 0.000398	0.00141 ± 0.00004	0.00004 ± 0.000128	0.00002 ± 0.000025	2.51E-05	99.87 %	48.5826	318.18 ± 1.23	0.39 %
au33.5l.mus.2o.txt	1.3	30	11.4163 ± 0.006754	0.23547 ± 0.000324	0.00313 ± 0.000064	0.00116 ± 0.000152	0.00002 ± 0.000054	5.40E-05	99.96 %	48.4625	317.45 ± 0.65	0.2 %
au33.5l.mus.2p.txt	1.4	30	3.75952 ± 0.004428	0.07679 ± 0.000107	0.00096 ± 0.000047	0.00005 ± 0.000127	0.00002 ± 0.000042	4.22E-05	99.85 %	48.8875	320.01 ± 1.21	0.38 %
au33.5l.mus.2q.txt	1.4	30	1.97669 ± 0.001182	0.0405 ± 0.000079	0.00051 ± 0.000042	0.00013 ± 0.000174	0.00002 ± 0.000022	2.17E-05	99.69 %	48.6545	318.61 ± 1.23	0.39 %
au33.5l.mus.2r.txt	1.5	30	1.19262 ± 0.000912	0.0245 ± 0.000172	0.00028 ± 0.00005	-0.00015 ± 0.000084	0.00002 ± 0.000024	2.38E-05	99.51%	48.4353	317.29 ± 2.94	0.93 %

Single Crystal Total-Fusion Analyses

28.2B (33° 04' 11.28" N, 85° 24' 15.25" W), Inner Piedmont, Milltown Quadrangle, Alabama

Monitor	P	t	40V	39V	38V	37V	36V	Mol 40Ar	%Rad	R	Age	%sd
au33.5m.mus.3a.txt	0.6	30	0.26136 ± 0.000423	0.01684 ± 0.000115	0.00041 ± 0.000037	0.00031 ± 0.000109	0.00011 ± 0.000029	2.90E-05	87.93 %	13.6484	95.2 ± 3.64	3.82 %
au33.5m.mus.3b.txt	0.7	30	0.85185 ± 0.001003	0.0226 ± 0.000145	0.0003 ± 0.000046	0.00028 ± 0.000147	0.0001 ± 0.000026	2.56E-05	96.62 %	36.4179	243.62 ± 2.78	1.14 %
au33.5m.mus.3c.txt	0.7	30	2.09619 ± 0.001958	0.0413 ± 0.000141	0.00056 ± 0.000048	0.00007 ± 0.000255	0.00028 ± 0.000027	2.70E-05	96.03 %	48.7389	319.11 ± 1.73	0.54 %
au33.5m.mus.3d.txt	0.8	30	2.60934 ± 0.002495	0.04965 ± 0.00013	0.00071 ± 0.000038	0.0002 ± 0.000155	0.00024 ± 0.000025	2.48E-05	97.33 %	51.1487	333.52 ± 1.36	0.41%
au33.5m.mus.3e.txt	0.8	30	4.69281 ± 0.001813	0.09203 ± 0.000255	0.00126 ± 0.000034	0.00007 ± 0.000201	0.00009 ± 0.000027	2.67E-05	99.44 %	50.7075	330.89 ± 1.09	0.33 %
au33.5m.mus.3f.txt	0.9	30	9.98171 ± 0.003178	0.20188 ± 0.00053	0.00266 ± 0.000055	0.0004 ± 0.000122	0.00007 ± 0.000025	2.52E-05	99.8 %	49.3463	322.75 ± 0.89	0.28 %
au33.5m.mus.3g.txt	0.9	30	7.69184 ± 0.008271	0.15686 ± 0.000354	0.00203 ± 0.000041	0.00044 ± 0.000163	0.0001 ± 0.000028	2.82E-05	99.62 %	48.8521	319.79 ± 0.87	0.27 %
au33.5m.mus.3h.txt	1	30	13.30664 ± 0.007234	0.27125 ± 0.000649	0.0034 ± 0.000041	0.00134 ± 0.000175	-0.00008 ± 0.000071	7.06E-05	100.19 %	49.0573	321.02 ± 0.93	0.29 %
au33.5m.mus.3i.txt	1	30	15.27031 ± 0.005531	0.3122 ± 0.000712	0.00411 ± 0.000093	0.00137 ± 0.000175	-0.00005 ± 0.000047	4.72E-05	100.09 %	48.9125	320.15 ± 0.79	0.25 %
au33.5m.mus.3j.txt	1.1	30	13.8039 ± 0.010271	0.28377 ± 0.000536	0.00374 ± 0.000072	0.00105 ± 0.000224	-0.00002 ± 0.000058	5.81E-05	100.04 %	48.6439	318.54 ± 0.76	0.24 %
au33.5m.mus.3k.txt	1.1	30	15.47731 ± 0.00779	0.3187 ± 0.001227	0.00415 ± 0.000055	0.00099 ± 0.000153	-0.00007 ± 0.000063	6.27E-05	100.13 %	48.5646	318.07 ± 1.29	0.41%
au33.5m.mus.3l.txt	1.2	30	20.50584 ± 0.01435	0.42085 ± 0.00047	0.00556 ± 0.000077	0.00123 ± 0.000197	0.00002 ± 0.000034	3.44E-05	99.97 %	48.7097	318.94 ± 0.45	0.14 %
au33.5m.mus.3m.txt	1.2	30	17.49282 ± 0.021687	0.36107 ± 0.000691	0.00473 ± 0.000069	0.00114 ± 0.000133	0.00001 ± 0.000084	8.44E-05	99.98 %	48.4382	317.31 ± 0.85	0.27 %
au33.5m.mus.3n.txt	1.3	30	14.89626 ± 0.010234	0.30598 ± 0.000756	0.00411 ± 0.0001	0.00152 ± 0.000184	0.00003 ± 0.000034	3.36E-05	99.95 %	48.657	318.62 ± 0.84	0.27 %
au33.5m.mus.3o.txt	1.4	30	19.27183 ± 0.018129	0.39439 ± 0.000664	0.00523 ± 0.000068	0.00138 ± 0.000225	-0.00015 ± 0.000077	7.65E-05	100.23 %	48.8654	319.87 ± 0.72	0.23 %
au33.5m.mus.3p.txt	1.5	30	5.43612 ± 0.002677	0.11091 ± 0.000245	0.00146 ± 0.000049	0.00013 ± 0.000252	-0.00002 ± 0.000037	3.68E-05	100.09 %	49.016	320.78 ± 0.97	0.3 %
au33.5m.mus.3q.txt	1.7	30	4.34809 ± 0.003884	0.08876 ± 0.000264	0.00116 ± 0.000048	0.00026 ± 0.000177	-0.00003 ± 0.00004	4.02E-05	100.21%	48.9845	320.59 ± 1.33	0.41%
au33.5m.mus.3r.txt	1.8	30	2.90883 ± 0.002608	0.05935 ± 0.00019	0.00083 ± 0.000045	0.00012 ± 0.000102	0.00002 ± 0.000048	4.75E-05	99.85 %	48.9372	320.3 ± 1.88	0.59 %
au33.5m.mus.3s.txt	2	30	5.22738 ± 0.003896	0.10735 ± 0.000412	0.00147 ± 0.000049	0.00036 ± 0.000191	0 ± 0.000021	2.08E-05	100.02 %	48.6963	318.86 ± 1.3	0.41%
au33.5m.mus.3t.txt	2.1	30	1.43193 ± 0.001829	0.02973 ± 0.000127	0.00044 ± 0.000047	0.00018 ± 0.00021	-0.00007 ± 0.00004	3.99E-05	101.48 %	48.165	315.67 ± 2.95	0.94 %

Single Crystal Total-Fusion Analyses

72.1B (33° 6' 13.67" N, 85° 29' 43.68" W), Jacksons Gap Group, Milltown Quadrangle, Alabama

Monitor	P	t	40V	39V	38V	37V	36V	Mol 40Ar	%Rad	R	Age	%sd
au32.5q.mus.7a.txt	0.6	30	1.8098 ± 0.001541	0.03863 ± 0.000171	0.00048 ± 0.000032	-0.00008 ± 0.000167	0.00003 ± 0.000027	2.75E-05	99.46 %	46.5889	306.17 ± 1.96	0.64 %
au32.5q.mus.7b.txt	0.7	30	3.44936 ± 0.002566	0.06929 ± 0.000175	0.00096 ± 0.000051	0.00022 ± 0.000154	0.00007 ± 0.000026	2.58E-05	99.37 %	49.4663	323.47 ± 1.12	0.35 %
au32.5q.mus.7c.txt	0.8	30	2.55366 ± 0.001623	0.05111 ± 0.000129	0.00062 ± 0.000047	-0.00081 ± 0.000337	0.00005 ± 0.000025	2.49E-05	99.41%	49.6685	324.68 ± 1.27	0.39 %
au32.5q.mus.7d.txt	0.8	30	2.90107 ± 0.002583	0.05799 ± 0.000194	0.00067 ± 0.000044	-0.00003 ± 0.000224	0.00002 ± 0.000027	2.75E-05	99.76 %	49.9046	326.1 ± 1.45	0.45 %
au32.5q.mus.7e.txt	0.9	30	4.02283 ± 0.002911	0.08095 ± 0.00019	0.00104 ± 0.00004	0.00015 ± 0.000177	-0.00001 ± 0.000026	2.58E-05	100.04 %	49.6956	324.85 ± 1.01	0.31%
au32.5q.mus.7f.txt	0.9	30	6.57828 ± 0.004178	0.13318 ± 0.000182	0.00167 ± 0.000061	0.00011 ± 0.000214	0.00004 ± 0.000026	2.56E-05	99.8 %	49.2965	322.46 ± 0.61	0.19 %
au32.5q.mus.7g.txt	1	30	8.92546 ± 0.008282	0.18314 ± 0.000381	0.00234 ± 0.000046	-0.00059 ± 0.000373	-0.00005 ± 0.000041	4.14E-05	100.17 %	48.7358	319.1 ± 0.85	0.27 %
au32.5q.mus.7h.txt	1.1	30	10.40123 ± 0.013687	0.21407 ± 0.000782	0.00286 ± 0.000067	0.00032 ± 0.000209	0.00004 ± 0.000029	2.85E-05	99.87 %	48.5272	317.84 ± 1.26	0.4 %
au32.5q.mus.7i.txt	1.1	30	10.94183 ± 0.006817	0.22678 ± 0.000287	0.00296 ± 0.000092	0.0012 ± 0.000179	-0.00019 ± 0.000062	6.20E-05	100.51%	48.2485	316.17 ± 0.69	0.22 %
au32.5q.mus.7j.txt	1.2	30	14.52022 ± 0.009505	0.30167 ± 0.000637	0.00399 ± 0.000061	0.00177 ± 0.000194	0.00005 ± 0.000031	3.06E-05	99.9 %	48.0868	315.2 ± 0.72	0.23 %
au32.5q.mus.7k.txt	1.3	30	13.23547 ± 0.004526	0.27553 ± 0.001128	0.00358 ± 0.000101	0.00116 ± 0.000155	0.00003 ± 0.000034	3.36E-05	99.94 %	48.0056	314.71 ± 1.31	0.42 %
au32.5q.mus.7l.txt	1.4	30	19.2131 ± 0.006989	0.40046 ± 0.000838	0.00517 ± 0.000085	0.00224 ± 0.000203	0.00003 ± 0.000035	3.48E-05	99.96 %	47.9567	314.41 ± 0.69	0.22 %
au32.5q.mus.7m.txt	1.5	30	19.4015 ± 0.010811	0.40299 ± 0.0008	0.00512 ± 0.000061	0.00143 ± 0.000232	0.00001 ± 0.000032	3.23E-05	99.98 %	48.1356	315.49 ± 0.67	0.21%
au32.5q.mus.7n.txt	1.7	30	3.83809 ± 0.002369	0.07877 ± 0.000194	0.00103 ± 0.000051	0.00004 ± 0.000202	0.00003 ± 0.000027	2.74E-05	99.8 %	48.6276	318.45 ± 1.05	0.33 %
au32.5q.mus.7o.txt	1.8	30	1.31621 ± 0.001189	0.02702 ± 0.000125	0.00028 ± 0.000049	0.00019 ± 0.000108	-0.00007 ± 0.000046	4.58E-05	101.54 %	48.7214	319.01 ± 3.61	1.13 %
au32.5q.mus.7p.txt	2	30	0.65935 ± 0.001144	0.01288 ± 0.000166	0.00015 ± 0.000042	-0.00011 ± 0.000102	-0.00003 ± 0.000026	2.60E-05	101.41%	51.201	333.83 ± 5.82	1.74 %
au32.5q.mus.7q.txt	2.2	30	0.74053 ± 0.001281	0.0147 ± 0.000187	0.00017 ± 0.000049	-0.00005 ± 0.000149	0.00002 ± 0.000028	2.75E-05	99.2 %	49.9706	326.49 ± 5.57	1.71%
au32.5q.mus.7r.txt	2.3	30	0.29297 ± 0.00063	0.0058 ± 0.000159	0.00002 ± 0.000053	0.00017 ± 0.00014	0.00002 ± 0.000024	2.38E-05	98.47 %	49.7478	325.16 ± 12.06	3.71%
au32.5q.mus.7s.txt	2.4	30	0.39521 ± 0.000802	0.00766 ± 0.000125	0.00012 ± 0.000045	0.00017 ± 0.000169	0.00001 ± 0.000027	2.73E-05	99.27 %	51.2215	333.95 ± 8.82	2.64 %
au32.5q.mus.7t.txt	2.5	30	0.29276 ± 0.000577	0.00545 ± 0.000119	0.00009 ± 0.000035	-0.00014 ± 0.000223	0.00005 ± 0.000046	4.58E-05	95.11%	51.1013	333.23 ± 17.93	5.38 %

Single Crystal Total-Fusion Analyses

49.2B (33° 4' 24.02" N, 85° 51' 1.16" W), Hog Mountain tonalite, Tunnel Vein, Alabama

Monitor	P	t	40V	39V	38V	37V	36V	Mol 40Ar	%Rad	R	Age	%sd
au33.5n.mus.4a.txt	0.6	30	0.21856 ± 0.000851	0.00561 ± 0.000164	0.00004 ± 0.000048	0.00008 ± 0.000172	0.00003 ± 0.000018	1.83E-05	95.6 %	37.2439	248.78 ± 10.03	4.03 %
au33.5n.mus.4b.txt	0.7	30	0.95488 ± 0.000798	0.01761 ± 0.000214	0.00015 ± 0.000072	-0.0001 ± 0.000157	0.00001 ± 0.000023	2.27E-05	99.64 %	54.04	350.65 ± 4.95	1.41%
au33.5n.mus.4c.txt	0.8	30	3.99222 ± 0.001554	0.07337 ± 0.000164	0.0009 ± 0.000058	-0.00001 ± 0.000126	0 ± 0.000024	2.40E-05	100.03 %	54.4127	352.84 ± 1.01	0.29 %
au33.5n.mus.4d.txt	0.9	30	6.60821 ± 0.004847	0.1201 ± 0.000311	0.00156 ± 0.000066	0.00015 ± 0.0002	0.00006 ± 0.00002	2.02E-05	99.71%	54.8619	355.49 ± 1.01	0.28 %
au33.5n.mus.4e.txt	1	30	9.31749 ± 0.009023	0.17271 ± 0.000354	0.0023 ± 0.000033	0.00029 ± 0.000226	-0.00005 ± 0.00004	4.02E-05	100.17 %	53.948	350.11 ± 0.91	0.26 %
au33.5n.mus.4f.txt	1	30	9.60133 ± 0.005671	0.17737 ± 0.000443	0.00235 ± 0.000052	0.00047 ± 0.000148	0.00001 ± 0.000021	2.10E-05	99.98 %	54.1216	351.13 ± 0.93	0.26 %
au33.5n.mus.4g.txt	1.1	30	9.71496 ± 0.011254	0.17768 ± 0.0003	0.00236 ± 0.000034	0.00018 ± 0.000159	0 ± 0.000044	4.44E-05	99.99 %	54.6726	354.37 ± 0.87	0.25 %
au33.5n.mus.4h.txt	1.1	30	10.43063 ± 0.007443	0.19349 ± 0.000727	0.00257 ± 0.000064	0.00111 ± 0.00015	0.00001 ± 0.000026	2.59E-05	99.98 %	53.8946	349.79 ± 1.36	0.39 %
au33.5n.mus.4i.txt	1.2	30	8.44297 ± 0.010896	0.15695 ± 0.00035	0.0021 ± 0.000059	0.00048 ± 0.00025	0 ± 0.000024	2.37E-05	100.01%	53.7943	349.2 ± 0.95	0.27 %
au33.5n.mus.4j.txt	1.2	30	2.8902 ± 0.002054	0.05349 ± 0.000179	0.00082 ± 0.000046	0.00036 ± 0.000214	0 ± 0.00002	2.01E-05	100.04 %	54.0372	350.63 ± 1.4	0.4 %
au33.5n.mus.4k.txt	1.3	30	1.90967 ± 0.001668	0.03628 ± 0.000149	0.00045 ± 0.000042	-0.00077 ± 0.000287	-0.00008 ± 0.00004	3.96E-05	101.28 %	52.6325	342.33 ± 2.54	0.74 %
au33.5n.mus.4l.txt	1.4	30	1.58964 ± 0.001235	0.02991 ± 0.000207	0.00038 ± 0.000042	0.00012 ± 0.000121	-0.00002 ± 0.00002	2.04E-05	100.38 %	53.1456	345.37 ± 2.74	0.79 %
au33.5n.mus.4m.txt	1.5	30	2.32602 ± 0.001703	0.04328 ± 0.000163	0.00059 ± 0.000038	-0.00004 ± 0.000197	-0.00003 ± 0.000021	2.06E-05	100.44 %	53.7477	348.92 ± 1.62	0.46 %
au33.5n.mus.4n.txt	1.6	30	2.45219 ± 0.002074	0.04545 ± 0.000145	0.00062 ± 0.000032	0.00018 ± 0.000141	0 ± 0.00002	1.99E-05	100.02 %	53.9492	350.11 ± 1.42	0.41%
au33.5n.mus.4o.txt	1.8	30	4.88661 ± 0.002274	0.0891 ± 0.000167	0.00116 ± 0.00005	0.00027 ± 0.000168	-0.00006 ± 0.000034	3.36E-05	100.39 %	54.8445	355.39 ± 1	0.28 %
au33.5n.mus.4p.txt	2	30	2.2725 ± 0.001037	0.04107 ± 0.000153	0.00057 ± 0.000038	0.0001 ± 0.000147	0 ± 0.000023	2.26E-05	99.98 %	55.3278	358.23 ± 1.71	0.48 %
au33.5n.mus.4q.txt	2.2	30	1.98473 ± 0.001552	0.03556 ± 0.000136	0.00034 ± 0.00006	-0.00018 ± 0.000195	0.00003 ± 0.000023	2.29E-05	99.55 %	55.5675	359.63 ± 1.87	0.52 %
au33.5n.mus.4r.txt	2.4	30	0.74694 ± 0.001106	0.01301 ± 0.000165	0.00021 ± 0.00005	0.0003 ± 0.000149	-0.00001 ± 0.000019	1.92E-05	100.43 %	57.4049	370.38 ± 5.5	1.49 %
au33.5n.mus.4s.txt	2.5	30	0.16394 ± 0.000751	0.00287 ± 0.000126	0.00002 ± 0.000042	-0.0003 ± 0.000305	-0.00013 ± 0.000046	4.57E-05	122.73 %	57.106	368.64 ± 34.62	9.39 %
au33.5n.mus.4t.txt	2.6	30	0.00889 ± 0.000665	0.00007 ± 0.000118	0.00002 ± 0.000044	-0.00021 ± 0.000147	0 ± 0.000024	2.41E-05	99.88 %	133.0151	64.94 ± 1492.4	195.1%

Single Crystal Total-Fusion Analyses

49.3B (33° 4' 18.92" N, 85° 51' 0.88" W), Hog Mountain tonalite, Barren Vein, Alabama

Monitor	P	t	40V	39V	38V	37V	36V	Mol 40Ar	%Rad	R	Age	%sd
au33.5p.mus.6a.txt	0.6	30	0.57374 ± 0.001477	0.01284 ± 0.000132	0.00017 ± 0.000034	0.00001 ± 0.000189	0.00001 ± 0.000021	2.11E-05	99.4 %	44.4008	292.89 ± 4.48	1.53 %
au33.5p.mus.6b.txt	0.7	30	1.29509 ± 0.001639	0.02484 ± 0.000118	0.0004 ± 0.000033	0.00037 ± 0.000143	0.00003 ± 0.000023	2.27E-05	99.29 %	51.7677	337.2 ± 2.43	0.72 %
au33.5p.mus.6c.txt	0.7	30	1.44387 ± 0.001713	0.02892 ± 0.000111	0.00026 ± 0.00005	-0.0001 ± 0.000221	-0.00003 ± 0.000022	2.19E-05	100.52 %	49.9324	326.26 ± 1.96	0.6 %
au33.5p.mus.6d.txt	0.7	30	1.45718 ± 0.00163	0.0278 ± 0.000158	0.00033 ± 0.000037	-0.00028 ± 0.000167	0.00001 ± 0.000022	2.19E-05	99.85 %	52.3444	340.62 ± 2.49	0.73 %
au33.5p.mus.6e.txt	0.8	30	1.00388 ± 0.001508	0.01944 ± 0.000153	0.00027 ± 0.000042	-0.00011 ± 0.000151	-0.00004 ± 0.000024	2.42E-05	101.08 %	51.6329	336.4 ± 3.61	1.07 %
au33.5p.mus.6f.txt	0.8	30	1.59754 ± 0.001611	0.03048 ± 0.000154	0.00041 ± 0.000031	-0.00013 ± 0.000147	-0.00001 ± 0.000021	2.06E-05	100.09 %	52.4114	341.02 ± 2.19	0.64 %
au33.5p.mus.6g.txt	0.9	30	4.61817 ± 0.002361	0.09033 ± 0.000209	0.00118 ± 0.000051	0.00003 ± 0.000145	0.00002 ± 0.000021	2.08E-05	99.88 %	51.0626	333 ± 0.91	0.27 %
au33.5p.mus.6h.txt	0.9	30	4.9947 ± 0.002921	0.09947 ± 0.000463	0.00129 ± 0.000053	0.00017 ± 0.000088	0.00006 ± 0.000024	2.39E-05	99.64 %	50.033	326.86 ± 1.61	0.49 %
au33.5p.mus.6i.txt	1	30	5.20208 ± 0.004021	0.1042 ± 0.000343	0.00132 ± 0.000047	0 ± 0.000098	-0.00001 ± 0.000023	2.34E-05	100.05 %	49.9257	326.22 ± 1.18	0.36 %
au33.5p.mus.6j.txt	1	30	8.39503 ± 0.007721	0.16991 ± 0.000584	0.00226 ± 0.00006	0.0001 ± 0.0002	0.00003 ± 0.000023	2.33E-05	99.89 %	49.3568	322.82 ± 1.18	0.37 %
au33.5p.mus.6k.txt	1.1	30	16.33427 ± 0.005527	0.33137 ± 0.00086	0.00443 ± 0.000086	0.00111 ± 0.000308	0.00002 ± 0.000039	3.85E-05	99.96 %	49.274	322.32 ± 0.87	0.27 %
au33.5p.mus.6l.txt	1.1	30	11.20828 ± 0.004133	0.22631 ± 0.000768	0.00297 ± 0.000067	0.00117 ± 0.000174	0.00004 ± 0.000054	5.44E-05	99.9 %	49.4764	323.53 ± 1.2	0.37 %
au33.5p.mus.6m.txt	1.2	30	15.03136 ± 0.010923	0.30642 ± 0.00065	0.00389 ± 0.000081	0.00164 ± 0.000187	0.00001 ± 0.00003	3.02E-05	99.99 %	49.0486	320.97 ± 0.74	0.23 %
au33.5p.mus.6n.txt	1.3	30	14.12149 ± 0.017339	0.28789 ± 0.000764	0.00366 ± 0.000092	0.00135 ± 0.000173	-0.00001 ± 0.000034	3.45E-05	100.03 %	49.0516	320.99 ± 0.97	0.3 %
au33.5p.mus.6o.txt	1.4	30	13.31657 ± 0.006884	0.27198 ± 0.000861	0.00337 ± 0.000057	0.00063 ± 0.000154	-0.00001 ± 0.000037	3.68E-05	100.01 %	48.9625	320.45 ± 1.06	0.33 %
au33.5p.mus.6p.txt	1.5	30	5.97426 ± 0.004961	0.12125 ± 0.000315	0.00153 ± 0.000045	0.00016 ± 0.000173	0.00002 ± 0.000027	2.74E-05	99.89 %	49.215	321.97 ± 0.98	0.3 %
au33.5p.mus.6q.txt	1.7	30	9.63431 ± 0.01155	0.19542 ± 0.000635	0.00252 ± 0.000046	0.00017 ± 0.000232	0.00003 ± 0.000027	2.75E-05	99.92 %	49.2635	322.26 ± 1.15	0.36 %
au33.5p.mus.6r.txt	1.8	30	10.24043 ± 0.004033	0.20812 ± 0.000705	0.00273 ± 0.000086	0.00154 ± 0.000277	-0.00011 ± 0.000047	4.68E-05	100.32 %	49.2057	321.91 ± 1.18	0.37 %
au33.5p.mus.6s.txt	2	30	7.81762 ± 0.008409	0.1576 ± 0.000325	0.00197 ± 0.000048	0.00028 ± 0.000103	0.00007 ± 0.000048	4.80E-05	99.73 %	49.4717	323.51 ± 0.96	0.3 %
au33.5p.mus.6t.txt	2.2	30	3.73576 ± 0.003752	0.07548 ± 0.000275	0.00094 ± 0.000056	-0.00002 ± 0.000151	0.00006 ± 0.000047	4.72E-05	99.51 %	49.2506	322.18 ± 1.72	0.53 %

Single Crystal Total-Fusion Analyses

50.1aB (33° 4' 12.29" N, 85° 51' 6.99" W), Hog Mountain tonalite, Trippel Vein, Alabama

Monitor	P	t	40V	39V	38V	37V	36V	Mol 40Ar	%Rad	R	Age	%sd
au33.5o.mus.5a.txt	0.6	30	0.71168 ± 0.000913	0.03479 ± 0.000108	0.00054 ± 0.00005	-0.00005 ± 0.000229	0.00003 ± 0.000021	2.12E-05	98.57 %	20.1631	138.92 ± 1.33	0.95 %
au33.5o.mus.5b.txt	0.7	30	1.82781 ± 0.001791	0.0523 ± 0.000163	0.00083 ± 0.000044	0.00001 ± 0.000141	0.00005 ± 0.000023	2.26E-05	99.2 %	34.7804	233.34 ± 1.16	0.49 %
au33.5o.mus.5c.txt	0.8	30	5.07922 ± 0.003573	0.10465 ± 0.00022	0.00151 ± 0.000055	-0.00005 ± 0.000195	0.00017 ± 0.000021	2.08E-05	98.99 %	48.047	314.96 ± 0.8	0.26 %
au33.5o.mus.5d.txt	0.9	30	7.89053 ± 0.007164	0.14506 ± 0.000345	0.00205 ± 0.000046	0.00045 ± 0.000198	0.00011 ± 0.000021	2.06E-05	99.58 %	54.1649	351.38 ± 0.94	0.27 %
au33.5o.mus.5e.txt	0.9	30	11.0768 ± 0.008825	0.2101 ± 0.00062	0.00284 ± 0.000073	-0.00028 ± 0.000302	-0.00007 ± 0.000058	5.77E-05	100.19 %	52.7226	342.86 ± 1.17	0.34 %
au33.5o.mus.5f.txt	1	30	7.70062 ± 0.002272	0.14829 ± 0.000423	0.00194 ± 0.000055	0.00032 ± 0.000219	-0.00003 ± 0.000037	3.73E-05	100.13 %	51.9291	338.16 ± 1.08	0.32 %
au33.5o.mus.5g.txt	1	30	14.98345 ± 0.008104	0.29589 ± 0.000758	0.00397 ± 0.000092	0.00154 ± 0.00014	0.00007 ± 0.000035	3.52E-05	99.87 %	50.5731	330.09 ± 0.9	0.27 %
au33.5o.mus.5h.txt	1.1	30	16.77112 ± 0.008606	0.33518 ± 0.000767	0.00432 ± 0.00008	0.00087 ± 0.000198	-0.00015 ± 0.000051	5.08E-05	100.26 %	50.0356	326.88 ± 0.82	0.25 %
au33.5o.mus.5i.txt	1.1	30	22.15041 ± 0.013379	0.44566 ± 0.00138	0.00576 ± 0.000087	0.00077 ± 0.00018	0 ± 0.000029	2.87E-05	100 %	49.7022	324.89 ± 1.03	0.32 %
au33.5o.mus.5j.txt	1.2	30	13.87296 ± 0.019968	0.28215 ± 0.000445	0.00372 ± 0.000045	0.00196 ± 0.000116	-0.00003 ± 0.00003	2.96E-05	100.06 %	49.1693	321.69 ± 0.72	0.22 %
au33.5o.mus.5k.txt	1.3	30	22.97379 ± 0.011894	0.46824 ± 0.000836	0.00614 ± 0.000107	-0.00031 ± 0.000449	-0.00007 ± 0.000053	5.25E-05	100.09 %	49.0641	321.06 ± 0.64	0.2 %
au33.5o.mus.5l.txt	1.4	30	17.14603 ± 0.011116	0.34832 ± 0.000811	0.0046 ± 0.00009	0.00158 ± 0.000218	0 ± 0.000033	3.31E-05	99.99 %	49.2209	322 ± 0.8	0.25 %
au33.5o.mus.5m.txt	1.4	30	18.50369 ± 0.011688	0.37439 ± 0.001085	0.00503 ± 0.000057	0.00175 ± 0.000234	-0.00009 ± 0.000053	5.27E-05	100.15 %	49.4242	323.22 ± 1	0.31%
au33.5o.mus.5n.txt	1.5	30	15.92208 ± 0.012106	0.3235 ± 0.001014	0.00435 ± 0.000078	0.00207 ± 0.000111	0.00001 ± 0.000033	3.33E-05	99.98 %	49.2067	321.92 ± 1.06	0.33 %
au33.5o.mus.5o.txt	1.6	30	10.27692 ± 0.013615	0.20947 ± 0.00059	0.00269 ± 0.000054	0.00058 ± 0.000209	-0.00004 ± 0.000032	3.17E-05	100.11 %	49.0604	321.04 ± 1.04	0.32 %
au33.5o.mus.5p.txt	1.7	30	7.20737 ± 0.004331	0.14509 ± 0.000329	0.0019 ± 0.00004	0.00013 ± 0.000148	0.00008 ± 0.000051	5.08E-05	99.66 %	49.5063	323.71 ± 1.02	0.31%
au33.5o.mus.5q.txt	1.9	30	8.26782 ± 0.0088	0.16721 ± 0.000544	0.00222 ± 0.000049	0.00079 ± 0.000264	0.00001 ± 0.000024	2.45E-05	99.96 %	49.4233	323.22 ± 1.14	0.35 %
au33.5o.mus.5r.txt	2.1	30	3.69566 ± 0.002694	0.07487 ± 0.000243	0.00108 ± 0.000043	0.00044 ± 0.000164	0.00002 ± 0.000018	1.83E-05	99.87 %	49.2968	322.46 ± 1.17	0.36 %
au33.5o.mus.5s.txt	2.2	30	2.33107 ± 0.002393	0.04734 ± 0.000162	0.00062 ± 0.000048	0.00024 ± 0.000213	0.00001 ± 0.00002	2.02E-05	99.86 %	49.1761	321.74 ± 1.42	0.44 %

Single Crystal Total-Fusion Analyses

50.1bB (33° 4' 12.29" N, 85° 51' 6.99" W), Hog Mountain tonalite, Trippel Vein, Alabama

Monitor	P	t	40V	39V	38V	37V	36V	Mol 40Ar	%Rad	R	Age	%sd
au33.5r.mus.8a.txt	0.6	30	1.21993 ± 0.001204	0.02583 ± 0.000095	0.0003 ± 0.000042	-0.00017 ± 0.000215	0 ± 0.000024	2.43E-05	99.9 %	47.1864	309.77 ± 2.18	0.7 %
au33.5r.mus.8b.txt	0.7	30	3.04512 ± 0.001603	0.05809 ± 0.000113	0.00081 ± 0.000054	0.00001 ± 0.000164	0 ± 0.000027	2.74E-05	99.98 %	52.4081	341 ± 1.14	0.33 %
au33.5r.mus.8c.txt	0.7	30	2.6665 ± 0.001992	0.05041 ± 0.000126	0.0006 ± 0.000035	-0.00023 ± 0.000158	-0.00008 ± 0.000042	4.22E-05	100.83 %	52.8938	343.88 ± 1.84	0.54 %
au33.5r.mus.8d.txt	0.8	30	2.59879 ± 0.002195	0.04954 ± 0.000187	0.00061 ± 0.000042	0.00045 ± 0.00012	0.00004 ± 0.000026	2.60E-05	99.55 %	52.2254	339.92 ± 1.66	0.49 %
au33.5r.mus.8e.txt	0.8	30	1.64742 ± 0.001503	0.03085 ± 0.000152	0.00045 ± 0.00004	0.00011 ± 0.000166	0.00012 ± 0.000025	2.52E-05	97.89 %	52.2651	340.15 ± 2.35	0.69 %
au33.5r.mus.8f.txt	0.9	30	2.75386 ± 0.001072	0.05271 ± 0.000091	0.00062 ± 0.000059	0.00007 ± 0.000203	-0.00001 ± 0.000027	2.66E-05	100.13 %	52.2475	340.05 ± 1.14	0.34 %
au33.5r.mus.8g.txt	0.9	30	2.61079 ± 0.001437	0.05004 ± 0.000134	0.00057 ± 0.00004	-0.00016 ± 0.000156	0 ± 0.00003	3.01E-05	99.98 %	52.1586	339.52 ± 1.48	0.44 %
au33.5r.mus.8h.txt	1	30	3.73409 ± 0.002811	0.07241 ± 0.000211	0.0009 ± 0.000039	-0.00008 ± 0.000281	-0.00004 ± 0.000033	3.28E-05	100.28 %	51.5701	336.02 ± 1.34	0.4 %
au33.5k.mus.8h1.txt	1	30	5.15326 ± 0.003794	0.1006 ± 0.000222	0.00125 ± 0.000039	0.00004 ± 0.000259	0.00001 ± 0.000026	2.60E-05	99.93 %	51.1908	333.77 ± 0.92	0.28 %
au33.5k.mus.8h2.txt	1.1	30	5.73981 ± 0.004849	0.11451 ± 0.00023	0.00147 ± 0.000037	-0.00002 ± 0.000186	0.00002 ± 0.000027	2.75E-05	99.89 %	50.0687	327.08 ± 0.85	0.26 %
au33.5r.mus.8i.txt	1.1	30	6.59071 ± 0.00503	0.13233 ± 0.000369	0.00169 ± 0.00005	-0.00065 ± 0.000306	-0.00005 ± 0.000035	3.47E-05	100.24 %	49.8032	325.49 ± 1.07	0.33 %
au33.5r.mus.8j.txt	1.2	30	9.99585 ± 0.013694	0.20118 ± 0.000366	0.00261 ± 0.000061	0.00017 ± 0.000218	0.00003 ± 0.000025	2.48E-05	99.91%	49.6436	324.53 ± 0.78	0.24 %
au33.5r.mus.8k.txt	1.3	30	16.61723 ± 0.011183	0.33871 ± 0.000732	0.00442 ± 0.000068	0.00095 ± 0.000148	0.00002 ± 0.000033	3.31E-05	99.96 %	49.0408	320.92 ± 0.75	0.23 %
au33.5r.mus.8l.txt	1.4	30	18.13617 ± 0.011902	0.36955 ± 0.000812	0.00488 ± 0.000064	0.00147 ± 0.000192	-0.00012 ± 0.000065	6.51E-05	100.2 %	49.0762	321.14 ± 0.81	0.25 %
au33.5r.mus.8m.txt	1.5	30	17.58264 ± 0.026393	0.358 ± 0.000553	0.00497 ± 0.000173	0.00125 ± 0.000176	0.00005 ± 0.000038	3.75E-05	99.91%	49.0708	321.1 ± 0.72	0.22 %
au33.5r.mus.8n.txt	1.7	30	13.76971 ± 0.010875	0.27985 ± 0.000556	0.00381 ± 0.00008	0.00151 ± 0.00023	0 ± 0.000031	3.14E-05	100.01%	49.2035	321.9 ± 0.72	0.22 %
au33.5r.mus.8o.txt	1.8	30	10.87393 ± 0.006332	0.22221 ± 0.000809	0.00278 ± 0.000081	0.00087 ± 0.000204	0.00003 ± 0.000038	3.78E-05	99.93 %	48.8992	320.08 ± 1.23	0.38 %
au33.5r.mus.8p.txt	2	30	16.02213 ± 0.013963	0.32698 ± 0.000798	0.00425 ± 0.000066	-0.00028 ± 0.000367	-0.00015 ± 0.000049	4.94E-05	100.27 %	49.001	320.69 ± 0.88	0.27 %

Appendix B: Muscovite electron microprobe analyses

Oxide Wt%	28.2B	28.2B	28.2B	65.4B	65.4B	65.4B	49.3B	49.3B	49.3B	49.2B	49.2B	49.2B	50.1B	50.1AB	50.1AB	8.3B	8.3B	8.3B	7.2B	7.2B	7.2B
Na_2O	0.23	0.58	0.45	0.82	0.94	0.83	0.65	0.00	0.69	0.85	0.68	0.82	0.47	0.50	0.47	0.28	0.25	0.23	0.72	1.23	1.65
MgO	1.34	1.44	1.34	0.72	0.76	0.73	1.36	0.00	1.44	1.48	1.63	1.72	1.95	1.81	1.85	1.95	2.01	1.90	0.84	0.78	0.99
Al_2O_3	34.99	35.16	34.31	33.73	34.10	34.55	33.36	0.00	34.55	33.79	33.96	33.38	33.92	33.95	34.34	30.59	30.47	30.61	36.76	37.15	36.98
SiO_2	46.08	46.86	46.73	44.56	45.12	45.05	45.84	100.13	47.01	46.46	46.71	47.90	46.59	47.03	47.05	47.07	46.58	47.30	49.57	49.00	48.48
K_2O	10.11	12.14	11.82	11.25	11.34	10.59	10.12	0.01	10.75	10.74	11.06	10.86	11.43	11.06	11.50	11.37	11.36	11.39	5.42	7.25	9.53
CaO	0.03	0.00	0.01	0.00	0.00	0.05	0.04	0.00	0.00	0.03	0.05	0.00	0.01	0.00	0.01	0.01	0.01	0.01	0.01	0.03	0.02
FeO	1.11	1.16	1.21	2.87	2.82	2.84	2.63	0.02	1.50	1.75	1.60	1.78	1.54	1.51	1.63	5.63	5.82	5.55	2.01	1.79	2.09
MnO	0.00	0.02	0.00	0.02	0.04	0.02	0.02	0.01	0.04	0.00	0.01	0.01	0.05	0.02	0.08	0.10	0.08	0.07	0.00	0.00	0.00
TiO_2	0.55	0.75	0.50	0.42	0.37	0.57	0.29	0.03	0.35	0.33	0.37	0.28	0.33	0.24	0.34	0.38	0.27	0.46	0.15	0.11	0.16
Total	94.44	98.11	96.39	94.39	95.49	95.24	94.31	100.20	96.33	95.43	96.07	96.74	96.30	96.12	97.26	97.38	96.85	97.53	95.49	97.34	99.90
Cations (on the basis of 22 O)																					
Si	6.163	6.267	6.250	5.960	6.035	6.025	6.131	13.392	6.288	6.214	6.247	6.407	6.231	6.290	6.293	6.296	6.230	6.326	6.630	6.554	6.484
iv AL	1.837	1.733	1.750	2.040	1.965	1.975	1.869	-5.392	1.712	1.786	1.753	1.593	1.769	1.710	1.707	1.704	1.770	1.674	1.370	1.446	1.516
vi AL	3.679	3.810	3.659	3.277	3.411	3.472	3.390	5.392	3.734	3.541	3.601	3.669	3.579	3.642	3.707	3.118	3.034	3.152	4.425	4.410	4.314
Ti	0.055	0.075	0.051	0.042	0.037	0.057	0.029	0.003	0.035	0.033	0.037	0.028	0.034	0.024	0.034	0.038	0.028	0.046	0.015	0.012	0.016
Fe	0.124	0.130	0.135	0.321	0.315	0.317	0.294	0.002	0.168	0.196	0.179	0.199	0.173	0.169	0.182	0.630	0.651	0.621	0.225	0.200	0.234
Mn	0.000	0.003	0.000	0.002	0.005	0.003	0.003	0.001	0.005	0.000	0.001	0.001	0.006	0.003	0.009	0.011	0.008	0.008	0.000	0.001	0.000
Mg	0.268	0.287	0.268	0.144	0.151	0.146	0.271	0.000	0.286	0.295	0.324	0.342	0.388	0.360	0.369	0.389	0.401	0.379	0.167	0.156	0.197
Ca	0.004	0.000	0.001	0.000	0.000	0.008	0.006	0.000	0.000	0.005	0.007	0.000	0.001	0.000	0.001	0.001	0.001	0.001	0.001	0.004	0.003
Na	0.060	0.149	0.118	0.214	0.244	0.215	0.169	0.000	0.178	0.221	0.177	0.213	0.121	0.131	0.121	0.073	0.064	0.060	0.187	0.318	0.427
K	1.725	2.072	2.017	1.920	1.935	1.807	1.727	0.002	1.835	1.833	1.888	1.853	1.951	1.888	1.963	1.941	1.939	1.944	0.925	1.237	1.627